Volcanic History of the Mount Misery Rhyolite Domes, Tauranga Volcanic Centre

A thesis

submitted in partial fulfilment

of the requirements for the degree

of

***Master of Science (Research)* – Earth Science**

at

The University of Waikato

by

Taya Kinley

THE UNIVERSITY OF
WAIKATO
Te Whare Wānanga o Waikato

2022

Abstract

The Mount Misery rhyolites are a group of three complex lava domes, which are part of the Minden Rhyolites within the Tauranga Volcanic Centre. The lava domes are a previously unstudied volcanic area and have in recent years been partially exposed by a series of quarries, creating an opportunity to understand the volcanic history. A pyroclastic succession flanking the side of the Pukunui dome was studied to compare it to the Otawera ignimbrite and potentially correlate it to the Pukunui succession. This study aims to determine the volcanic emplacement and post-emplacement processes of the Mount Misery series domes and pyroclastics, achieved through field work, thin section microscopy, X-ray diffraction, scanning electron microscopy, and X-ray fluorescence.

Key findings from this study show similar phenocryst assemblages but the groundmass textures are complex. The rhyolite groundmasses analysed varied between glassy, crystalline and devitrified, while key phenocrysts found were plagioclase and quartz, and within Maungatūtū/Mount Misery and Greenpark domes also minor clino- and orthopyroxenes. Quartz polymorphs such as cristobalite were common in the groundmass as needle-like structures, while at Pukunui, pure quartz composed the thin bands. The thin bands found at Pukunui and Greenpark formed as a strain feature that caused segregation of quartz along preferential axial planes. Sanidine was found at all three locations as devitrification of glass within the groundmasses. Maungatūtū/Mount Misery had sanidine present as radiating spherulites, while Greenpark had a new find of sub-circular crystalline inclusions which appeared to be some variation of a spherulite.

The domes have similar geochemical and mineralogical compositions, proving they are linked to the same source magma, but would have erupted at different points in time, likely with Maungatūtū/Mount Misery as the oldest and Pukunui as the youngest. The flow banding and flow folding present at Pukunui and Greenpark, and the lack of shearing features, have been used to identify the domes as endogenous. The Pukunui pyroclastic succession included multiple flow units that were correlated to the Otawera ignimbrite elsewhere, which was likely emplaced as a proximal ignimbrite from a dome collapse event at Pukunui. This was one of the final volcanic events in the Mount Misery series area.

Acknowledgements

To Adrian Pittari, my number one supervisor, for the opportunity to complete this thesis and to grow and learn as a volcanologist. The endless hours we spent in our catch-ups, looking over samples, and being able to give me the help I needed has been imperative to the completion of this thesis. I am so very grateful for your time and support.

I have been very lucky to have Marlena Prentice as my rock throughout, sharing invaluable knowledge with me. Thank you for always taking the time to listen no matter how busy you were, guiding me in the right direction and being the best support I could've asked for.

Thank you to the owners of the J Swap quarry at Pukunui, the Oropi quarry at Greenpark, and the landowner of Maungatūtū/Mount Misery for allowing me access to these sites, without which there would have been no research.

A special thank you to Kirsty Vincent, for the endless support in the labs and for guiding me through the most vital part of this thesis. I absolutely could not have done the key parts of this study without you and your ongoing patience. To Helen Turner in the SEM room, your ability to work in my last-minute bookings and your kind words were much appreciated. The staff at the University of Waikato, Earth and Science that helped me in many ways throughout, thank you for your assistance.

I would also like to thank my office for the laughs and moral support on both good and bad days. You guys made this experience more than enjoyable, and I'm so grateful I got to spend the time with you!

Finally, to my family, thank you for the ongoing love and support in the completion of this study. Mum, dad, my sisters, grandparents and especially my partner; always giving a kind word when things were feeling tough, for listening when things felt hard and the endless encouragement has been something I am truly grateful for. My flatmates too; you guys have been awesome and I love you all a lot!

This thesis is dedicated to the late Colleen Blyth (1942-2018),
who would have been so proud of this achievement.

Table of Contents

List of Figures

Chapter One

Introduction

1.1 Introduction

Lava domes are a common feature in the Tauranga Volcanic Centre (TgaVC), and are classified as the Minden Rhyolites subgroup (Leonard et al. 2010). The three lava domes that make up the Mount Misery rhyolite domes (Pukunui, Maungatūtū/Mount Misery and Greenpark), which have been previously grouped based on geochemical data (Briggs et al. 2005). The area has been mapped and dated (Briggs et al. 1996, 2005), and now there are active quarries that expose two of the three domes, which provides the chance to examine different rhyolite dome lithologies and the composition of the flow units. The opportunity to understand their geological history will be a key part of the current knowledge development of the TgaVC.

The Mount Misery dome series are, from a volcanic perspective, relatively unstudied. Volcanism in the TgaVC has been previously addressed (Rutherford, 1978; Hughes, 1993; Briggs, et al. 1996, 2005) but the quarry exposure in this area can provide new insights into lava dome growth processes and alteration processes in silicic dome centres. Volcanological studies will outline the history of these three volcanic centres; including an understanding of the emplacement processes, magma compositions, and the effect of post-emplacement processes on the texture and mineral characteristics. These insights will also be useful for understanding the rock resource from the quarry perspective.

1.2 Research Objectives

This thesis focusses on the three Minden Rhyolite subgroup lava domes that comprise the Mount Misery series: Pukunui, Maungatūtū/Mount Misery and Greenpark. A pyroclastic succession on the flanks of the Pukunui dome is also included here. To understand the eruptive history of each dome and processes, the following objectives have been addressed:

- A field examination, to determine the lithology, facies and structure of the rhyolites at each location;
- A petrographic study of the primary volcanic and secondary alteration minerals and textures. This is achieved using thin section microscopy, X-ray Fluorescence (XRF), and Scanning Electron Microscopy (SEM), which utilises Energy Dispersive X-ray Spectroscopy (EDS) to determine mineral compositions;
- Geochemical studies to determine chemical compositions from each site, with an aim to identify similarities and correlate between domes where necessary. X-ray Diffraction (XRD) for both major and trace elements determines the elemental compositions comprising each sample.

1.3 Location of Study

The Mount Misery rhyolites are three separate rhyolite lava domes located within close proximity to each other in the Bay of Plenty region, north-east of Tauranga. Each dome location is shown in Figure 1.1 below. All field locations are located alongside Ohauiti Road and Kaitemako Road. Pukunui and Greenpark rhyolites are exposed in active quarries, while Maungatūtū/Mount Misery is a sheep and cattle farm that is privately owned. An outcrop along Rowe Road was also visited, with a sample being taken to determine if there would be a match to one of the domes.

The Mount Misery series lies in the Papamoa Range (Figure 1.2B), alongside the Mamaku Plateau. The Pukunui dome straddles the Otawa andesite, which is seen in the field as a hilly, forest-covered expansive space to the east. The terrain surrounding the Mount Misery series is steep and hilly, with few surrounding streams such as Kirikiri and Waitao, which have tributaries throughout the area.

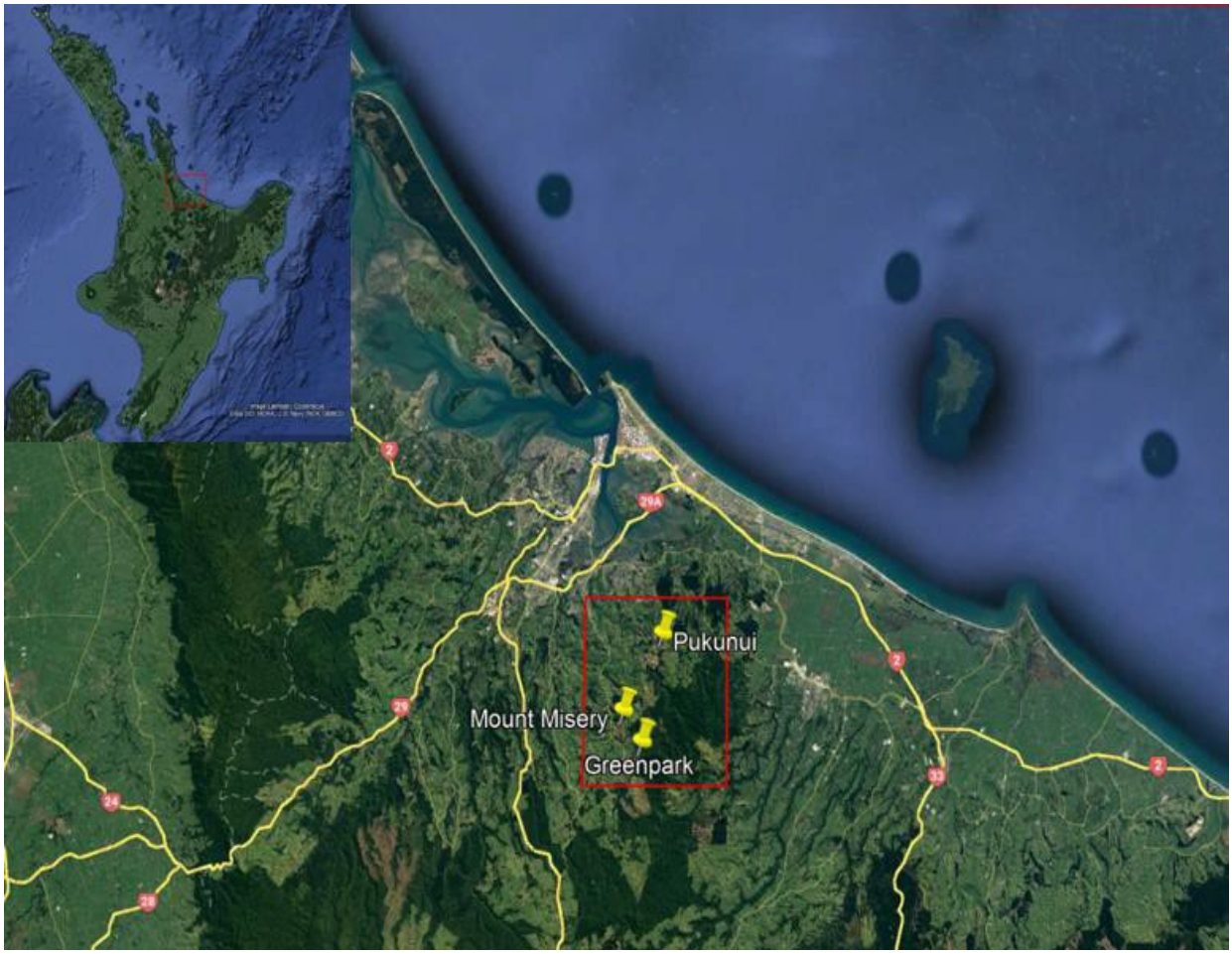

Figure 1.1: Field area map of the North Island, New Zealand compared with East Tauranga. The highlighted red area shows the three Mount Misery peaks, part of the Minden Rhyolites (sourced from Google Earth).

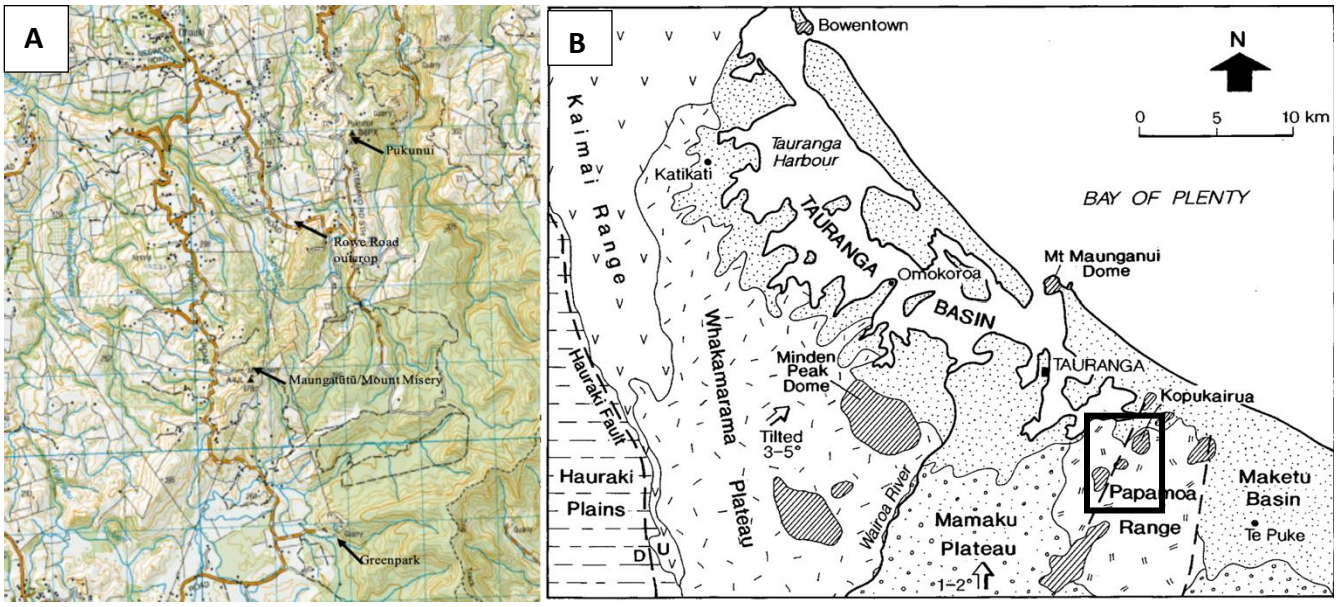

Figure 1.2: (A) Topographic labelled map showing the Mount Misery domes and the Rowe Road outcrop. (B) geological map of the Tauranga area (Mount Misery series locations shown in the black box). From Briggs et al. (1996), reproduced with permission.

1.4 Previous Work

There have been previous geological studies completed looking at the Tauranga Volcanic Centre, specifically the eastern aspect. Briggs et al. (1996; 2005) undertook fundamental work on all four of the Minden Rhyolite groups. This included dating the domes in each group through $^{40}Ar/^{39}Ar$ dating resulting in a range of 1.95 – 2.89 Ma. Briggs et al. (2005) used $^{40}Ar/^{39}Ar$, to date Maungatūtū/Mount Misery at 2.69 ± 0.03, and highlighted an average SiO_2 of 72.2 wt. %. Rutherford (1978) studied the Minden Rhyolites, but not each subgroup, giving obsidian fission-track ages, and trace element analyses. In Rutherford's study, Mount Maunganui was dated at 2.29 ± 0.21 Ma. Maps of the Minden Rhyolites (Figure 1.2B) have also been included in the Tauranga geological map (Briggs et al. 1996) and the Rotorua 1:250,000 QMP (Leonard et al. 2010).

There is minimal research on the Mount Misery domes. Hughes (1993) mapped and discussed the Mount Misery rhyolites and their common features, including the ages previously given. Hughes (1993) mapped the Minden Rhyolites. Pittari et al. (2021) redefined the TgaVC and also dated several domes of the Minden Rhyolite subgroup by U-Pb and (U-Th)/He, and zircon dating methods. Prentice et al. (2022) redefined the stratigraphy of the Papamoa Formation ignimbrites in eastern Tauranga.

1.5 Structure of thesis

- *Chapter two explains the methods used in the field and laboratory.*
- *Chapter three is a literature review, giving background information on general geological settings and in-depth analysis of lava domes and the Mount Misery area.*

- *Chapter four presents the field data taken for the Mount Misery series. This includes the field areas used in this thesis, field observations that were made, and how the data was collected from each field site.*
- *Chapter five is a petrography section, which has petrographic microscopy, XRD data, and SEM analysis of selected samples from each location.*
- *Chapter six outlines geochemical data taken from XRF analysis.*
- *Chapter seven is a summary of the important findings, and an interpretation of the volcanic and alteration processes associated with the domes.*

Chapter Two

Methodology

2.1 Introduction

This chapter outlines the methods used to collect data in the field and laboratories. This includes field work, thin section preparation, microscopic petrography, scanning electron microscopy (SEM), X-Ray diffraction (XRD) and X-Ray Fluorescence (XRF).

2.2 Field Work

Field work was undertaken to examine the internal structuring, lithology and layering of the Mount Misery rhyolites: Pukunui, Maungatūtū/Mount Misery and Greenpark. Pukunui and Greenpark are currently open quarries, which meant that there were large sections of these two domes exposed, while Maungatūtū/Mount Misery had multiple exposed outcrops. Samples of the rhyolite and the pyroclastic succession at Pukunui were collected, as it was emplaced along the side of the Pukunui rhyolite. The field work for this thesis was completed during the summer of 2021/2022. There were three different locations visited; two quarries, a privately-owned farm and a smaller outcrop along Rowe Road, between Pukunui and Maungatūtū/Mount Misery.

In the field, I usually started at the lowest exposed part of the rhyolites and work upwards, making observations, measurements and taking samples where exposure of each face was sufficient. Each stop was determined by the change in outcrop characteristics, or in the case of Maungatūtū/Mount Misery wherever good exposure occurred of the rhyolite. At each location GPS coordinates, as well as elevations, were measured. A field description of each unit was taken, including the textures and components of the facies and the textures present. Each unit was photographed with a scale, and most were sampled with a rock hammer or spalling hammer for a fresh sample to be taken. At locations with flow banding, dip and strike measurements were taken. Each time a sample was taken, they were individually bagged and labelled after being photographed, so that they would be easily identified. The Pukunui pyroclastic succession was described in a stratigraphic log, which characterised pumice, lithics, crystals and the matrix. Estimations of grain sizes and abundance percentages were also taken.

2.3 Thin Section Preparation

38 thin sections were prepared for optical microscopy, with 29 of these from the three Mount Misery rhyolite domes and 9 from the pyroclastic succession at Pukunui. Each sample was individually cut into small blocks to fit onto glass slides, leaving margins of 1-5 mm depending on the size and structure of the original rock. After cutting and drying, the blocks were impregnated with Nuplex Resin at a 2:1 ratio of resin to hardener. They were then dried and ground down, using a #600 polish powder on a frosted glass plate to remove excess impregnation resin. Each rock required a flat surface that would be mounted onto a frosted glass slide, and samples were dried on a heating plate periodically to ensure each round of resin would absorb and adhere correctly. The flat, smooth surface of each block was then mounted onto frosted slides with Hillquist epoxy using a 2.3:1 ratio of resin to hardener. When

mounting the glass slides, bubbles that initially appeared were removed with circular motions alongside heat, and then left to set overnight. Following block mounting, each sample was cut to approximately 1 mm in thickness using the Struerd Discoplan-TS, then trimmed to ~ 10 µm on the same machine. The slides were checked periodically under a microscope to ensure the correct final thickness, which was determined when plagioclase phenocrysts were the right birefringence. Cover slips were applied to seal the thin sections of each sample with a petropoxy using a 1:0.1 ratio of resin to hardener, and once applied left to dry overnight. Each thin section was labelled on the original block from hand samples and then scribed with a diamond-tipped pen onto thin section glass to identify them.

Polished thin sections were prepared for scanning electron microscopy (SEM) as above, except instead of cover slip application, the thin sections were polished. 12 polished thin sections were prepared for SEM. This was a process of sanding down the thin section on the Struers LaboPol-25 machine, first by hand with Struers #500 sandpaper, and then on the machine grinding disc using #1200 sandpaper. After the thin section had been sanded to the point where all necessary minerals were visible, it was then held sample side down onto the Buehler Metaserv Grinder Polisher. This was to remove all scratch marks from polishing, and was typically achieved after 20 minutes.

2.4 Microscope Petrography

The 38 thin sections made were then used for bulk rock analyses to look at the phenocrysts and groundmass within each type of rhyolite. Each thin section was looked at individually, and from there common features were identified. Thin sections were viewed under plane (PPL) and cross polarised light (XPL) to highlight different features. Certain interesting components were photographed for identification purposes and to compare similar features. The groundmass and individual phenocrysts were identified using characteristics common to each mineral, and compared to what would be expected of rocks in this area.

2.5 Scanning Electron Microscopy (SEM)

Polished thin sections and whole rock pieces were analysed through two different methods; backscatter (BSE) and secondary electron (SE) mode. The machine used was the Hitachi SU8230 FE SEM. Thin sections and whole rock pieces were analysed, and so to go into the SEM machine both were required to be coated in platinum, which allowed a layer for electrons to escape through. Before the platinum coating, carbon paint was applied to the mounting block and slides on each corner to also allow the movement of electrons. The platinum coating was at 5 µm thickness, applied by the Quorum Q150V Plus machine. The thin sections and pieces were mounted onto a block to fit on the stage of the SEM, and upon correct placement, modes were selected on the computer for BSE, SE, and EDS analysis. Thin sections were looked at using all three modes, using Point ID to identify minerals within the

groundmass, and whole rock was in SE mode to look at textures. Energy Dispersive X-ray Spectroscopy (EDS) was used to analyse the chemistry of specific points within a sample, using a voltage of 20.0 kV.

2.6 X-Ray Diffraction (XRD)

Whole rock samples were selected for XRD based on the microscopic petrography. Once a selection of 13 rhyolites had been identified, hand samples were cut into blocks. Samples were labelled and placed into glass jars, and dried at 105°C overnight to remove all moisture from the sample, making it easier for the next stage of crushing. The samples were crushed in the tungsten carbide ring mill, turning the block samples into a fine powder which was put back into the designated glass jar, ready for analysis. Samples were then run through XRD after being pressed into a pellet. This was done in the Panalytical Empyrean Series 2 XRD machine at the University of Waikato. The bulk samples were run for 5-80 °2θ at 50 seconds per step using a Copper Kα source. Recorded mineral peaks and their diffraction patterns were then recorded and analysed using Highscore Plus indexing software.

2.7 X-Ray Fluorescence (XRF)

Once the selected 13 rhyolites and 6 pumice samples were crushed into a powder and XRD had been run, XRF preparation began. Fusion discs were prepared by measuring 8 g of 12:22 flux (Lithium Tetraborate 35.3%: Lithium Metaborate 64.7%) with 0.8 g of sample in a crucible. Ammonium iodide was added as a releasing agent, and the sample was then placed into the furnace. The furnace melted the sample and flux at 1050°C, and once at melting point, the liquid was poured into a mould and then cooled to form a disc in a half hour period. The loss of ignition (LOI) was calculated by measuring ~ 2 g of sample in a crucible, then heated to 1000°C. Once heated overnight at this temperature, the crucibles were removed, and once cool were weighed to see the difference. Pressed pellets were made using 6-7 g of sample and ~ 20 drops of PVA binding glue, mixed thoroughly and placed into an aluminium holder. The sample was then pressed using a hydraulic press to set it firmly, with the final step to be dried for 2-3 hours at 70°C to evaporate the PVA binder. The samples were then run through the XRF process, taking approximately 3 hours to complete a singular sample. The XRF samples are run through the Bruker S8 Tiger in the School of Science, at the University of Waikato.

Chapter 3

Literature Review

3.1 Volcanic Regional and Geological Setting

New Zealand is located on the Pacific Ring of Fire, in the south-western Pacific Ocean. It is a rifted continental fragment composed of two main islands, the north and south (Scott, 2013). New Zealand was not a separate geological area until late Cretaceous times, and previously formed part of the Pacific -facing Gondwana continental margin (Laird et al. 2003). The eastern side of New Zealand was a representation of the youngest part of the convergent margin system, where subduction occurred until 105 ± 5 Ma then being replaced with crustal extension that resulted in New Zealand separating from Gondwana (Laird et al. 2003). Between 85 – 55 Ma, the Pacific-Australian plate boundary consisted of the Tasman Sea spreading ridge, and further east, the Lord Howe Rise, New Zealand and Norfolk Ridge that formed Zealandia (Mortimer et al. 2007). Zealandia was a rifted continental borderland, and since approximately 5 Ma the convergent Pacific-Australian boundary has been close to its present-day position.

The northern and eastern margins of New Zealand had the first onset of subduction occur at the beginning of the Miocene period (Rait et al. 1991). Arc-related volcanoes in Northland were the first to occur in New Zealand, aged 25 – 23 Ma, and have been associated with offshore volcanic chains that have since been displaced eastwards (Pittari et al. 2021). The oldest andesitic volcanism has been dated at 22 Ma based on deposits in Northland, and ultramafic rocks are present only in North Cape. This implies that these volcanic rocks originated from a thick oceanic plateau that formed adjacent to Northland in the early Cretaceous/early Paleogene (Rait et al. 1991). Calc-alkaline igneous eruptions began in the early Miocene, continuing into the Holocene to central Taupō and Taranaki areas. Volcanism has migrated in an oceanward pattern, from north-west to south-east towards the Hikurangi Trench (Brothers, 1984).

North Island volcanism is comprised of many components, such as shown in Figure 3.1 (Pittari et al. 2021). Slab rollback at 6 Ma started the rifting of the Vitiaz Arc into the Colville and Kermadec ridges, opening the Havre Trough (Pittari et al. 2021). The rifted Havre Trough is the remnant of an older volcanic arc which has been preserved within the Coromandel Volcanic Zone, the Taupō Volcanic Zone, as well as continued through the Kermadec Arc and rift basins. There is a back-arc present which developed with the migration of a southeast arc, and this movement was responsible for the development of the Hamilton Basin, and the presently active Hauraki Fault (Pittari et al. 2021). There are also andesitic volcanic centres in the south-west, such as Taranaki, and basaltic intraplate volcanism in Auckland, to the north-west (Pittari et al. 2021).

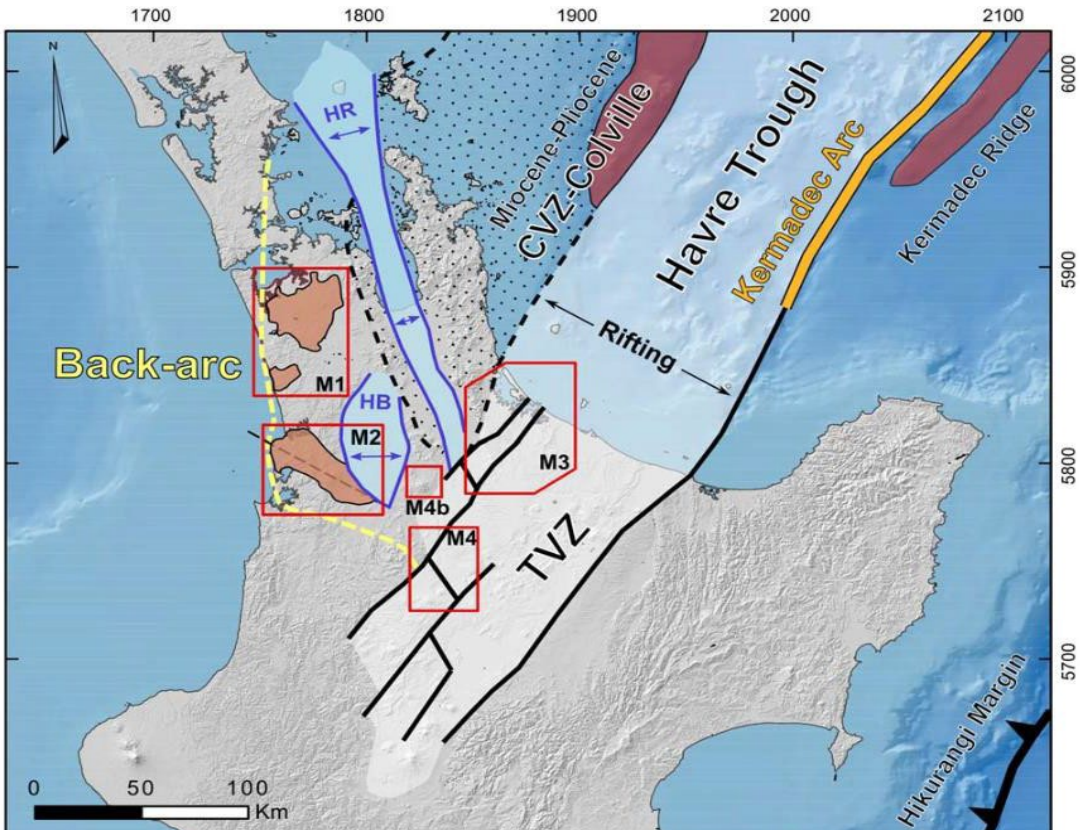

Figure 3.1: Magma tectonic components represented within the North Island, highlighting the rifted Havre Trough bound by the Colville and Kermadec ridges (dark red). Oblique rift basins such as the Hamilton Basin (HB), Hauraki Rift (HR) are shown (light blue). From Pittari *et al*. (2021), reproduced with permission.

3.1.1 Coromandel Volcanic Zone

The Coromandel Volcanic Zone (CVZ) is the southern portion of a NNW andesite, dacite and rhyolite belt extending south from the Poor Knights Islands. The CVZ is a 200 km-long by 35 km-wide continental volcanic arc, and is the largest as well as the oldest area of andesite-dacite volcanism in New Zealand (Moore, 2011). Onshore, the CVZ encompasses the Coromandel Peninsula as far south as the Kaimai Range, which includes the Kiwitahi Volcanic Zone. The Kiwitahi Volcanic Zone now lies to the west due to the opening of the Hauraki Rift. The Coromandel Peninsula is comprised of Miocene to Quaternary volcanics, with the central CVZ evolving from 18 to 4 Ma ago (Adams et al. 1994). It is bound to the west by the Hauraki Rift, which is a graben that has been infilled by Quaternary and Tertiary sediments (Smith et al. 2006). The Tauranga Volcanic Centre has been acknowledged previously as part of the CVZ, but this is now considered a transition period between the CVZ and the Taupō Volcanic Zone (Briggs et al. 2005; Pittari et al. 2021). The geomorphology of the Tauranga area is a representation of the transition that occurred between the Miocene-Pliocene CVZ and the current Pleistocene-Recent Taupō Volcanic Zone (Briggs et al. 2005).

The CVZ is notably made up of igneous rocks ranging from basalt to rhyolite, which formed on Mesozoic low-grade metagreywacke basement. During 9 to 7 Ma, bimodal basalt and basaltic andesite-rhyolite filled the landscape following major caldera collapses, ignimbrite eruptions and postcaldera andesitic eruptions (Adams et al. 1994). CVZ volcanism began 7 Ma, leading to the emplacement of rhyolite domes, ignimbrites, and pumice breccias. These presently make up the subgroups of the Whitianga group. Multiple silicic volcanic centres situated within the CVZ occur as negative gravity anomalies (Malengreau et al. 2000; Smith et al. 2006), arcuate or circular structures, and include thick intracaldera ignimbrites, and silicic dome complexes (Briggs et al. 1990). The Waihi Caldera is the youngest rhyolite-dominant volcanic centre, lying south of the CVZ and north-west of Tauranga, having formed c. 3.9 – 3.5 Ma (Briggs et al. 2005; Vincent 2012; Julian 2016; Pittari et al. 2021).

3.1.2 Taupō Volcanic Zone

Active North Island volcanism is a rifted, north-east trending, predominantly silicic volcanic arc that runs through the centre of the island, known as the Taupō Volcanic Zone (TVZ). The TVZ represents the southernmost area of the 300 km continental extension, part of the ~ 2800 km Tonga-Kermadec arc (Figure 3.1). TVZ volcanism began c. 2 Ma and is spatially concurrent with a 15 – 40 km wide zone, a crustal extension known as the Taupō rift (Rissmann et al. 2011; Wilson et al. 2016). The TVZ is renowned for its frequent and voluminous silicic volcanism and abundant geothermal systems (Barker et al. 2020). There is regional magmatic segmentation with andesite-dominated volcanism in the south-west and north-east areas, and centrally rhyolite dominated volcanism, with at least eight large caldera volcano systems as shown in Figure 3.2 (Barker et al. 2020).

In the last 1.6 Ma within the central TVZ, there have been 25 separate caldera forming eruptions that have in total resulted in over 6000 km^3 of silicic magma being discharged. The overall magma volume is only comparable to Yellowstone Caldera regarding Quaternary silicic volcanic systems (Chambefort et al. 2014). Calderas within the TVZ exhibit strong regional structural control, and the prior fault structures may have a significant impact on the structure and location of caldera collapses, which can form irregularly shaped calderas (cf. Okataina Caldera: Seebeck et al. 2010) and act as pathways for ignimbrite eruptions and lava dome growth (Ashwell et al. 2013). Many of the smaller eruptions led to the extrusion of rhyolitic and dacitic lava to produce intra-and extra-caldera lava domes and complexes, and such associations have been well documented in the TVZ (Ashwell et al. 2013; Bebbington, 2020). Domes found in the TVZ are aligned along major regional faults, and the modern-day hydrothermal

systems are known to still use these regional pathways, as it has been proven that buried lava domes serve as conduits for hydrothermal fluids (Leonard, 2003).

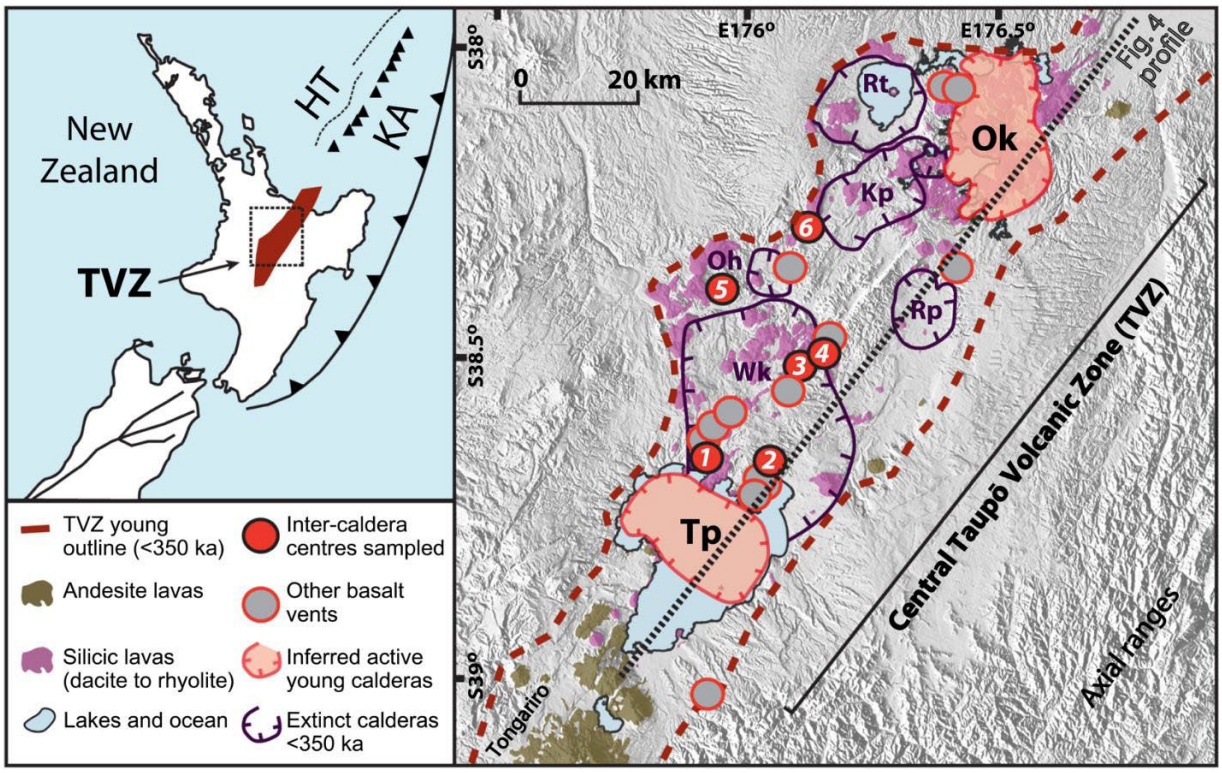

Figure 3.2: Regional magmatic segmentation of volcanism in the TVZ, and the eight large caldera systems (from Barker et al. 2020, reproduced with permission).

3.2 Tauranga Volcanic Centre

The Tauranga Volcanic Centre (TgaVC) was active from 2.95 to 1.9 Ma (Briggs et al. 1996, 2005; Leonard et al. 2010) and is located in the eastern Bay of Plenty region, which extends from Bowentown and Waihi Beach in the northwest, to the Papamoa Hills in the southeast (Hollis, 1995). Most of the volcanic deposits are confined within the Tauranga basin which covers an area of 520 km^2 and is restricted to an area bounded by the Papamoa Hills located in the east, the southern Kaimai Range to the west, and the Mamaku plateau to the south. The central part of the Tauranga basin is the Tauranga harbour, a large and shallow estuary comprised primarily of tombolos, and the barrier island complex of Matakana Island (Briggs et al. 2005).

The Tauranga harbour is the largest geographical feature within the Tauranga basin, covering a 400 km^2 area and containing two estuarine systems which are Waimapu and Waikareao (Hollis, 1995). The rhyolite domes of Mount Maunganui and Bowentown form the mouth of both entrances to the harbour (Hollis, 1995). Large flat regions are composed of ignimbrite sheets of both TgaVC and TVZ origin. The geomorphology of the Tauranga area is a representation of the volcanic deposits which were

erupted during the transition between the Miocene-Pliocene CVZ and the present-day Pleistocene-Recent TVZ (Briggs et al. 2005).

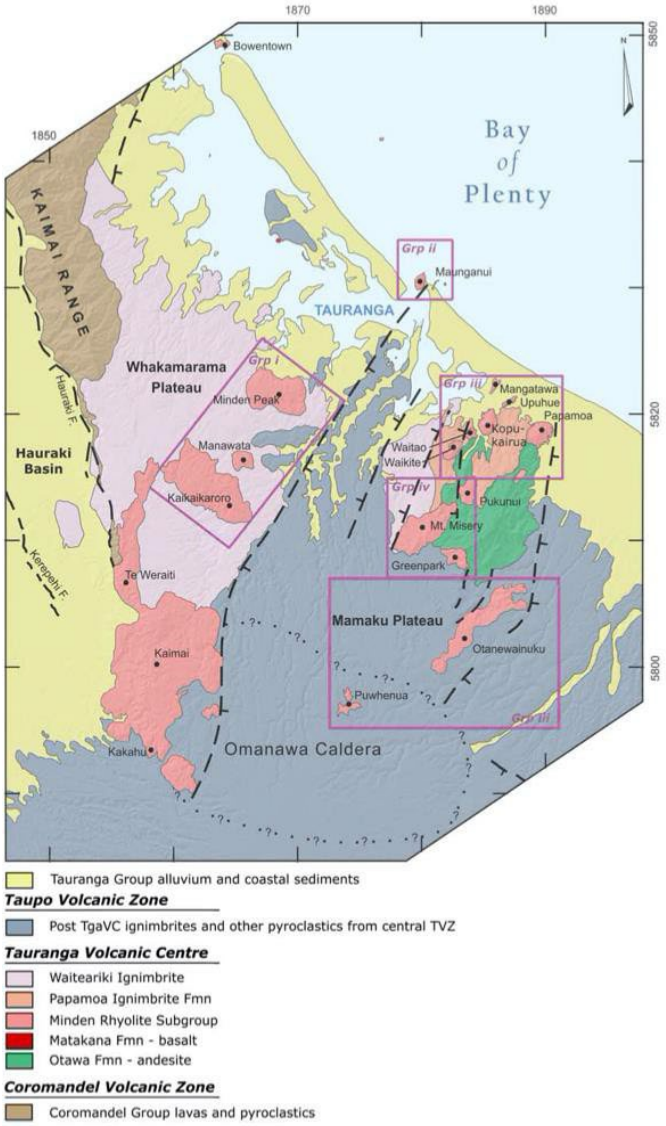

Figure 3.3: A geological map of the Tauranga Volcanic Centre (from Pittari et al. 2021, reproduced with permission) redefined to show units of features, as well as spaces covered by pyroclastic or sedimentary deposits. The four Mount Minden groups are identified, as is the Omanawa Caldera.

Previously, the volcanic vents of this period in the Kaimai and Tauranga areas were considered as two separate volcanic centres defined through spatial separation, however this has been reviewed and they are now regarded as one (Pittari et al. 2021). This new centre combined TgaVC comprises an eroded andesitic stratovolcano (Otawa formation), roughly 17 rhyolite-rhyodacite lava dome complexes (the Minden Rhyolites), a small basalt lava flow (Matakana Formation), two distinct ignimbrite formations (Waiteariki and Papamoa) and a graben caldera structure (Pittari et al. 2021). Often, they are overlain by younger, partially welded ignimbrites. The entire Tauranga basin is covered in a thick layer of Pleistocene-Recent silicic tephra, derived from the TVZ and the Mayor Island Volcanic Centre (Briggs

et al. 2005). The complexity and size of the TgaVC is comparable to younger volcanic centres within the TVZ.

3.2.1 Minden Rhyolites

The topographic highs of the Tauranga basin are numerous dacite-rhyolitic lava domes and complexes which make up the Minden Rhyolites, such as Maungatūtū/Mount Misery at 478 m a.s.l, Mount Maunganui at 252 m a.s.l, and Mount Minden at 286 m a.s.l (Hollis, 1995). The Minden Rhyolites (Minden Group) are upper Miocene-Pliocene dome and flow rhyolites, as well as welded pumice breccias across the TgaVC (Rutherford, 1978). The Minden Group cover an extensive area of andesitic eruptives ranging from 16 to 7 Ma (Rutherford, 1978).

The Minden Rhyolite domes are prominent landforms in the TgaVC, and includes all rhyolites in the Tauranga and Bay of Plenty area (Briggs et al. 2005). Many of the rhyolite and dacite domes in the TgaVC are crystal rich, with up to 40% phenocrysts, but this excludes the crystal poor Maunganui dome and the Bowentown dome (Pittari et al. 2021). The clusters of rhyolites in the TgaVC, which are spatially associated, may imply genetically related silicic magmas which have been synchronously derived (Briggs et al. 2005). Their genesis when compared to TVZ silicic magmas is very similar, suggesting a relationship which may be as a result of fractionation or partial crustal melting (Briggs et al. 2005).

Samples taken from individual rhyolite domes and flows show distinct textural differences. Differences within rhyolite samples may include their spherulite occurrences, and biotite or quartz content. Within spherulites there are often radiating feldspar aggregates, which may contain cristobalite and tridymite, located in a glassy carapace (Hughes, 1993). Spherulites may be super-imposed onto flow structures, which can imply that the crystallisation of the feldspars occurred after the lava was deposited and the flow was at a minimum rate (Hughes, 1993). There are four groups which define the Minden Rhyolites and these are based on factors such as spatial association, phenocryst mineral assemblage, and geochemistry. Some of the Minden Rhyolite domes also have associated ignimbrite deposits with them which are included in the groups.

3.2.2 Minden Peak Group

The Minden Peak group forms crystal rich hornblende-rhyolite domes located north-west of the Wairoa River and include Minden Peak, Manawata and Kaikaikaroro domes. It has been dated at 2.39 – 2.16 Ma. The rhyolite is geochemically defined by high silica, high potassium and intermediate zirconium contents (Briggs et al. 2005).

3.2.3 Mount Maunganui Group

This grouping includes the crystal-poor rhyolite of Mount Maunganui, Mount Drury, Moturiki Island and Motuotau Island, with a date of 2.35 Ma. The phenocryst mineralogy is biotite ± hornblende ± orthopyroxene. Defining geochemistry is very high silica, very high potassium and low zirconium content. The Mount Maunganui group are a tight spatial cluster, with a highly evolved mineral composition (Briggs et al. 2005).

3.2.4 Mangatawa Group

The Mangatawa group is the largest, with 10 domes classified under it, including Papamoa, Upuhue and Mangatawa. They are crystal-rich hornblende and orthopyroxene rhyolites/dacites with lesser biotite. They are defined as having low silica, high potassium, and intermediate zirconium content. The Mangatawa group is aligned on north-east trending faults along the TgaVC basement that borders the eastern segment. The faults are not exposed at the surface, however, there are multiple deep, older faults that occur in the basement and are shown on seismic reflection profiles offshore (Briggs et al. 2005).

3.2.5 Mount Misery Group

The Mount Misery group includes Pukunui, Maungatūtū/Mount Misery and Greenpark domes which have previously been classified as crystal rich hornblende – orthopyroxene rhyolites. Geochemistry is characterised by low silica, high potassium and the highest zirconium content of the four groups, that can exceed 200 ppm. The high zirconium content is what separates the Mount Misery series from Mangatawa, as geographically they occur in the same area (Briggs et al. 2005).

3.2.6 Ignimbrites of the TgaVC

There are numerous ignimbrites and fall deposits found in the TgaVC (Figure 3.4). From oldest to youngest, these are the Aongatete Formation, a succession of ignimbrites within the Papamoa Formation, which includes the Waiteariki ignimbrite, the Ongatiti ignimbrite; and other ignimbrites of the Pakaumanu Group, which are the Chimp Formation, the Pokai Formation and the Mamaku ignimbrite (Prentice et al. 2022). Many of the sources are yet to be formally defined, but are likely of local origins. Gravity maps of the Tauranga area show a large, negative anomaly which may be indicative of a caldera structure that has been infilled with low density volcanic materials, known as the Omanawa Caldera. This gravity map feature could represent a caldera that historically has collapsed and been buried, potentially a source of these undefined ignimbrites (Briggs et al. 2005). The volcanic lithologies of the Tauranga basin vary from basalt to rhyolite, and these rock types form the surrounding edges of the basin, such as the Papamoa Hills and the Kaimai Range (Hollis, 1995). The lower area of the basin is covered in pyroclastic deposits which form topographic features such as low ridges and interfluves.

The Ongatiti ignimbrite is a major feature landscape forming partially welded ignimbrite of the Waikato region and was sourced from the Mangakino Volcanic Centre. Non-welded equivalents extend through the west and east coasts of the North Island. There are two small outcrops in the Tauranga basin, situated west of the Waiora River which represent the furthermost extent of the welded area of the Ongatiti Ignimbrite (Briggs et al. 2005).

The Te Puna and Te Ranga ignimbrites found in the TgaVC are localised to the central basin, representing locally derived eruptives, or more likely are distal equivalents of widespread, unidentified ignimbrites from the TVZ. Components within Te Puna are hornblende, pumice, and crystals within the non-welded to partially welded ignimbrites, found in several outcrops around Tauranga (Briggs et al. 2005). Phenocrysts include plagioclase, hornblende, biotite, quartz and orthopyroxene. The biotite present in this unit has a distinctive golden colouring. The Te Puna ignimbrite is a non-welded, crystal rich ignimbrite, found in coastal sections of western Tauranga Harbour and Matakana Island (Prentice et al. 2022).

The Chimp Formation (including the Te Ranga ignimbrite) is a sandy textured ignimbrite, found in the field as non-welded, crystal poor and ranging from pumice poor to rich (Prentice et al. 2022). It is noted for holding coarse glass shard textures, charcoal and obsidian. The Chimp Formation is notably restricted to low lying areas of the central Tauranga basin. It has been found to be intercalated with lower lake derived silts and upper fluvial volcaniclastic sands, implying it may have been emplaced sub-aqueously (Briggs et al. 2005).

The Pokai Formation (formerly Waimakariri ignimbrite) overlies the Te Ranga ignimbrite, and is found as a large, partially welded ignimbrite. The exact source of the Pokai ignimbrite is undetermined presently, but is likely derived from south of the TgaVC, possibly from the Rotorua Volcanic Centre (Briggs et al. 2005). Its age is currently unknown but has been determined to be between 275 ± 10 ka (Downs et al. 2014).

The overlying Mamaku ignimbrite is the youngest significant eruptive of the Tauranga-Kaimai area, and a major component of the landscape. It has been linked to the collapse of the Rotorua caldera because of its date, determined by $^{40}Ar/^{39}Ar$ to be 0.22 ± 0.01 Ma (Briggs et al. 2005). The Pokai Formation and Mamaku ignimbrite forms the Mamaku plateau, which surrounds the rhyolite domes of Kaimai, Puwhenua, Otanewainuku and Maungatūtū/Mount Misery. The Mamaku plateau is intercalated with volcanic units that postdate the Waiteariki ignimbrite, forming a range of terrestrial and estuarine sediments known as the Matua subgroup (Houghton and Cuthbertson, 1989).

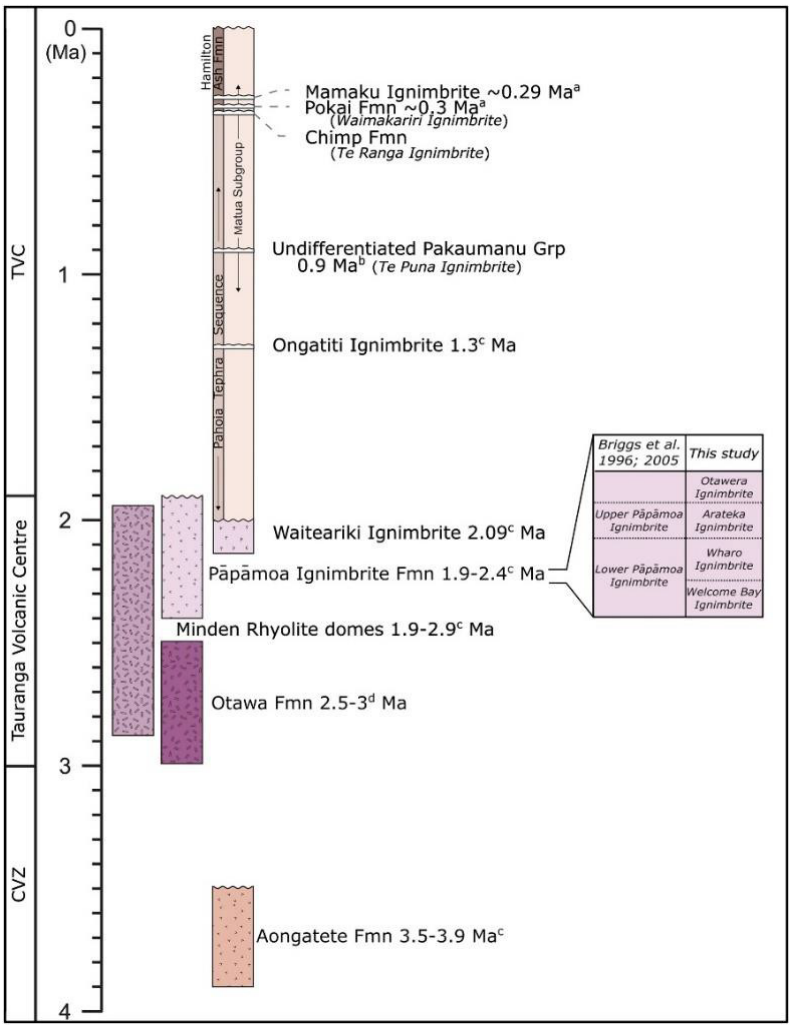

Figure 3.4: Generalised figure (from Prentice et al. 2022, with permission from Elsevier) showing deposits in the Tauranga region associated with the TgaVC.

3.3 Lava Domes

Lava domes are a common feature in the TgaVC, and the three field areas of Pukunui, Maungatūtū/ Mount Misery and Greenpark are lava domes. This section describes common features of lava domes, their structures and potential collapse.

3.3.1 Geomorphology and Dome Structure

Lava domes vary widely in structure and texture, forming as high silica magma cools down and degasses soon after eruption (Calder et al. 2015). The fundamental framework of each lava dome reflects processes relating to the internal conditions of magma ascending its way through the upper crust, and the local emplacement conditions at the vent (Hale et al. 2009). These factors control the permeability of a lava, and thus their ability to lose gas. In turn, this affects their buoyant driving force and whether the eruption is passive or explodes catastrophically (Druitt et al. 2002; Kokelaar, 2002). Lava domes are a frequent style of volcanism. They can occur in isolation, appear as linear formations, or in arcuate chains extending up to 20 km long (de Silva and Lindsay, 2015). Growth of a lava dome can be episodic or steady, with eruption durations ranging

from hours to decades. Lava types expelled from domes may range from basaltic eruptions (cf. Semeru 1946), to rhyolitic eruptions (cf. Chaitén 2010), but the majority are composed of intermediate lavas that are andesitic to dacitic (Calder et al. 2015).

Dome dimensions may vary from metres to kilometres in diameter and hundreds of metres in height, and present as steep sided, circular, elliptical, irregular and uniform landforms. The morphological characteristic of a dome is linked to high viscosity magmas that form them, and the extrusion rate is generally responsible for the shape of a lava dome (Huppert et al. 1982).

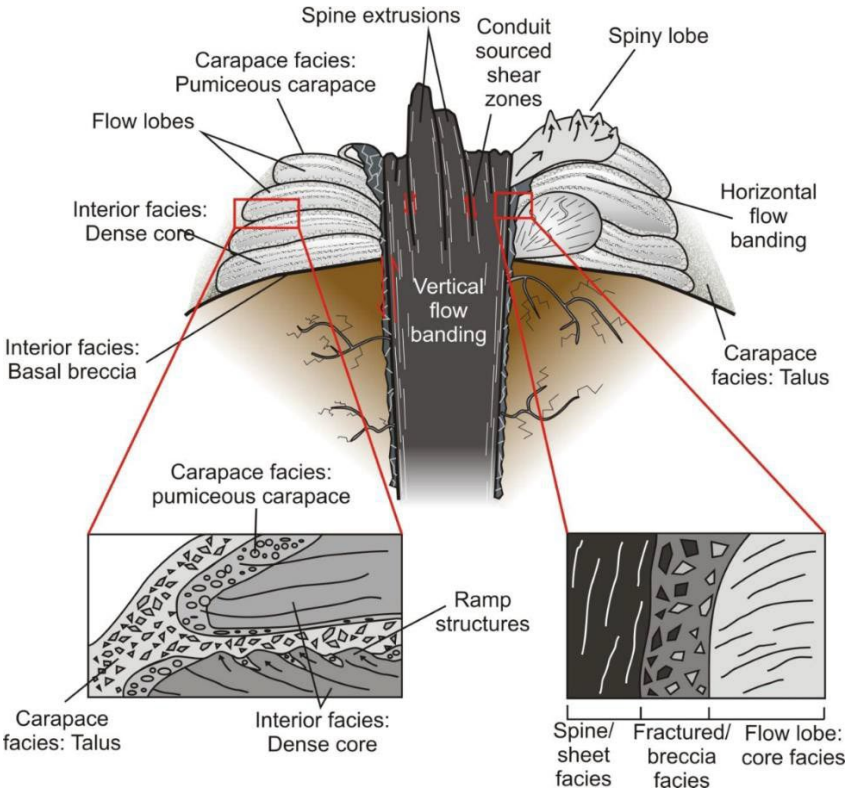

Figure 3.5: Hypothetical lava dome structure consisting of lobes (spiny and flow), carapace features and internal structures (from Ashwell, 2014, reproduced with permission).

Lava domes comprise an inner core and an outer rock carapace, with a brecciated talus situated to the side (Figure 3.5). Deformation and flow variations within each rock typically determine what aspect of a lava flow forms the core, the carapace, and the talus (Ashwell, 2014). The core deforms in a ductile fashion, whereas the carapace often fails by brittle fracture, and the talus is composed of brittle fragmented blocks. The extrusion of a low-viscosity dome can shape a very smooth surface, though it is usually a temporary feature. Eruptive stress, degassing, and thermal contraction enhance the brittle deformation of the lava, inducing further brecciation and occasionally columnar-like jointing (Sparks, 1997). During the eruption of a lava dome, clastic and brecciated components increase to greater than 50 vol% of the erupted products, and nearly 100 % of the total volume upon cooling (Sparks, 1997).

Flow banding is an internal lava dome structure directly linked to the method of extrusion that occurs. Features such as flow banding and fractures are used to reconstruct the morphology of eroded or exposed domes (Ashwell et al. 2013). Flow banding is created as a result of viscous flow during lava ascent within the conduit, and lesser so during dome growth. Looking at exposed lava bodies, flow banding is associated with the modal distribution of crystals that form the rock (Jerram et al. 2018). A viscous flow creates shearing between conduit walls and the free moving material already present. The shear will elongate and flatten air bubbles within, as well as align phenocrysts and microlites into the thin banded features (Ashwell et al. 2013). Flow banding can be used in exposed areas to determine the direction of the lava flow, and the dip in such places is commonly high. Flow folding may cause large ranges in dip, however strike is expected to remain similar to pre-folded lavas under the assumption that folding was stalling the flow of dome slopes. Thin banding can therefore help to reconstruct the structure of a lava dome, including the shape or location of the conduit (Ashwell et al. 2013). Flow bands typically present horizontally on a dip away from its origin vent, if the magma had moved down a steeper slope. Lava flows may demonstrate complex flow folding, which is a result of variations in localised flow conditions or from viscosity variations (Ashwell et al. 2013).

The carapace of lava domes are made up of blocks varying from millimetres up to 5 metres. The placement of these blocks can seem random but are a reflection of the eruption processes, with average block size decreasing with distance from the vent (de Silva and Lindsay, 2015). Blocks are more abundant where a lava flow has had a low extrusion rate, which results in less intense fragmentation, forming larger blocks in the area. Most blocks will form in the vent region, however some may be produced downslope through fracturing linked to compressional folding or crease structure formation. The blocks found within lava dome surfaces often show a spectrum of glassy and vesicular textures which can develop at different flow depths (de Silva and Lindsay, 2015).

Surface geomorphological features of lava domes include compressional ridges and crease structures. Domes have a complex stratigraphy with changing textures. Rhyolitic extrusions generally have a surface layer of finely vesicular pumice, with a zone of obsidian underneath, followed by coarsely vesicular pumice where volatiles from the flow may accumulate between the first two layers (de Silva and Lindsay, 2015). These features can then deform into fold and compressional ridges as a result of flow surface compression. Surface ridge formation is a response to compressional parallel flow during the movement of silicic lavas. For surface folds to occur, a viscous fluid is required to enhance stress and rheologic conditions (de Silva and Lindsay, 2015). Circumstances required for compressional ridges and crease structures are for the upper surface of the flow to have a higher viscosity than the interior, and for the compression to be high enough to overcome gravitational forces (Fink and Griffiths, 1998). If the contrasting viscosity is too high, the top lava flow will fracture instead of deforming in a ductile manner. Wavelengths within a crease structure are proportional to the thickness of the upper cooled carapace, while the ratio of wavelength to carapace is reliant on flow composition.

Flow surfaces may experience more than one folding episode (Fink and Griffiths, 1998). Crease structures develop where the lava flow can experience lateral spreading, where the flow moves across a flat surface or along a surface ridge crest perpendicular to the direction of maximum compression. These structures also vary in size, from 3 m, exceeding 250 m. In some instances, the entire surface of a lava dome may be a singular crease structure.

3.3.2 Dome Eruption Processes

Lava dome growth occurs passively for long periods, but there is also the potential to erupt explosively, due to the intermittent build-up of gas, or produce pyroclastic flows resulting from gravitational dome collapse, exposing the pressurised magma beneath (Sparks, 1997).

Mild eruptions, such as ash venting, are a common form of activity that lasts seconds and comes from concentric fissures or vents close to the dome source (Calder et al. 2015). This centrality to the centre implies that the dome remains mostly intact and the degassing process is simultaneous with ongoing magma extrusion; this process is sustainable within lava domes for months to years, as it occurs in the shallow plumbing fracture systems. Vulcanian or plinian eruption events commonly involve the removal of large amounts of dome material. In many cases, explosive events access hotter and more gas-rich magmas lower in the conduit, but the magmas are only partially crystal-bearing. Vulcanian and plinian styles result in moderate to substantial lithic and pumice-laden eruption plumes, which can reach a height of about 15 km (cf. Soufriere Hills; Calder et al. 2015). These large explosive events can create column or fountain collapse pyroclastic flows, reaching several kilometres radially around the volcano. The deposits from pyroclastic flows may be abundant in pumice, referred to as ignimbrites. Deposits from explosive eruptions are likely to be a poorly sorted mixture of pumice and lithic lapilli with a matrix of vitric shards and crystal fragments, while the pyroclastic flow deposits can be loose and uncompact, or partly welded.

3.3.3 Lava Dome Collapse

Dome instability can often be a precursor to collapse. A sign of instability can be rockfalls, which form small, end-member collapse phenomena from lava domes and can occur frequently. Sections can collapse along high-angle failure planes on outer, mostly degassed lava dome carapaces and may involve blocks that roll, bounce, or slide downhill (Calder et al. 2015). There are several potential mechanisms for dome collapse, including gravitational collapse because of over steepening, internal gas overpressures, interaction with intense rainfall, change in extrusive direction, topography beneath

the dome, the fracture state of the dome and large scale local tectonic faulting and hydrothermal alteration (Voight, 2000).

Secondary mineral formation, such as hydrous silica, could increase internal pressure of lava domes by reducing gas permeability, provoking collapse through explosive decompression. Dome morphology will also play a significant role in a dome's overall stability (Harnett and Heap, 2021). Collapses from an actively extruding recent lava dome are frequent during eruptive phases, but those that occur from post- emplacement dome weakening by hydrothermal alteration are moderately infrequent and harder to anticipate (Ball et al. 2015).

Pyroclastic flows and lava dome collapse are often linked, and deposits are recognised as block and ash flows as they comprise dense blocks of fragmented lava within an ash matrix. Pyroclastic density currents are formed when lava domes produce energetic flow pulses during collapse, forming turbulent ash clouds and dense basal avalanches (Calder et al. 2015). Pyroclastic density currents typically form low profile sheets and fans, which can cover areas as large as 45,000 km^2 and tend to bury landscapes of pre-eruption topography; marked thickness is noted in topographic depressions. On occasion, mild lava dome eruption styles may be linked to collapsing plumes, which result in thin pyroclastic deposits dominated by fine ash (Calder et al. 2015).

3.3.4 Lava Dome Textures

Typically, rhyolite lavas and lava domes have characteristic porphyritic textures, and not all phenocrysts are euhedral (Allen and McPhie, 2003). From a homogenous lava, a texture is likely to be evenly distributed with euhedral phenocrysts in either a flow banded or massive groundmass which is typical of an effusive eruption style (Allen and McPhie, 2003). Phenocrysts crystallise within the melt before an eruption has occurred, whereas antecrysts are inherited from crystal rich ‘mush’ that was leftover from prior eruptions (Higgins, 1996). The crystals within a groundmass, such as microlites, could be a product of the current eruptive crystallisation, or from accompanying slow cooling as a result of high temperatures during or after the emplacement of the lava (Lofgren, 1971; Swanson et al. 1989). These groundmass crystals can include spherulites, micropoikilitic textures and granophyric textures (Lofgren, 1971).

3.3.5 Alteration Textures

Hydrothermal alteration is a type of diagenesis that causes physical and chemical changes, therefore changing mineralogy and texture within a rock (Fisher and Schmincke, 1984). Volcanic glass is often altered to more stable phases, such as smectites, kaolinite or alunite (Cerling et al. 1985). Clay rich alteration minerals have low strength and have the capacity to absorb and channel groundwater, which will locally increase fluid pore pressure (Ball et al. 2015). Low temperature alteration of volcanic glass

can involve ion exchange, hydration, or an oxygen and hydrogen isotope exchange (Cerling et al. 1985). If volcanic glass has high water content, the texture is usually perlitic, where there are a network of hydrated and arcuate cracks which have been made during the cooling phase. Perlites in an altered rock may create interconnected cracks, leading to rehydration or dehydration (Marshall, 1961). Spherulites may be found surrounded by cracks, which are similar to fractures resulting from bubble growth (Romano et al. 1996). Spherulites are typically composed of radiating crystal fibres, where each fibre is a singular crystal that has a minorly different crystallographic orientation from the adjacent crystals (McPhie et al. 1993). In silicic igneous rocks that have been formerly glassy, the glass may then alter to alkali feldspars, or quartz, to form spherulites. They are not spherical throughout the growth process, and tend to consist of open clusters of widely spaced crystal fibres (McPhie et al. 1993).

Interaction with geothermal fluids are responsible for producing post-depositional hydrothermal alteration in the host rocks. Circulating hydrothermal fluids produce three-dimensional zones which are characterised by discrete mineral assemblages (Shanks et al. 2005).

Chapter Four

Field Geology

4.1 Introduction

This section introduces the three field areas of Pukunui, Maungatūtū /Mount Misery and Greenpark, as well as the Pukunui pyroclastic succession. It outlines the rock units found at each location, with field descriptions, relevant maps and field images.

4.2 Pukunui

4.2.1 Introduction

Pukunui is a lava dome located on Kaitemako Road, in Welcome Bay. It is currently a J Swap quarry which was purchased in 1984, and has historically been two separate quarries on the site. The Pukunui dome was split into upper and lower zones by the quarry owners, with the base rock noted as being volcanic dacite. This area includes both the Pukunui rhyolite dome and the Otawa andesite which have both been quarried for different purposes. The upper quarry supplied over one million tons of structural fill for the Tauranga PJK toll road (J Swap Contractors Ltd, 2022).

The Pukunui lava dome has been quarried and there was an exposed area at the top, which showed the different textures within the Pukunui rhyolite. The ignimbrite and interbedded ash succession attached to the side of Pukunui may be correlated to an ignimbrite of the Papamoa Formation, and so a stratigraphic log was an important part of the field geology work.

Figure 4.1: Pukunui field area showing the Otawa andesite, Otawera ignimbrite and Pukunui rhyolite. Otawa is shown as 1, the rhyolite is listed as 2 – 4, and the Otawera ignimbrite is 5 – 7 (base image sourced from Google Earth).

4.2.2 Otawa Andesite

The Otawa andesite is the remains of an ancient strato-volcano, and has been quarried at lower elevations (Figure 4.1, stop 1). The andesite outcrop here had platy and columnar jointing. Texturally, the andesite is porphyritic, with large visible crystals predominantly plagioclase, and minor pyroxenes.

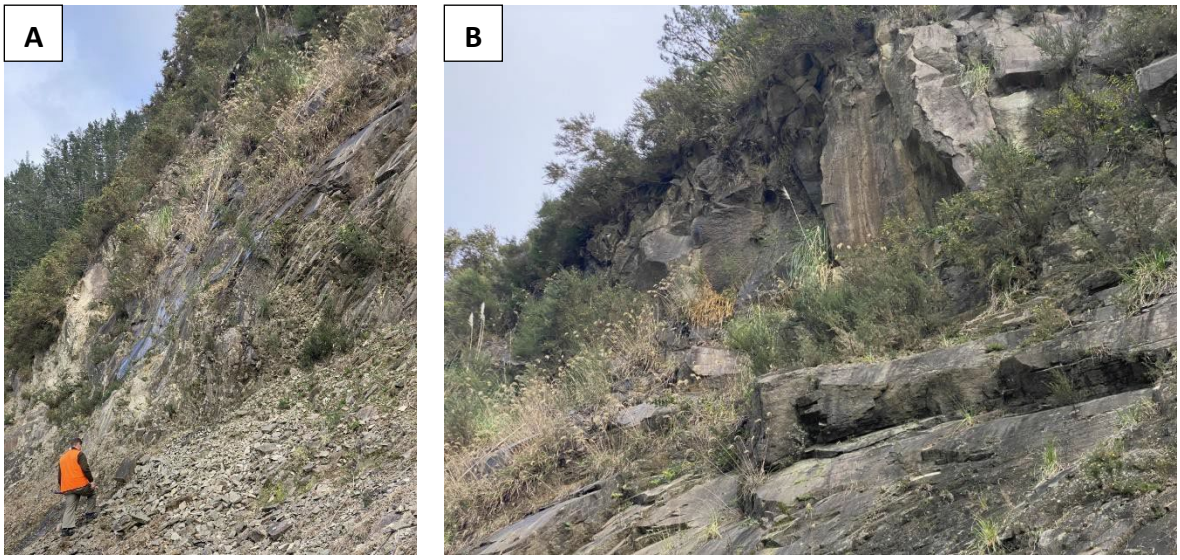

Figure 4.2: Otawa Andesite face (A) showing platy jointing, and a closer image (B) showing columnar jointing higher up the face.

4.2.3 Pukunui Rhyolite Dome

At higher levels of the quarry (Figure 4.1, stop 2 – 4), there was a voluminous rhyolite deposit that had a massive appearance. Flow banding was a major feature, and the frequent jointing was the reason the quarry face was very unstable. The jointing appeared to be blocky, and most rocks in the outcrop were orange, likely due to exposure and weathering.

The rhyolite structure varied spatially from massive, to thin banded (Figure 4.3B), to coarse banded (Figure 4.3C), and coarse zones that had been infilled as a result of weathering. There was a brown vertical to diagonal unconformity visible which was soft and crumbly (Figure 4.3A), clearly an altered rhyolite but very unstable. Certain faces in the outcrop had obvious crumble zones due to folding.

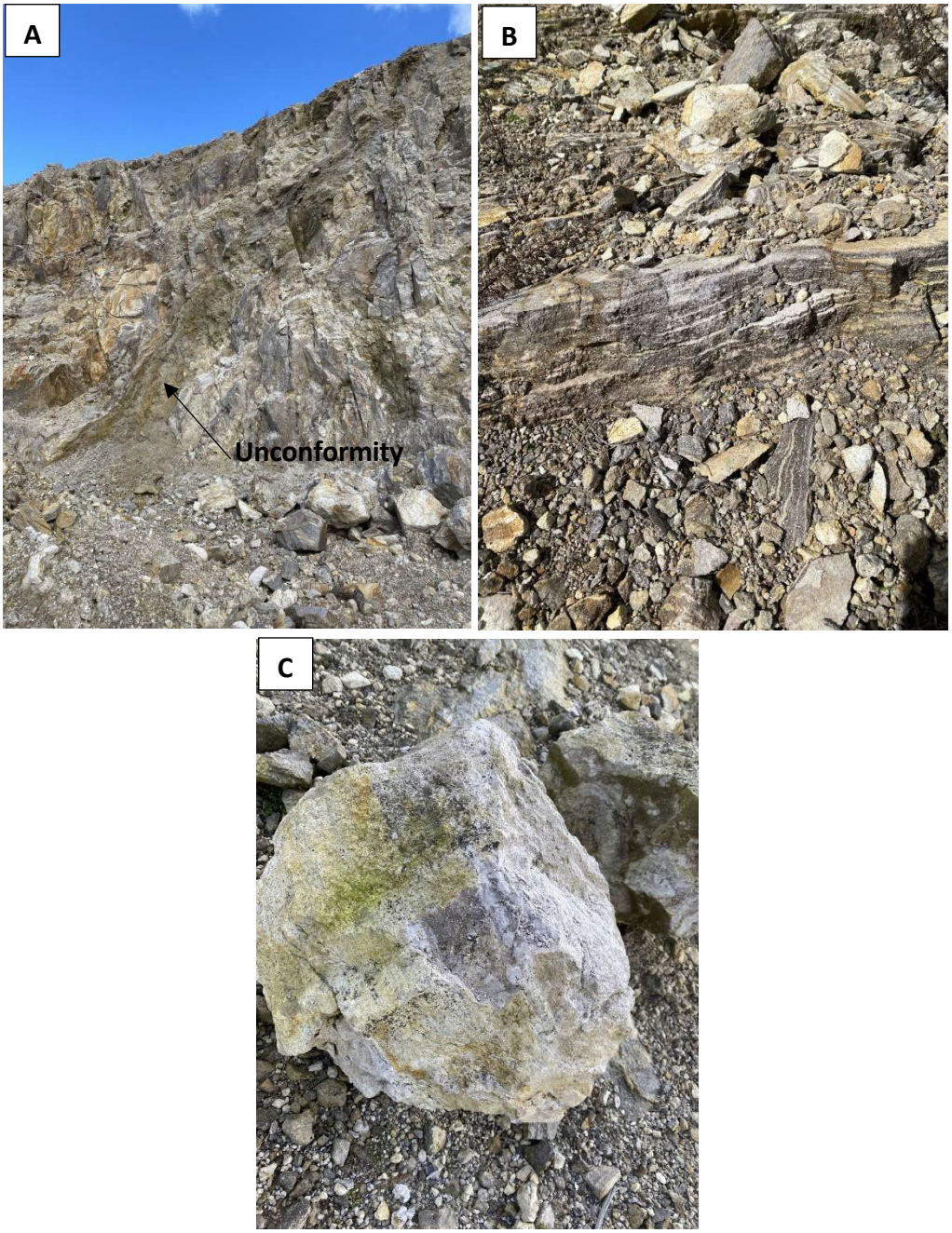

Figure 4.3: Features of the Pukunui Rhyolite, (A) brown vertical/diagonal unconformity, (B) thin banded rhyolite, and (C) block from a coarse banded rhyolite.

4.2.4 Pyroclastic Succession

A succession of pyroclastic units, including ignimbrite was exposed on the northern side of the lava dome. The outcrop was comprised of a soft and friable rock face, and pumice clasts. There were three flow units that held large andesitic clasts. There were two exposed areas of this pyroclastic succession that were studied, and the succession was divided into six units (A – F), shown in Figure 4.5.

Unit A was a matrix supported lithic-rich ignimbrite, and occurred at the base of the succession. It was at least 1.5 m thick, however the base was not exposed. There were andesite lithics present, up to 15 cm

in length with an average length of 9.6 cm. Pumice average size was <1.5 cm and the maximum pumice size was 5 cm. The pumice clasts had a moderately vesicular, woody texture (fibrous).

The lower 0.9 m was massive, while the upper 0.6 m was reversely graded changing to normally graded. This upper zone had large lithics up to a maximum size of 35 cm, which appeared to be a variety of rhyolites and andesites.

Unit B was an ash layer ~ 0.5 m thick and a well sorted fall deposit, with normal graded coarse to fine ash. It was crystal rich, with 1 – 2 cm sized pumice present in the lower part of the layer. Mafic minerals were concentrated in the bottom of the ash layer.

Unit C was a massive, fine grained layer ~ 5 cm thick with grain sizes <2 mm.

Unit D was a possible fine-grained ignimbrite ~ 20 cm thick, appearing as a massive, fine to coarse ash and visibly crystal rich. Accretionary lapilli were present in the upper 15 cm and were 2-10 mm in size, and this layer was right below the flow boundary.

Unit E was ~ 10 m thick. In the lower 4 m of the unit, there was small lithics with a maximum size of 7 cm, and an average size of 3 - 4 cm. The pumice present in this layer was up to 1 cm in size. The upper 6 m of the unit was massive, coarse grained, and case hardened, with slight to moderate welding. There was sub-vertical jointing through the centre, with a large, undulating sub-horizontal crack representing the flow unit boundary. The dip was 60°W, and lithics were visible in the upper half, but couldn't be measured as it was too high to reach.

Unit F was a bedded ignimbrite, white to beige in colour and ~ 4 m thick. There were slight changes in the ignimbrite texture within unit F, implying changes during the eruption. The lower layer was a continuous ignimbrite bed of massive coarse ash, 3 m thick. The layer above the lower unit was a 30 cm thick massive ignimbrite. The contact between the 3 m unit and the 30 cm unit was sharp and straight. Above this, there was a 40 cm thick, fine, laminated zone likely as a result of a fine/coarse ash fall. The next layer was 20 cm thick, with ~ 5% lithic content with small pumice. There were pumice lenses present that were clast-supported in this layer. The 10 – 15 cm of the unit above the 3 m bed was 20% pumice that was 0.5 – 1 cm on average, and poorly sorted.

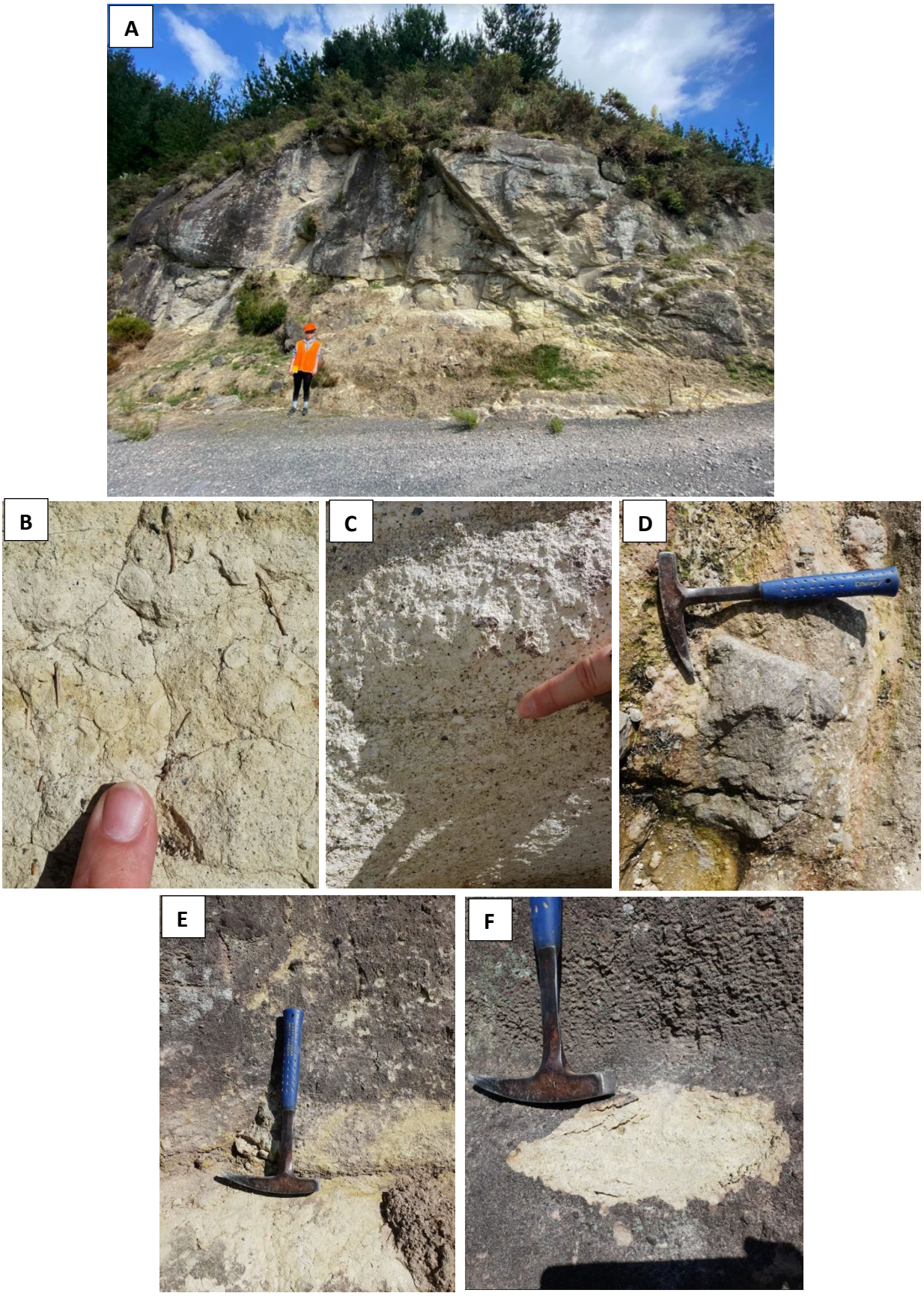

Figure 4.4: Field geology images showing textures and stratigraphy of the Pukunui pyroclastic succession. (A) lower ignimbrite succession face. (B) accretionary lapilli in unit D. (C) Unit F upper layer showing poor sorting and coarse-grained pumice. (D) Large andesite lithic in the lower half of unit A. (E) Upper 0.6 m of unit A. (F) Unit C, fine grained ignimbrite layer.

4.2.5 Stratigraphic Log

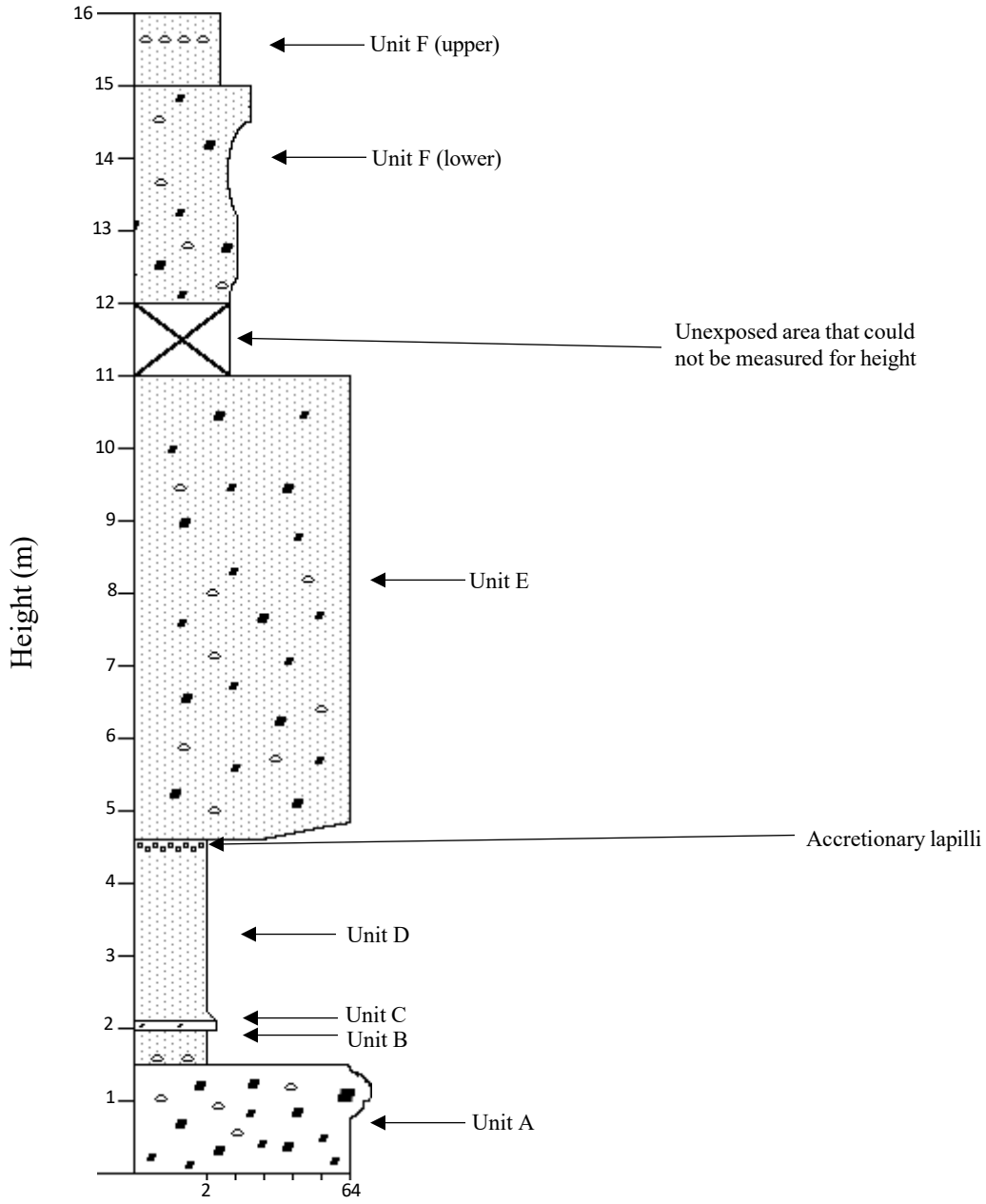

Figure 4.5: Stratigraphic log showing the ignimbrite succession on the northern flank of the Pukunui Rhyolite, as described in section 3.1.4.

4.3 Maungatūtū /Mount Misery

4.3.1 Introduction

This section describes the location, field and outcrop characteristics of the rhyolite present at the Maungatūtū/Mount Misery lava dome. The lava dome forms a 478 m hill situated 10 km south of Tauranga, at the head of Mangarewarewa Stream and Kirikiri Stream. Beaconed trig A4JL is located at its summit. Historically, Maungatūtū/Mount Misery was unsuccessfully used to run sheep and cattle due to bush sickness, before cobalt supplementation was discovered (Tauranga Historical Society, 1972).

Today, Maungatūtū /Mount Misery is farmland, used for beef and sheep. The geomorphology is rolling to steep hills and most outcrops have minimal exposure, causing access to be limited. All small outcrops were extremely weathered. Seven stops, denoted in Figure 4.6, were made to assess the rhyolite in this field area.

Figure 4.6: Maungatūtū /Mount Misery field area, with stops 1-7 listed (base image sourced from Google Earth).

4.3.2 Rhyolite variations

At the southern end of Maungatūtū/Mount Misery (Figure 4.6, stop 1), at the end of the spur, the exposed rhyolite was ~ 3.8 m thick, including the upper 0.9 – 1 m of soil. The rhyolite was grey to purple in colour, with white phenocrysts and orangey-black mottles (Figure 4.7B). The phenocrysts visible were 1 – 5 mm in size, and comprised 10 – 15% of the bulk rock. This rhyolite had a massive appearance and lacked jointing.

A short distance uphill, there was a rhyolite outcrop which had ~ 7 m exposure from ground level. There was visible layering within the rhyolite, ranging from 10 – 50 cm wide. Joints and fractures were also visible, from 1 – 1.2 m wide.

At the third stop there was a smooth large outcrop, which was a round slab of rhyolite located next to a farm track, downslope from the first two stops. In this outcrop, there was less visible fracturing and layering. The top side of this rhyolite had a texture similar to breccia or as a result of weathering. There were round, knobbly intrusions and some of these had bread-crust fracturing internally (Figure 4.7F).

Near the summit (stops 4 – 7), were rhyolite outcrops with large fractures (Figure 4.7C).

The last stop of this field area was to an outcrop on Rowe Road that had been previously looked at as a rhyolite face in older research. The outcrop appeared massive, with similar characteristics to the Mount Misery rhyolites such as a pale purple colour and orange mottles.

4.3.3 Tephra- paleosol succession mantling the rhyolite dome

The rhyolite seen at the second stop had a soil layer on top. The soil layer was 1.3 m thick, of bedded tephra above the exposed rhyolite, comprising seven layers (Figure 4.7E). From bottom to top, there was an orange clay paleosol; a cream clay or fine ash; very coarse yellow/orange sand with pumice that had crystals and lithics present, which was well sorted; a grey/brown thick coarse sand; a light orange/brown silty soil, interbedded with lenses made of fine sand; a very coarse sand with pumice between the contact and sand; and a silt layer. All contacts between the tephra units were sharp and planar.

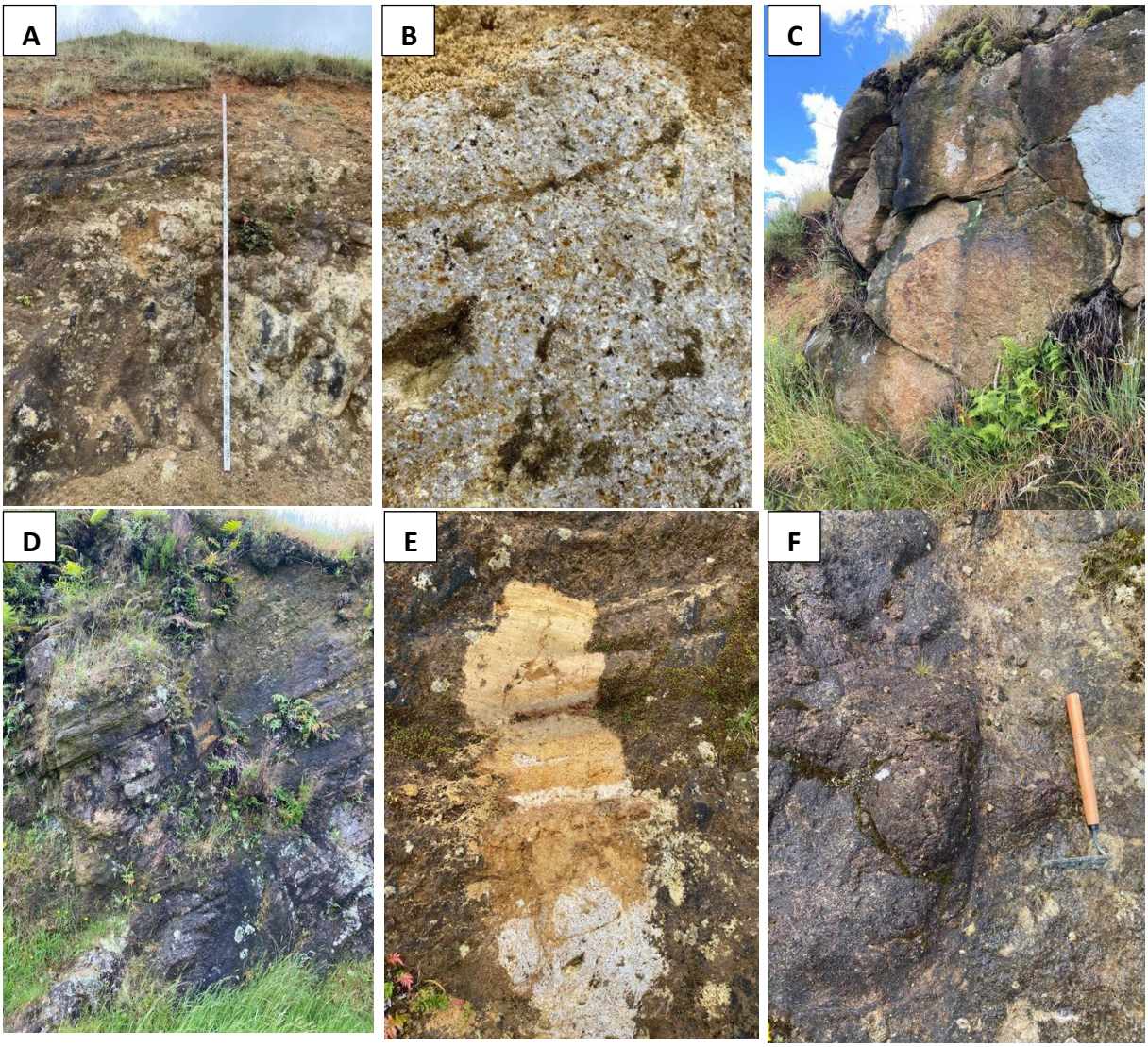

Figure 4.7: Photos of the Maungatūtū/Mount Misery rhyolites. (A) Stop 1 massive rhyolite. (B) close up of stop 1 rhyolite showing orange motley texture and purple colouring. (C) fractured rhyolite from stop 5. (D) rhyolite at the top of Maungatūtū/Mount Misery. (E) tephra sequence at stop 1 that rested above the rhyolite. (F) autobreccia rhyolite found at stop 3.

4.4 Greenpark

4.4.1 Introduction

This section describes the Greenpark rhyolite found at the Oropi Quarry. The quarry was established in 1956, with the purpose of supplying aggregate for new Tauranga subdivisions and infrastructure. Based on Oropi Road, the quarry provides speciality rocks, base rock, metal aggregate or drainage metal depending on requirements (RPL Services, 2022).

The eastern side of the quarry has been classified as dark-coloured ‘andesite’, whereas on the western side the light-coloured rock has been described as a rhyolite. Samples were taken from all parts to compare and determine what it is. Examination of the quarry began at the lowest level of exposure, on the ground of the quarry close to the main buildings. Most aspects of the rhyolite were visible here and had been recently blasted, so it was relatively unaltered and good for taking hand samples.

Figure 4.8: Greenpark quarry as seen from above, showing the location of each stop 1 - 6 (base image sourced from Google Earth).

Figure 4.9: Greenpark Quarry showing a light-coloured rhyolite on the left hand side and a darker rhyolite on the right hand side, which has been previously classified as andesite.

4.4.2 Rhyolite descriptions

Near the base of the quarry on the western side (stop 1), the rhyolite was a >3 m face with thin banding and light grey in colour. Strike and dip of flow banding was 075/35°N, which was consistent across the outcrop with only slight variations. Flow banding ranged from 0.5 – 2 cm to 2 – 10 cm in thickness. The banding was generally linear, although some folds were visible within bands. Above 4 m from the base, the banding alternated between dark, porphyritic, glassy, to white crystalline bands. Lithics were observed throughout this outcrop.

At stop 2 (Figure 4.11A) above 4 m from the base, convoluted and irregular banding was visible. At about 4 – 10m above base, on the western side (stop 2), two rhyolite facies are defined. There were thin banded zones (Figure 4.11B) and coarse banded zones that were predominantly linear with flow folding present. The bands in the thin zones ranged from 2 mm to 2 cm thick and were dark grey and glassy, but alternated between grey and purple in colour. Intercalated between the thin zones were internally massive bands ranging from 10 – 25 cm thick. Banding patterns were irregular; strike and dip of flow banding here was 040/30°NW laterally across the outcrop to the north (stop 3). There were darker banded areas that appeared to be broken into a breccia, with some parts still intact. Visually it is a chaotic zone, likely an auto breccia (Figure 4.11C).

Near the top of the quarry (stop 4) the rhyolite showed tabular jointing that measured 3 m wide, 1 m deep and 2 + m high. Jointing was massive and columnar. Thin banding ranged from 2 mm to 2 cm and alternated between light and dark in colour. The flow banding was linear, with few folds.

Further west on the upper level of the quarry (stop 5), the outcrop varied from flow banded on the lower east side to thick-banded and massive on the upper west side. The east side was oriented 085/32°S whereas the west orientation was 120/32°SW. The two areas were split by a large fracture (Figure 4.10), where the lower east side features were tabular jointing and thin banding, compared to the upper east which was mostly massive and darker in colour.

On the upper eastern side of the quarry (stop 6), there was a massive 15+ m outcrop (Figure 4.12A). Almost linear flow banding was observed, with flow folding present (Figure 4.12B). The face was dark purple to grey on the surface. There was curvy planar jointing, almost columnar with some bends. Strike and dip of the flow banding was 018/16°E.

Figure 4.10: Panoramic photograph of stop 5, showing the textural differences between the lower east (left hand side) and upper west (right hand side) rhyolites.

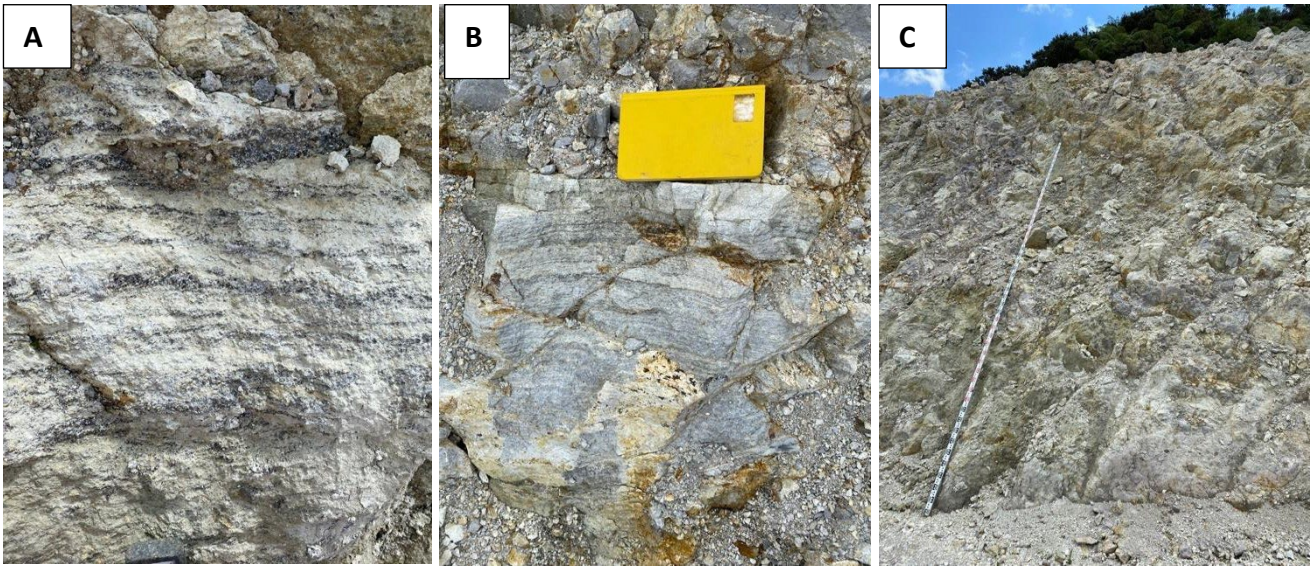

Figure 4.11: Photos of the Greenpark rhyolite type and textures. (A) coarse banded rhyolite. (B) thin banded rhyolite. (C) chaotic autobreccia zone.

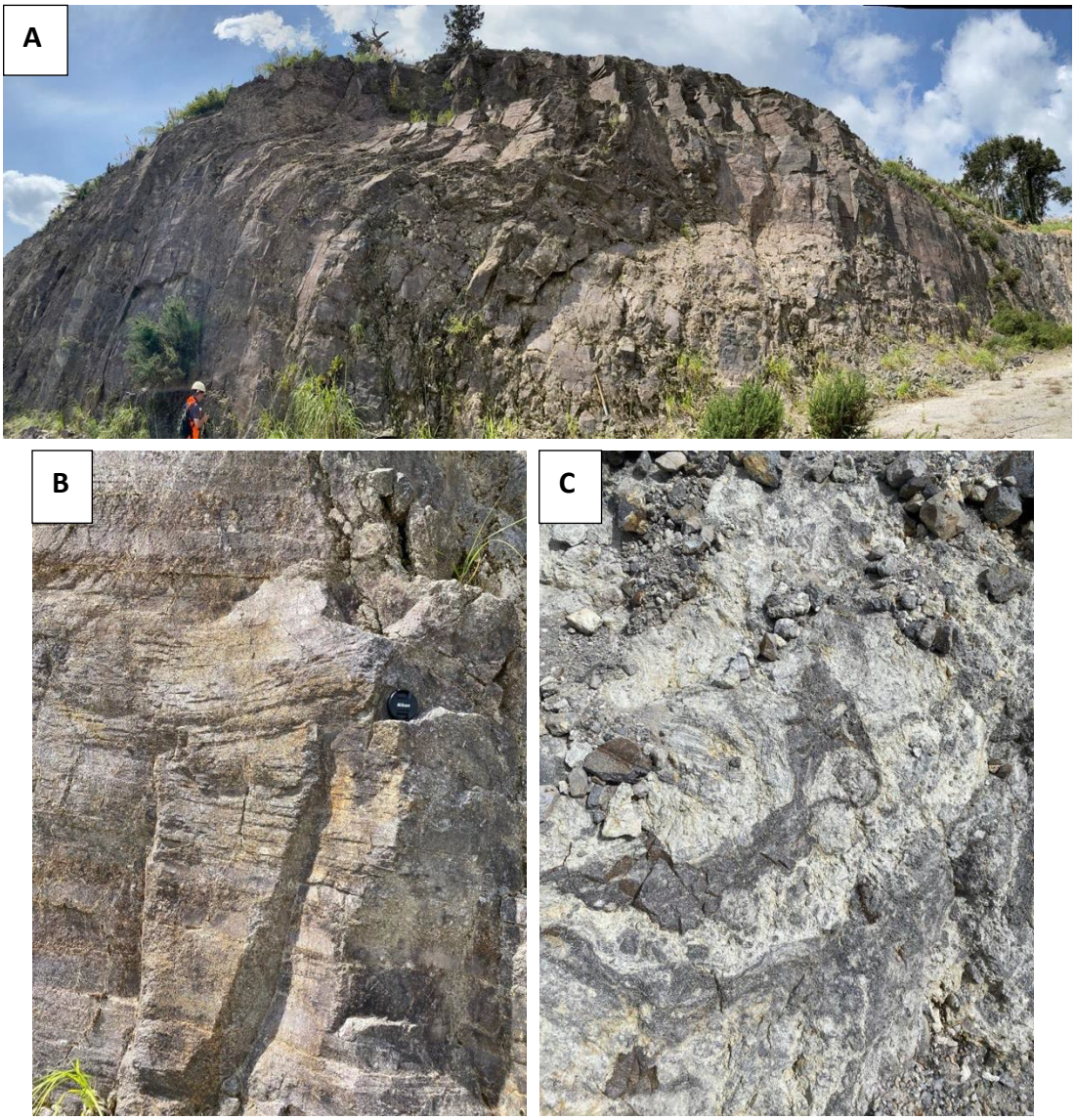

Figure 4.12: Photographs of the Greenpark rhyolites showing features of the west side of the quarry, (A) panoramic image of stop 6 showing the flow folding. (B) darker texture and semi linear flow banding of stop 6 darker coloured rhyolite. (C) Lighter coloured rhyolite from western side for comparison to the darker eastern rhyolite.

Chapter 5
Petrography

5.1 Introduction

This chapter outlines methods used and presents the results for the petrographic analysis of the Mount Misery series rhyolites and the Pukunui pyroclastic succession. Methods used were thin section microscopy, X-ray diffraction analysis (XRD) and semi-quantitative Scanning Electron Microscopy (SEM-EDS). The methods were chosen as they would provide the greatest amount of insight to secondary alteration and general textures relative to each lava type.

5.2 Thin Section Microscopy

A total of 42 thin sections with cover slips were made for analysis under the optical microscope, and 11 more were polished to use under the SEM, to provide a greater understanding through petrographic microscopy. Pukunui had 9 thin sections made, Maungatūtū/Mount Misery had 6, Greenpark had 12, the Pukunui pyroclastic succession had 13, and 2 additional pumice samples were cut from the Otawera ignimbrite. The microscopic petrography laid a foundation for following testing, to determine the best samples to look further into.

The rhyolite samples from the Mount Misery group lavas were all non-vesicular with porphyritic textures. Phenocrysts were set in a fine-grained groundmass, primarily composed of devitrified glass. Some samples showed flow banding, and many had large areas that were affected by weathering or alteration.

5.2.1 Pukunui Rhyolite

Eight samples from which nine different thin sections were cut, were examined under the optical microscope. Samples being analysed included weathered rhyolite, thin-banded rhyolite, coarse-banded rhyolite and altered rhyolite. Most samples had similar mineral compositions, and key features were the mineral types present as well as their sizes, as seen in Figures 5.1 - 5.5. Most thin section samples for Pukunui featured brown to yellow domains, which often appeared to be central to flow banding, which would wrap around them. The main features consisted of thin banding, medium-sized euhedral plagioclase, and few smaller quartz phenocrysts, and feldspar minerals (Figure 5.6).

Plagioclase

Plagioclase was the most common mineral observed in the Pukunui rhyolites (Figure 5.1), making up >50% of the phenocrysts in each sample. The average size of plagioclase phenocrysts within the Pukunui samples was 0.4 – 0.8 mm, with the maximum size range being 1.3 – 1.7 mm. Recurring features were simple and oscillatory twinning, in typically euhedral to subhedral plagioclase. Few samples showed oscillatory zoning in a radiating pattern. Most phenocrysts tended to appear altered, with sieving textures and occasional melt inclusions.

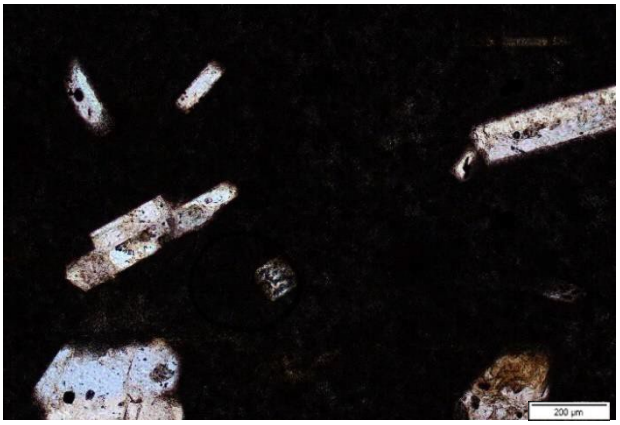

Figure 5.1: Plagioclase phenocrysts observed under the petrographic microscope under XPL, showing relatively small sizes and euhedral shapes.

Quartz

Quartz phenocrysts range from euhedral to anhedral, with an average size of 0.8 mm (Figure 5.2). Quartz appeared to be the mineral that forms the veins that are frequently seen throughout the Pukunui lavas, as the veins tend to have straight extinction angles with a white birefringence. Features shown in quartz and quartz polymorphs were small embayments and melt inclusions.

Quartz polymorphs

Quartz polymorphs such as cristobalite or tridymite were frequent in the groundmass, as quartz present in an altered form. The quartz polymorphs appeared to form some the altered flow bands and veins.

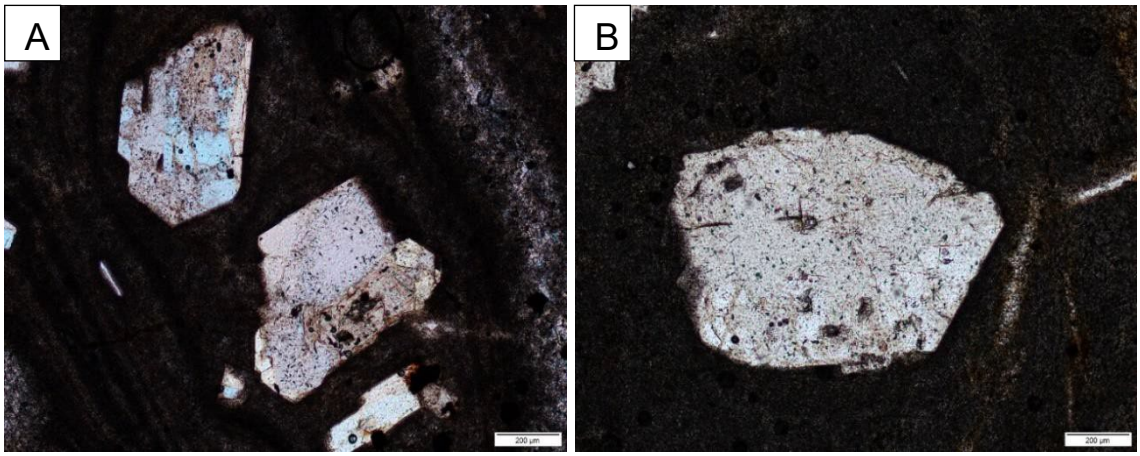

Figure 5.2: Quartz phenocrysts from the Pukunui rhyolites under XPL Note small embayments in (A) and the euhedral to subhedral shapes. (B) large intact quartz mineral.

Opaques

Opaque minerals were found in the brownish domain areas (Figure 5.3). Most were Fe-Ti oxides or altered mafic minerals, with an average size of 0.2 mm. Few phenocrysts, such as hornblende that were altered, contained opaques inside of them. In the more weathered Pukunui samples, there was an

abundance of opaque minerals as well as near-amorphous material, with typical shapes being anhedral to subhedral.

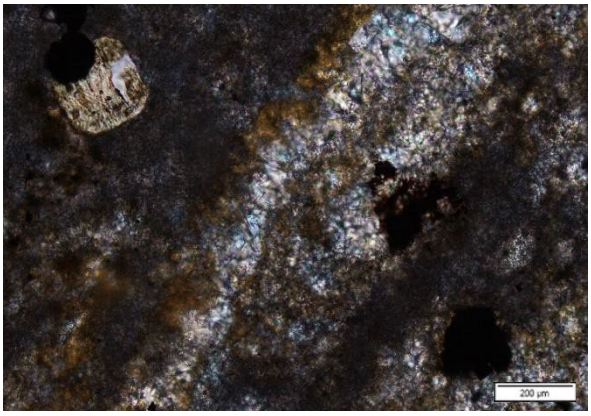

Figure 5.3: Opaque minerals observed under PPL. Notice the surrounding brown domains, and opaques that sit on top of other phenocrysts.

Hornblende

The few hornblende crystals found had microcrystalline seam alteration with opaque rims, and were mainly found in the brownish domains (Figure 5.4). They were euhedral to subhedral, and small in size, ranging from 0.1 to 0.4 mm and identifiable in more weathered areas.

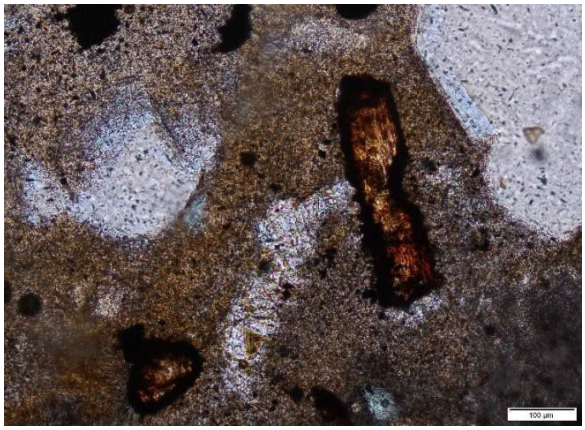

Figure 5.4: Hornblende phenocrysts within the Pukunui lavas under PPL.

Groundmass

Characteristics of the groundmass were consistent throughout each sample. Many featured flow banding, shown as light and dark alternating bands of which the majority were fine-grained. The flow bands wrapped around the phenocrysts with an irregular fluidal form, and were often cut through by a series of small quartz veins. Under the microscope, the thin bands were composed of alternating glass and devitrified glass. Few samples had a more fine-grained homogenous groundmass with less banding present, while others had abundant bands. Microlites were present as euhedral laths of feldspar, but typically each groundmass featured either silica quartz polymorphs or devitrified glass. In some samples, the groundmass was perlitic within flow bands whereas other bands appeared as quartz veins.

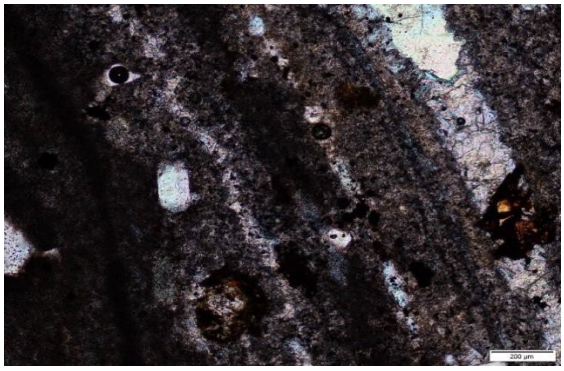

Figure 5.5: Groundmass textures of the Pukunui lavas under XPL, note the flow banding in both and the fine grained, devitrified microlite textures.

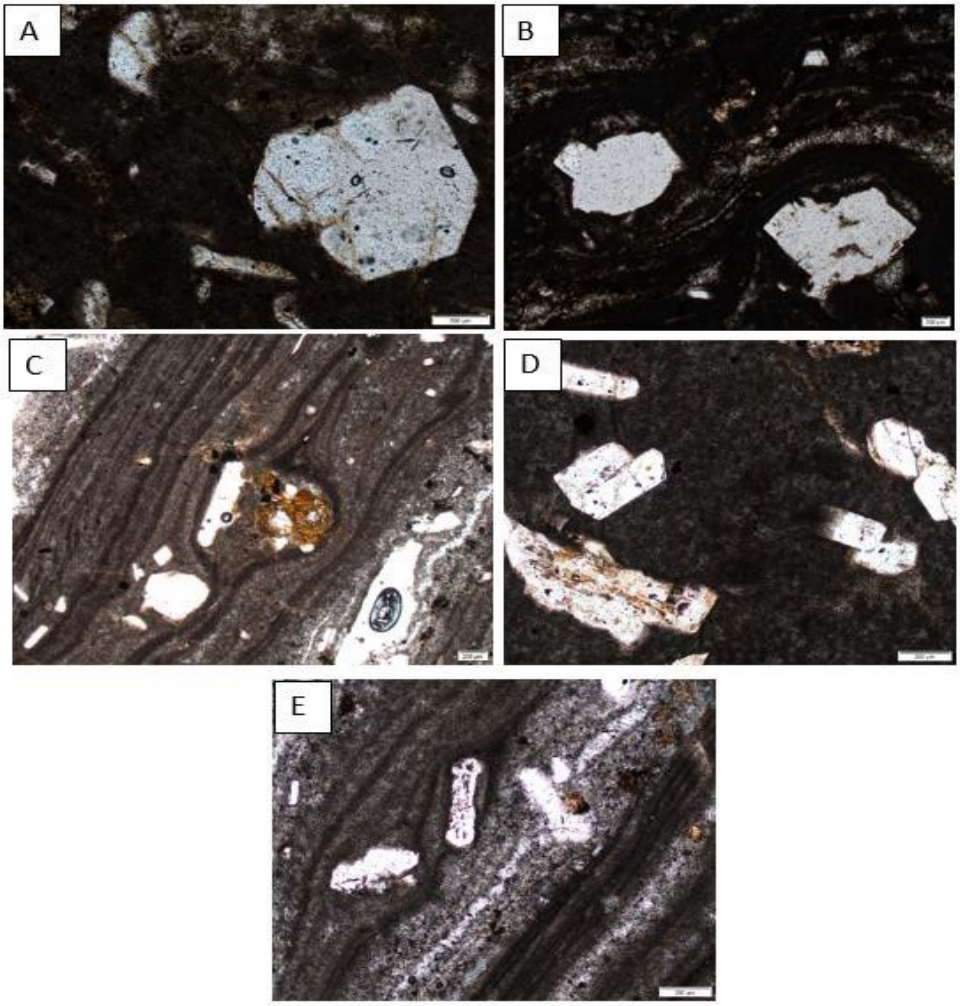

Figure 5.6: Features of the Pukunui rhyolites, including crystals and groundmass variations under plain polarized light. (A) Large plagioclase mineral. (B) Plagioclase minerals in a flow banded groundmass. (C) Thin banding groundmass surrounding plagioclase. (D) Smaller euhedral plagioclase phenocrysts. € Flow bands under PPL with phenocryst plagioclase inclusions.

5.2.2 Pyroclastic Succession on flank of Pukunui Dome

Of the 13 thin sections made from this succession, 2 were of lithics, and 11 bulk ignimbrite samples. In addition, two samples of pumice of the Otawera ignimbrite. The two lithics were plucked in the field and expected to be an andesite and a rhyolite, but thin section microscopy showed them to both be andesite. From the 11 bulk samples, most were welded ignimbrite, and two were ash. In the ash samples, all present minerals appeared generally smaller, less developed with plagioclase in high numbers and potentially micas or lithics. The ignimbrite thin sections featured large phenocrysts, some showing embayments and melt inclusions.

The Otawera pumice samples were cut to compare them to the pumice inside the ignimbrites from the Pukunui quarry, to identify similarities between the two. The pumice thin sections were mostly composed of large pumice, with small plagioclase phenocrysts throughout, as well as a crystal and glass-shard rich matrix.

Crystals of Ignimbrite and Ash

Pyroxene

Small and large pyroxenes were present in the majority of the ignimbrite samples, and were abundant throughout. These were mostly clinopyroxenes, rarely orthopyroxene and were euhedral to subhedral in shape. The clinopyroxene phenocrysts are a pale grey under PPL, and under XPL went extinct on inclined angles. The pyroxenes in the Pukunui pyroclastic succession are fragmented, on average ≤ 1 mm in size, reaching a maximum of 1.6 mm.

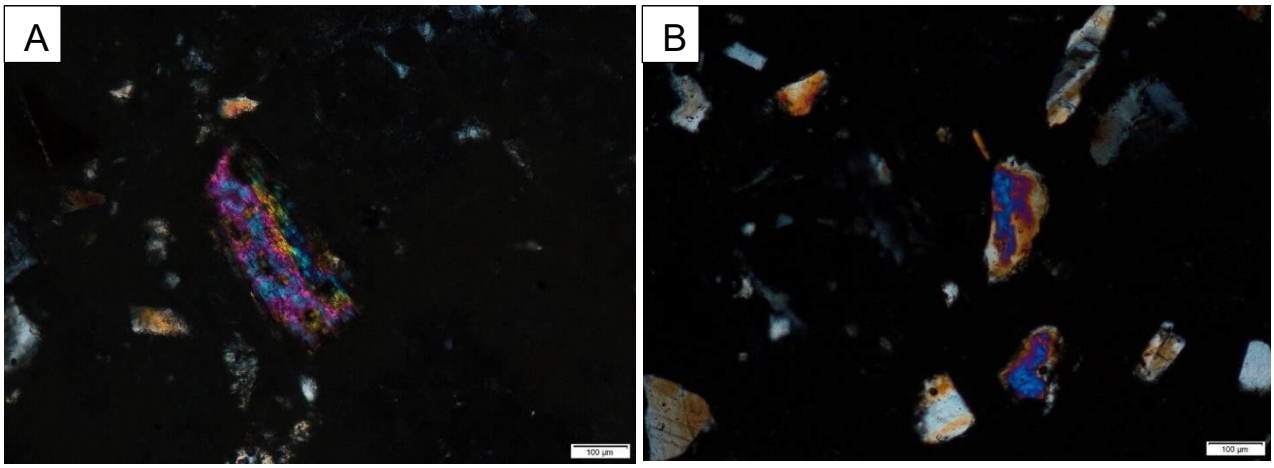

Figure 5.7: Pyroxene phenocrysts observed under the petrographic microscope in XPL. (A) a large pyroxene phenocryst surrounded by smaller plagioclase, (B) multiple pyroxene phenocrysts showing a variety of shapes.

Plagioclase

Plagioclase phenocrysts were highly abundant in the ignimbrite, ash and pumice samples. 1.5 mm was the maximum size of plagioclase phenocrysts found, but most were restricted to 0.2 – 0.5 mm on average. Most plagioclase showed strong simple twinning, and while some are fragmented, most show strong euhedral to subhedral shapes. The colour under XPL is a grey-white to beige colour, showing extinction angles as seen in Figure 5.8.

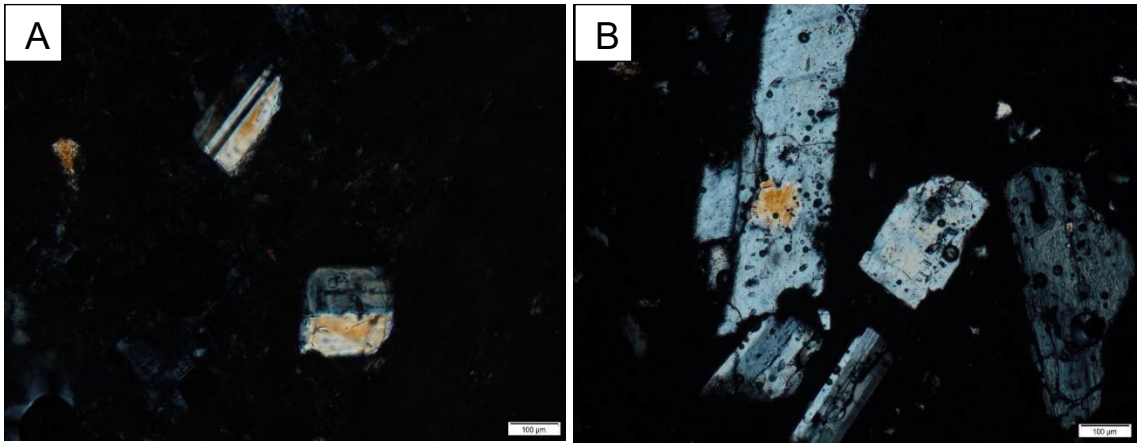

Figure 5.8: Plagioclase phenocrysts observed under the petrographic microscope, in XPL. (A) showing strong simple twinning and euhedral shapes, while (B) shows more subhedral varieties.

Opaques

From 0.1 mm to 0.5 mm, opaques were low in abundance and notably anhedral to subhedral in shape. The shape and colour of the opaques seen in the Pukunui ignimbrite show a similarity to those seen in the Pukunui lavas, which are also black and semi-circular.

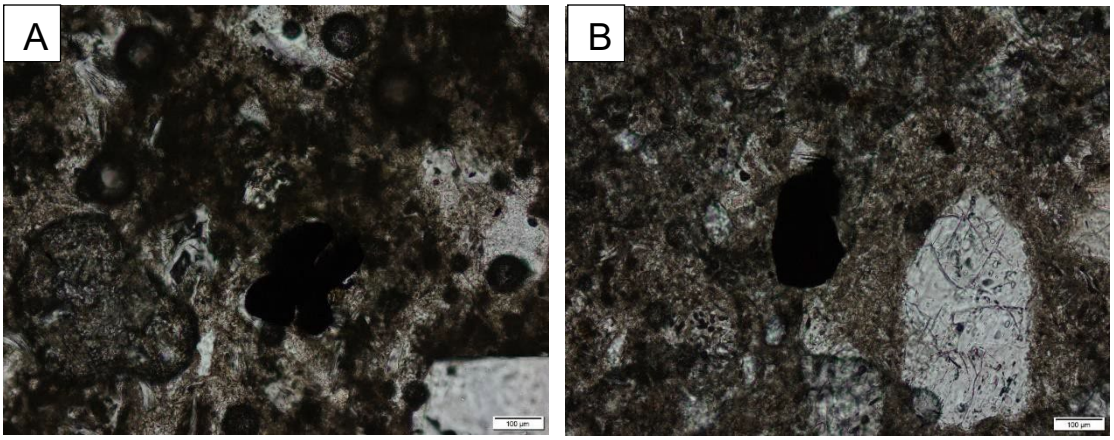

Figure 5.9: Opaque phenocrysts observed under the petrographic microscope in PPL. Note the dark black colour of both, and the slightly rounded shapes.

Hornblende

Hornblende was a small aspect of these lava samples, and the least commonly occurring phenocryst. Ranging from 0.2 to 1 mm, shapes varied from anhedral to subhedral. Under PPL the colour of hornblende was as a soft beige/brown, as shown in Figure 5.10.

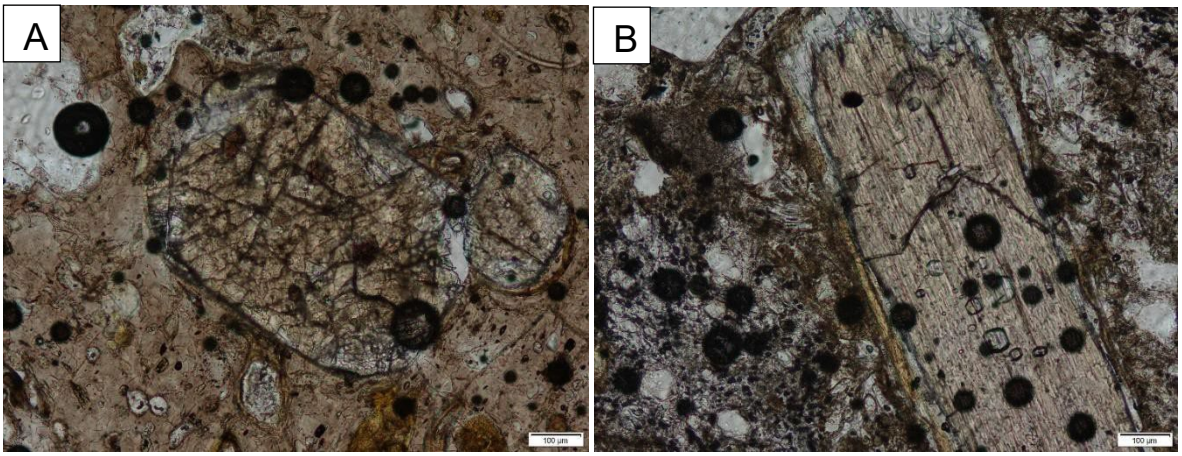

Figure 5.10: Hornblende observed under the petrographic microscope in PPL. Notice the soft brown colour, and in (A) the anhedral appearance, (B) large euhedral hornblende crystal.

Pumice

The rhyolitic pumice found in the ignimbrite averaged 1 mm but exceeded 2mm, with plagioclase embedded within the pumice in some cases. The texture is fibrous, with flattened vesicles. The pumice tended to be massive, and while low in abundance still occurs in the majority of many thin sections.

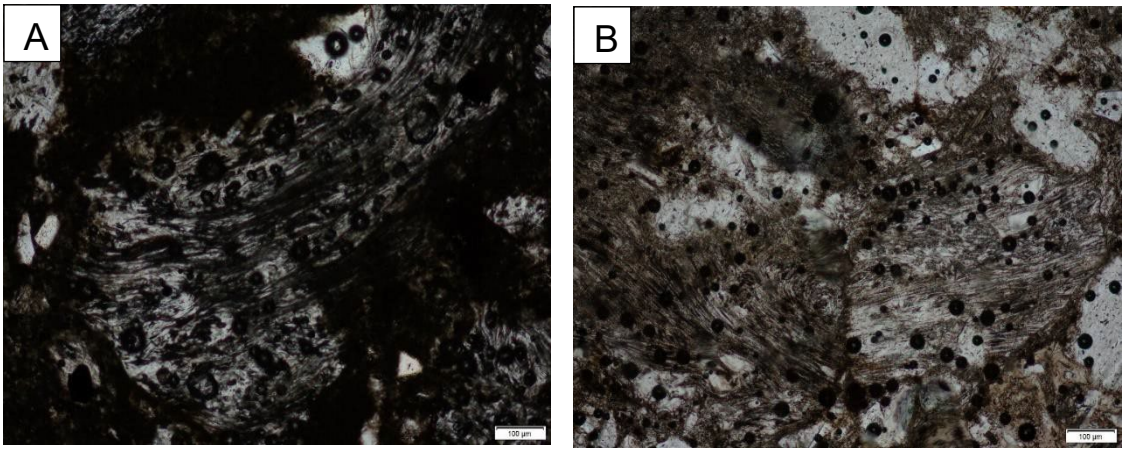

Figure 5.11: Pumice textures observed under the petrographic microscope. Note in both (A) and (B) the flattened vesicles and wavy textures.

Lithics

As seen in Figure 5.12 (E, F) the andesite lithics were crystal rich. Large plagioclase minerals were the most abundant, with euhedral to subhedral shapes and exceeding 4 mm in size, with an average of 0.4 mm. The plagioclase tended to have sieve textures. Pyroxenes were also abundant. Augite was the most

common pyroxene, seen with a 40° inclined extinction angle. Opaques were present in smaller numbers, anhedral to subhedral and 0.2 mm on average in size. Both lithics were highly porphyritic.

Matrix of ignimbrite units A - F

The ignimbrite of the Pukunui pyroclastic succession comprise a crystal and glass-shard rich, yet comparatively pumice and lithic poor matrix, with a eutaxitic texture. The matrix comprised 70 – 80 % of the bulk rock and was fine-grained, and difficult to resolve under high magnification because of its small grain size. The glass shards in the matrix ranged from 50 – 250 μm and are shown in Figure 5.12A.

The glass shards were a cuspate to tabular shape, and show advanced devitrification. The glass shards occasionally show original cuspate C to Y shapes, but the majority had a deformed appearance. They were frequently observed wrapping around phenocrysts found (as described above). Under PPL, the glass shards are brown to grey in colour.

Ash from unit B and upper F

Both ash samples consisted of abundant small plagioclase phenocrysts. There was a small number of opaques and orthopyroxenes. The opaques tended to be anhedral to subhedral and were around 0.3 mm in size, while the orthopyroxenes were euhedral to subhedral and around 0.5 mm in size.

Otawera Pumice

The pumice samples from Otawera were comprised of small plagioclase phenocrysts and flattened vesicles (Figure 5.12B-D). The plagioclase was small, euhedral to subhedral and 0.4 mm in size. The flattened vesicles were narrow and elongated, and highly abundant. Few opaques were scattered throughout.

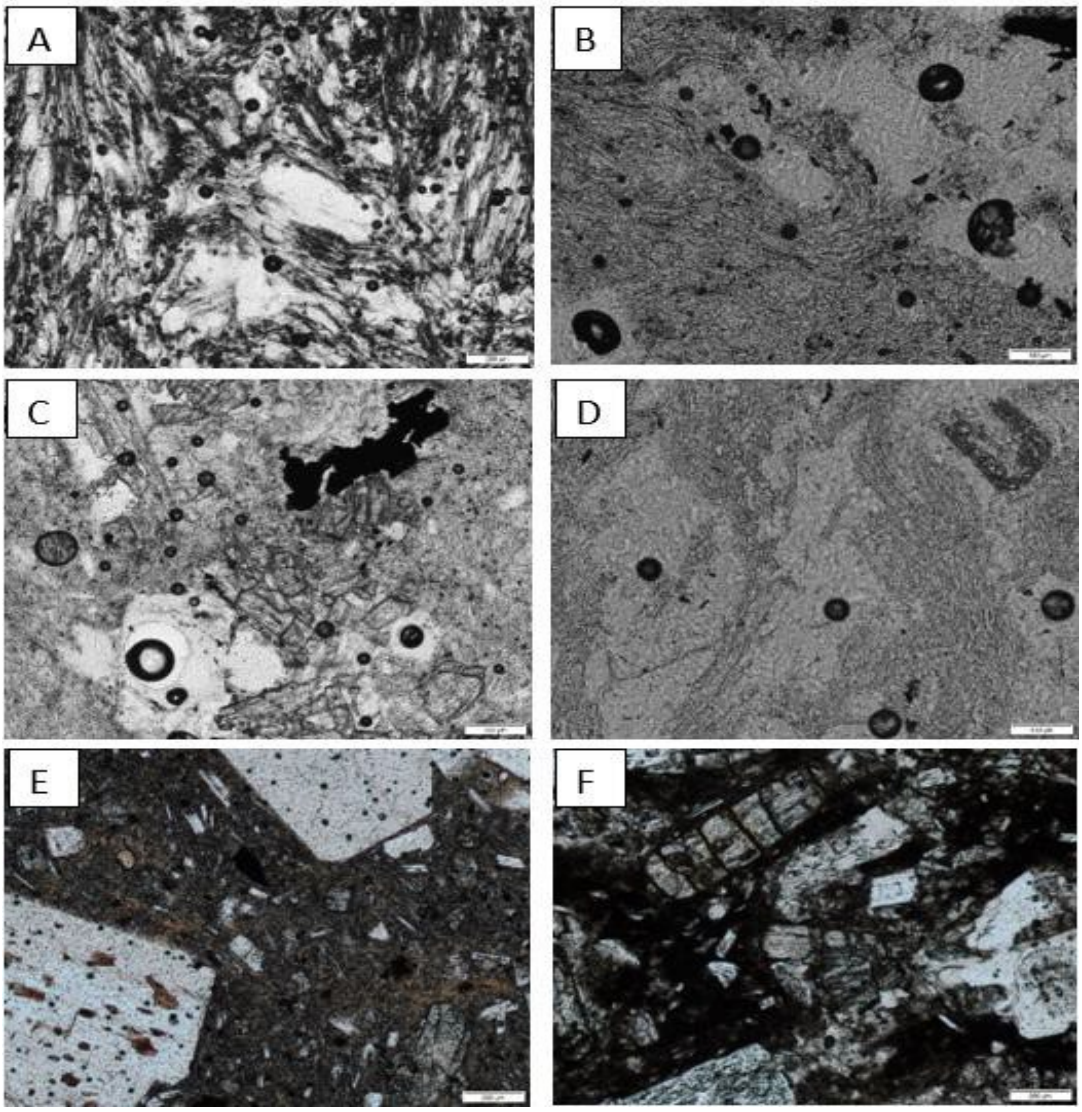

Figure 5.12: Features of the Otawera pumice and Pukunui pyroclastic succession, including pumice and Andesite lithics. (A) glass shards in the matrix of the Pukunui succession. (B - D) Otawera pumice showing flattened vesicles, opaques and plagioclase. (E, F) Large pyroxenes and smaller minerals found in andesite lithics within the Pukunui pyroclastic succession.

5.2.3 Maungatūtū/Mount Misery Rhyolite

From Maungatūtū/Mount Misery, six rock samples were taken from the field and made into thin sections. The main factor in characterisation of the Maungatūtū/Mount Misery rhyolites was the size of the phenocrysts within each sample. Many of the thin sections made were very weathered, with large brown domains as seen in the Pukunui samples. Most of the phenocrysts were highly altered or had been plucked out.

The groundmass in each sample was largely devitrified glass, or secondary quartz such as cristobalite. A spherulitic groundmass is seen in sample S2, with radiating spherulites present in darker coloured, potentially altered zones. Sample S2 was the only sample where a spherulitic groundmass was identified. Quartz veining was also a feature within the groundmass, and in a few samples, there was both devitrified glass and larger crystals infilling the vein. Two thin sections showed minerals with a high birefringence within veins.

Quartz

The most abundant phenocryst mineral in the Maungatūtū/Mount Misery lavas is quartz. When found, they tended to be massive, with embayments and melt inclusions. Quartz was roughly 1 mm on average, reaching 2.5 mm in size. They typically had a weathered and altered appearance (Figure 5.13A), and shapes ranged from euhedral to anhedral. Some of the quartz phenocrysts had concave fractures through the centre as shown in Figure 5.13B.

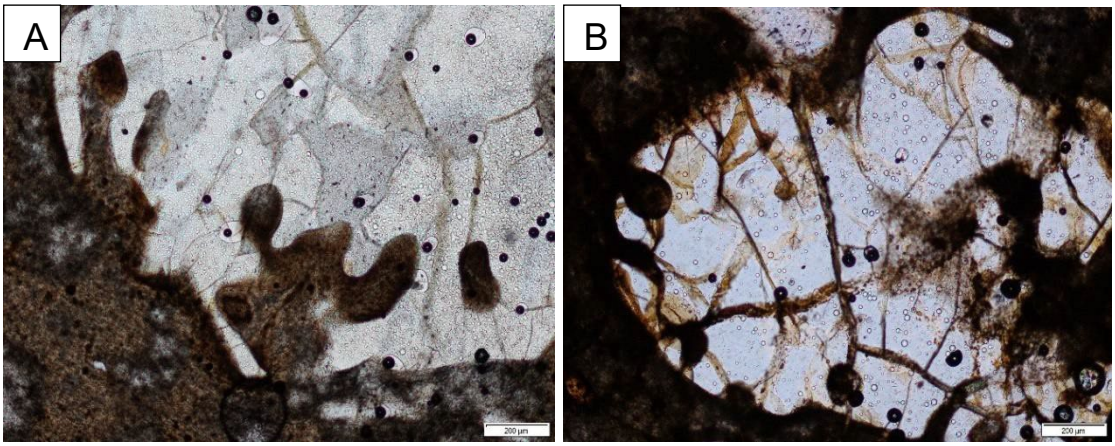

Figure 5.13: Quartz phenocrysts observed under the petrographic microscope under PPL. (A) a large quartz phenocryst with embayments along one side, (B) is a more altered quartz showing cracks through the centre and embayments.

Pyroxenes

Pyroxenes were abundant in the Maungatūtū/Mount Misery samples. They were large in size (maximum of 3 - 4 mm) and were mostly clinopyroxenes and few orthopyroxenes. They had a strong weathered appearance, with alteration along the rims and were subhedral to anhedral.

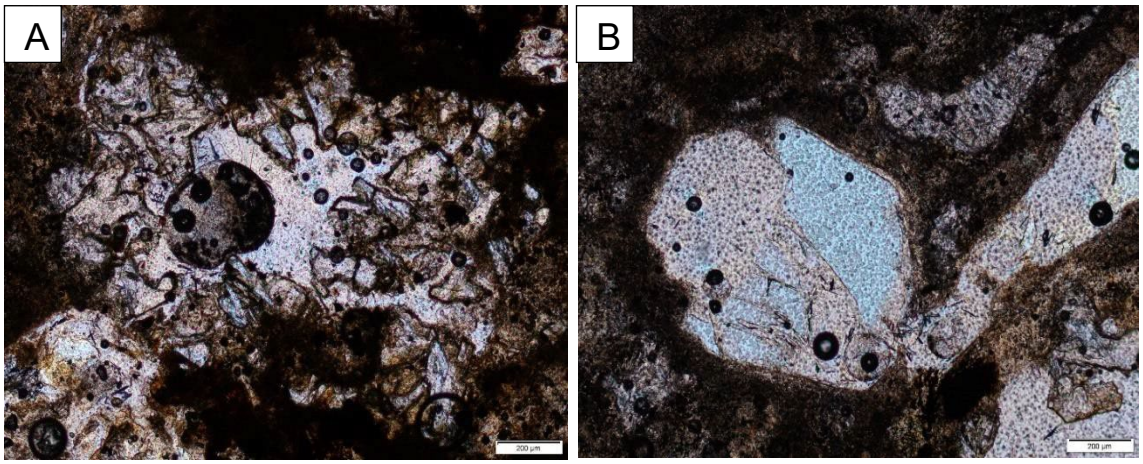

Figure 5.14: Pyroxene phenocrysts observed under the petrographic microscope under PPL. (A) a highly altered or weathered pyroxene, while (B) demonstrates the physical subhedral shape of a medium sized phenocryst.

Plagioclase

The plagioclase phenocrysts in the Maungatūtū/Mount Misery samples tended to be smaller compared to Pukunui and Greenpark. There tended to be less plagioclase feldspars found in the Maungatūtū/Mount Misery lavas, and much of the original plagioclase was absent. There were empty spaces where plagioclase looked to have been plucked out, so the remaining ones tended to be about 0.5 mm in size. Polysynthetic and simple twinning was a common feature, as well as euhedral to subhedral shapes.

Opaques

Opaques were the least abundant phenocryst in these samples, making up <5 %. The majority of opaques were 0.1 – 0.25 mm, and anhedral to euhedral. In some samples, there was visible iron leaching near the pyroxene phenocrysts.

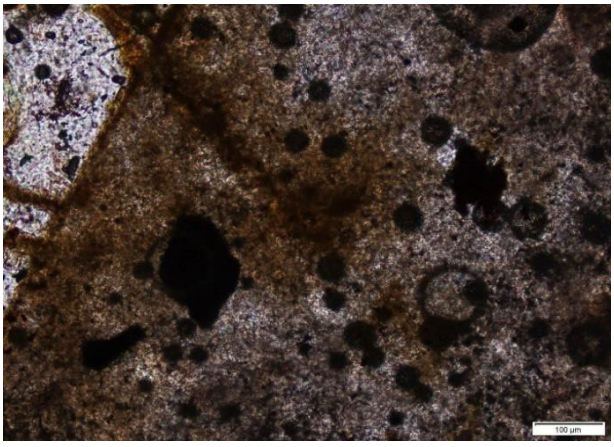

Figure 5.15: Opaque minerals as seen under the petrographic microscope.

Spherulites

Spherulites were found in a few of the samples, such as S2 and TM. A spherulitic groundmass was only present in S2, but they occurred individually throughout other samples. They were found close to phenocrysts or sometimes attached to a crystal, within the brown domains, some in radiating patterns (Figure 5.16). The composing fibres are needle like and crystalline, typically dark in colour. Most of the spherulites found were radiating, but few were non-radiating and the sizes varied.

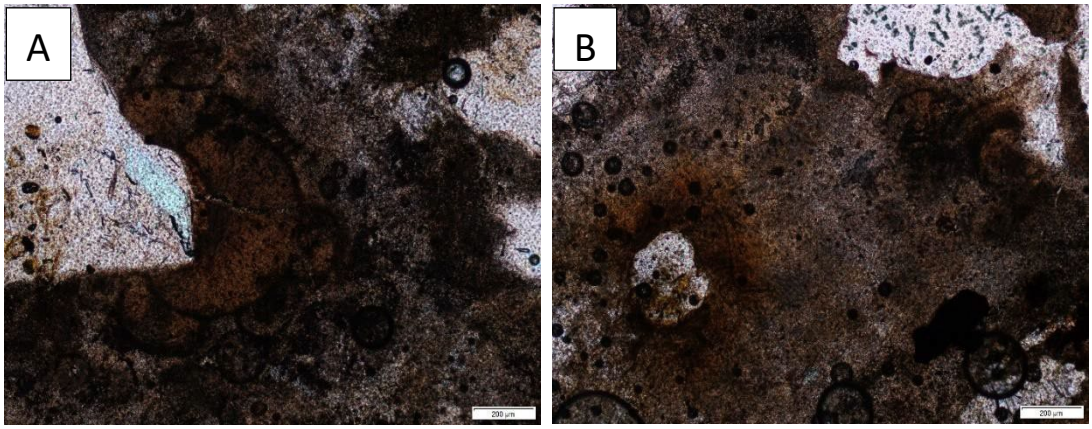

Figure 5.16: Photomicrographs of spherulite features. (A) Spherulite surrounding a pyroxene phenocryst. (B) Multiple spherulites in a brown domain, shown in shades of orange/red and in lighter brown.

Groundmass

Common groundmass features were devitrified glass, and darker brown domains which occasionally contained spherulites. The groundmass was fine-grained, and non-vesicular. In thin sections where the sample had been weathered or altered to a high level, most of the thin section was composed of a devitrified glass groundmass. There were darker brown areas which did not look like domains, but potentially iron oxide leaching surrounding mafic minerals.

5.2.4 Greenpark Rhyolite

The 12 samples analysed from the Greenpark Quarry showed a wide variation of petrographic features. A unique characterisation of these rocks were sub-circular crystalline inclusions which were present in five of the twelve samples. Many of the thin sections made for this area were of highly weathered samples, and had devitrified groundmasses; several crystals were plucked in the preparation of the thin sections.

Sub-circular crystalline inclusions

The most common feature of the Greenpark rhyolite was an unusual observation of sub-circular inclusions in the groundmass (Figure 5.17A-C). These were circular to sub-circular, and were found in samples S1.1, S2MB, S3MB, S5E/L and S6-AR. They were slightly larger in sample S6-AR than in S1.1. Under both PPL and XPL they had a grey to white birefringence. They were roughly 0.13 mm in diameter in S1.1 and up to 0.3 mm diameter in S6-AR, occurring in clusters in large numbers. Under high magnification they appeared to be a part of the groundmass, and not phenocrysts, with strong interlocking granular textures (Figure 5.17A). In sample S5E/L they were small and less frequent, covering approximately 20% of the thin section and were found mostly near veins interlocking the plagioclase crystals. The average size of crystals within the inclusions were 0.2 – 0.3 mm. In thin section S3MB, the inclusions tended to have more ragged edges and a less circular shape. However, they tended to have sharp boundaries within the surrounding groundmass, and were often linked together.

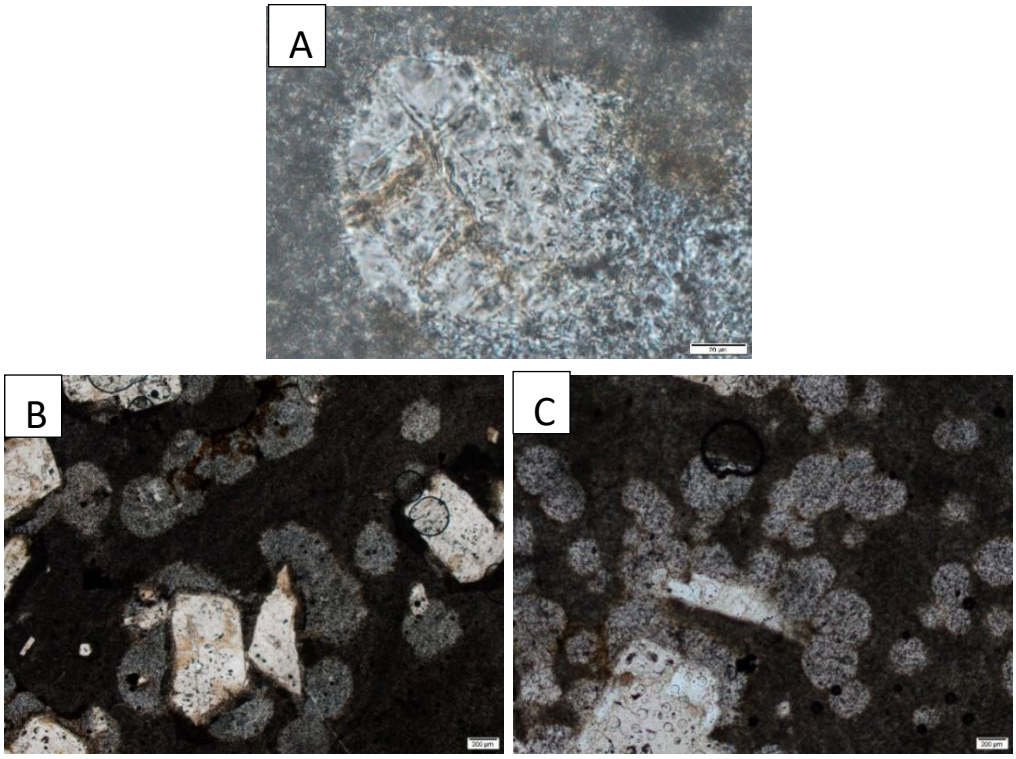

Figure 5.17: Sub-circular inclusions shown under PPL. (A) 50x magnification of a sub-circular inclusion under PPL. (B) Sub-circular inclusions concentrated around a phenocryst, and (C) attached to phenocrysts.

Plagioclase

The maximum size of a plagioclase phenocryst found in the Greenpark rhyolite lavas was 3.8 mm, with an average size of 1 mm. The smaller plagioclase phenocrysts were roughly 0.2 mm. They had oscillatory zoning, lamellar twinning and simple twinning, while being euhedral to subhedral in shape. Melt inclusions were common features. Thin veins also connected whole plagioclase phenocrysts (Figure 5.18). These were a common feature, and many plagioclase phenocrysts were connected by veins that looked like quartz as they were colourless under PPL, and the XPL view showed the typical off-white colour.

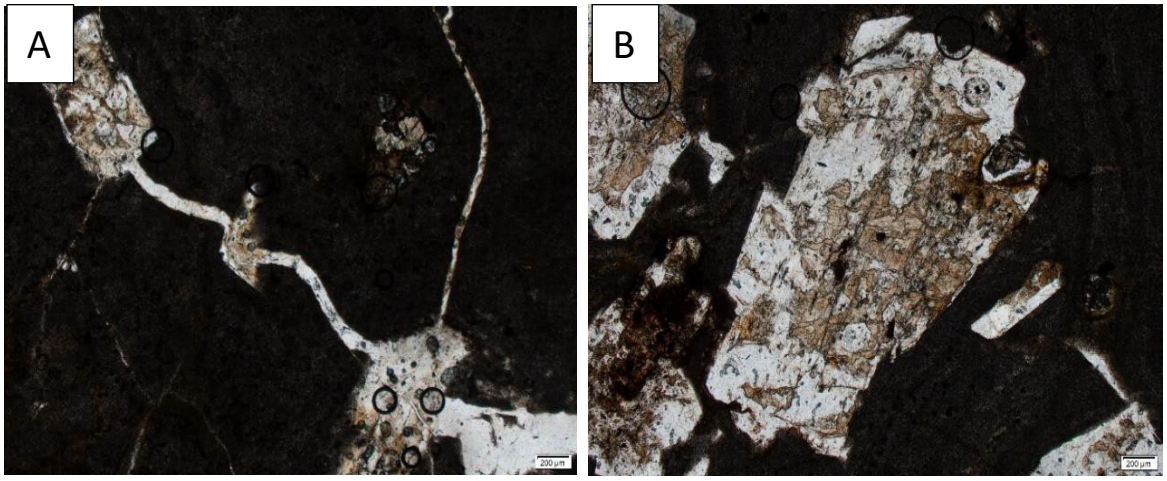

Figure 5.18: Plagioclase phenocrysts and veining observed under petrographic microscope, under PPL. (A) quartz veining connected to smaller plagioclase phenocrysts. (B) highly altered plagioclase mineral.

Pyroxene

Pyroxenes were common in the Greenpark rhyolite, occasionally these were 1.5 mm maximum, but most were on average 1 mm. They were euhedral in shape and were clinopyroxenes. These appeared with darker colours under PPL, but seemed to be highly altered. Few opaques were found within a pyroxene.

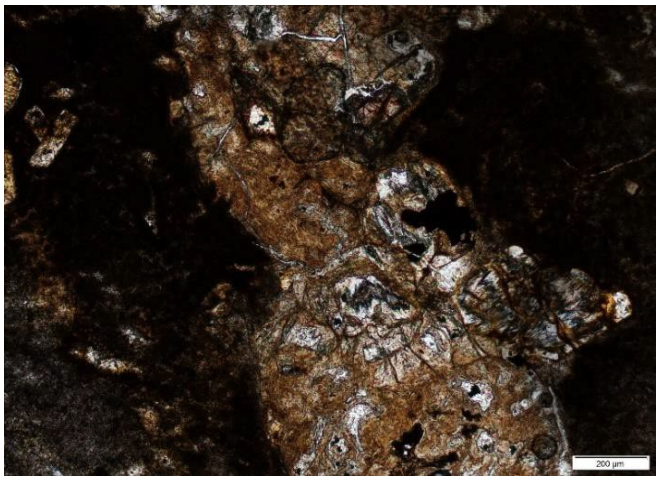

Figure 5.19: A highly altered pyroxene phenocryst under a petrographic microscope, in PPL.

Quartz

Quartz phenocrysts commonly were euhedral to subhedral in shape, with concave fracturing. The average observed sizes ranged from 0.8 – 1.1 mm, but were infrequent within the Greenpark Rhyolites.

Opaques

Opaques were featured in many of the thin sections but had a low abundance, small in size and appeared well-rounded. Sizes of opaques were ≤ 0.1 mm.

Groundmass

Flow banding was a common occurrence throughout many of the Greenpark lavas. It was often very fine grained, almost cryptocrystalline with alternating dark and light areas. There were dark brown domains present, which was common in the other two Mount Misery group domes. The groundmass was mostly devitrified glass and microlites.

5.3 XRD Results

XRD was run on a smaller number of samples, which were selected based on uncertainties raised from thin section observations. 13 powdered rocks were analysed. From Pukunui, three samples were tested (2CB, 2TB and 3CB). Maungatūtū/Mount Misery had four samples tested (TM, S1, S2 and S3). Greenpark held samples with many unknowns and so additional samples were run (S1.1, S2TB, S2MB, S4DAR and S6DAR). Within the Pukunui pyroclastic succession, only one lithic sample was analysed, in an attempt to confirm whether or it was andesite or rhyolite. Figures 5.22 through 5.26 show diffraction patterns which identify the mineral peaks in each sample, calculated through d-spacings (Appendix C). The most common minerals were cristobalite, tridymite and sanidine, followed by plagioclase feldspars. Additional minerals were observed and recorded, including alkali feldspars and augite.

5.3.1 Pukunui

The most common minerals identified in the Pukunui rhyolite were tridymite and cristobalite, which made up the majority of all three samples. Tridymite had intense peaks at [Å]: 4.104, [Å]: 4.332 and [Å]: 3.826, while cristobalite recorded peaks at [Å]: 4.049 and [Å]: 2.525. Sanidine has recorded intense peaks at [Å]: 3.256 and [Å]: 3.219. Plagioclase feldspars were very common. Peaks for the plagioclase feldspars occurred at [Å]: 4.049 [Å]: 3.187 and [Å]: 3.219. These peaks are represented in Figure 5.20.

5.3.2 Maungatūtū/Mount Misery

Quartz was a significant mineral within the Maungatūtū/Mount Misery rhyolites, especially samples TM and S3. Plagioclase feldspars were detected and identified at peaks [Å]: 3.774, [Å]: 3.186. Sample S3 recorded no significant entries for plagioclase feldspars, unlike the other two. Cristobalite, tridymite and quartz record intense peaks. The intense peaks for cristobalite were found at [Å]: 4.051 and [Å]: 2.462. Tridymite peaks were recorded at [Å]: 4.100 and [Å]: 4.312. Quartz had a strong presence, with intense peaks at [Å]: 4.262, [Å]: 3.349 and [Å]: 1.819. Sanidine has recorded peaks in all four samples, shown at [Å]: 3.217 and [Å]: 3.257 (Figure 5.21).

5.3.3 Greenpark

S1.1, S2TB and S3MB all had large amounts of quartz, cristobalite and tridymite as the main components. In smaller amounts are plagioclase feldspars that were identified with peaks at [Å]: 3.834 and [Å]: 3.766. Quartz has intense peaks at [Å]: 4.264 and [Å]: 3.351, while cristobalite has peaks at [Å]: 4.053 and [Å]: 2.490 (Figure 5.22). Tridymite was present and associated with intense peaks at [Å]: 4.107, [Å]: 4.334 and [Å]: 3.820. Sanidine was most common in S2MB, with peaks at [Å]: 3.256 and [Å]: 3.222.

Comparatively, S4DAR and S6DAR had more plagioclase feldspars than the other samples, which were more quartz dominant. Cristobalite had intense peaks at [Å]: 4.054 and [Å]: 2.526, while plagioclase feldspars peaks were recorded at [Å]: 4.107, [Å]: 3.220 and [Å]: 3.189. Tridymite also recorded peaks at [Å]: 4.108, [Å]: 4.334 and [Å]: 3.833 (Figure 5.23).

5.3.4 Ignimbrite Lithic

There was a large percentage of plagioclase feldspars that were identified by peaks occurring at [Å]: 3.186, [Å]: 3.784 and [Å]: 3.760. Augite was present in moderately high amounts, with one peak identified at [Å]: 2.955, a mineral that was not found in any of the other samples. Cristobalite was detected, with intense peaks at [Å]: 4.052 and [Å]: 2.501, followed by quartz showing a peak at [Å]: 4.334. Sanidine was also found in this andesite sample, with peaks at [Å]: 3.217 and [Å]: 3.258 (Figure 5.24).

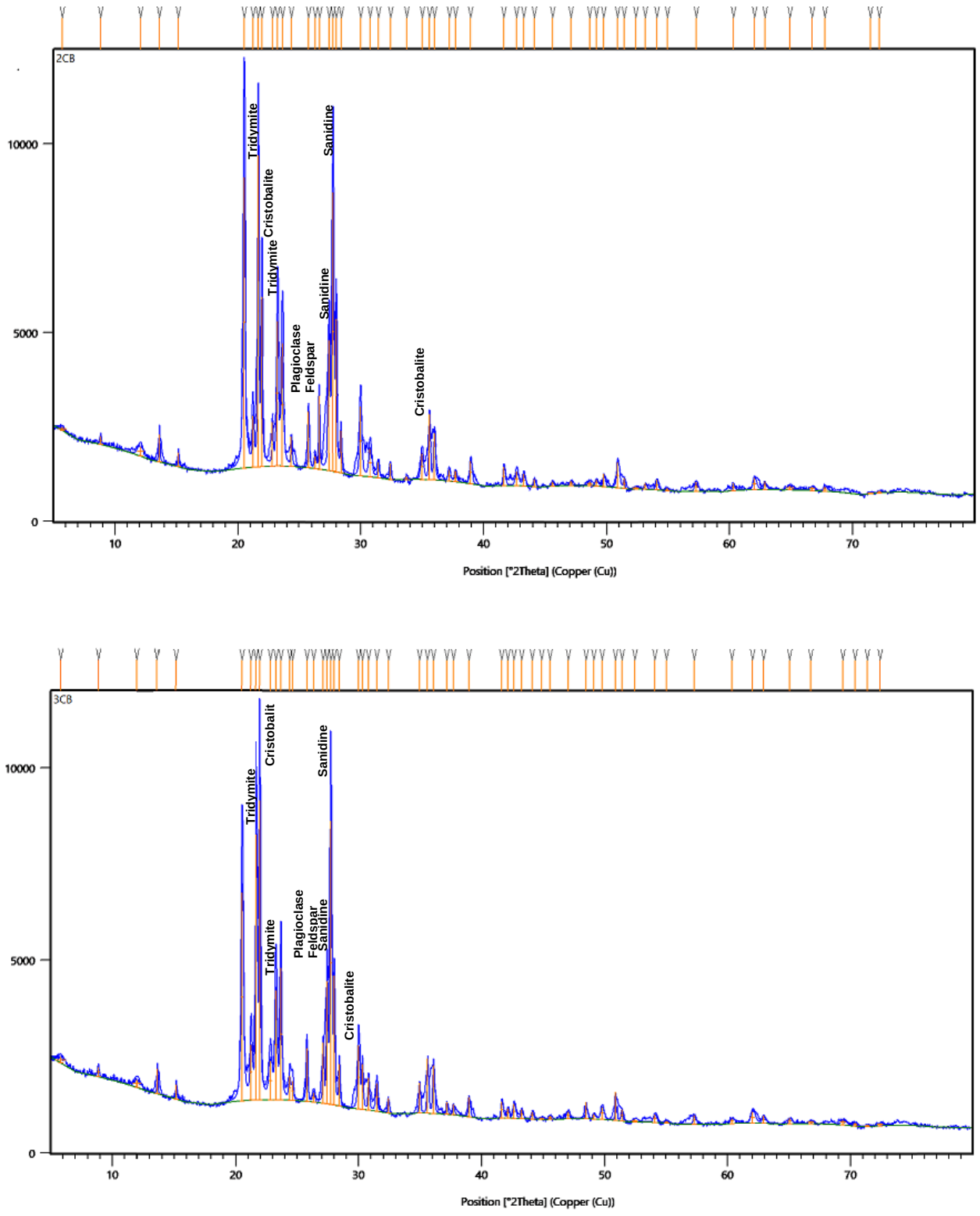

Figure 5.20: Diffraction patterns showing the presence of sanidine, cristobalite, tridymite and plagioclase feldspars in samples 2CB and 3CB from the Pukunui lavas.

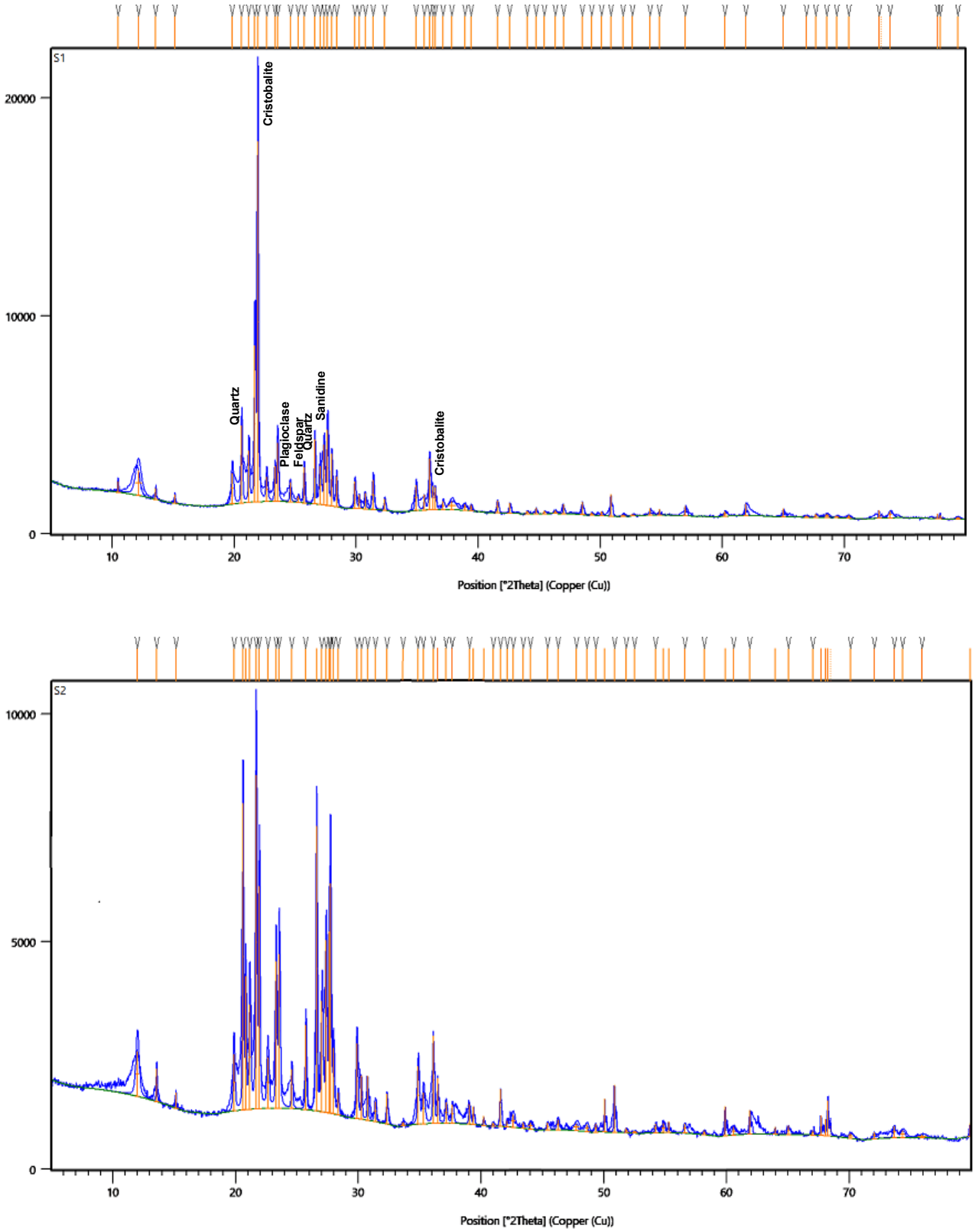

Figure 5.21: Diffraction patterns showing the presence of alkali feldspars, quartz, tridymite, cristobalite, sanidine and plagioclase feldspars for the Mount Misery lavas.

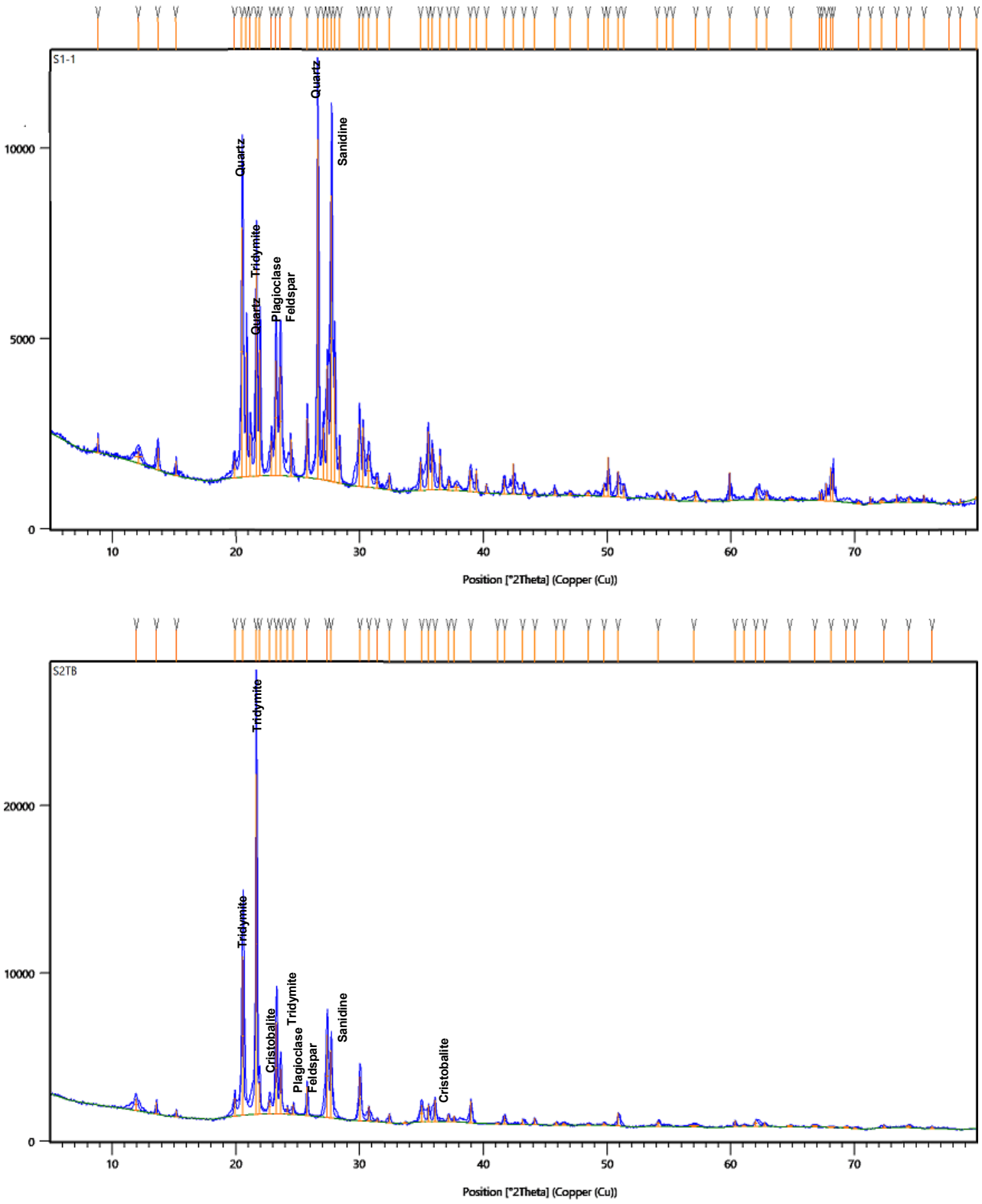

Figure 5.22: Diffraction patterns showing the presence of sanidine, quartz variations and plagioclase feldspars of the mineralogically differing Greenpark rhyolites, S2TB and S1.1.

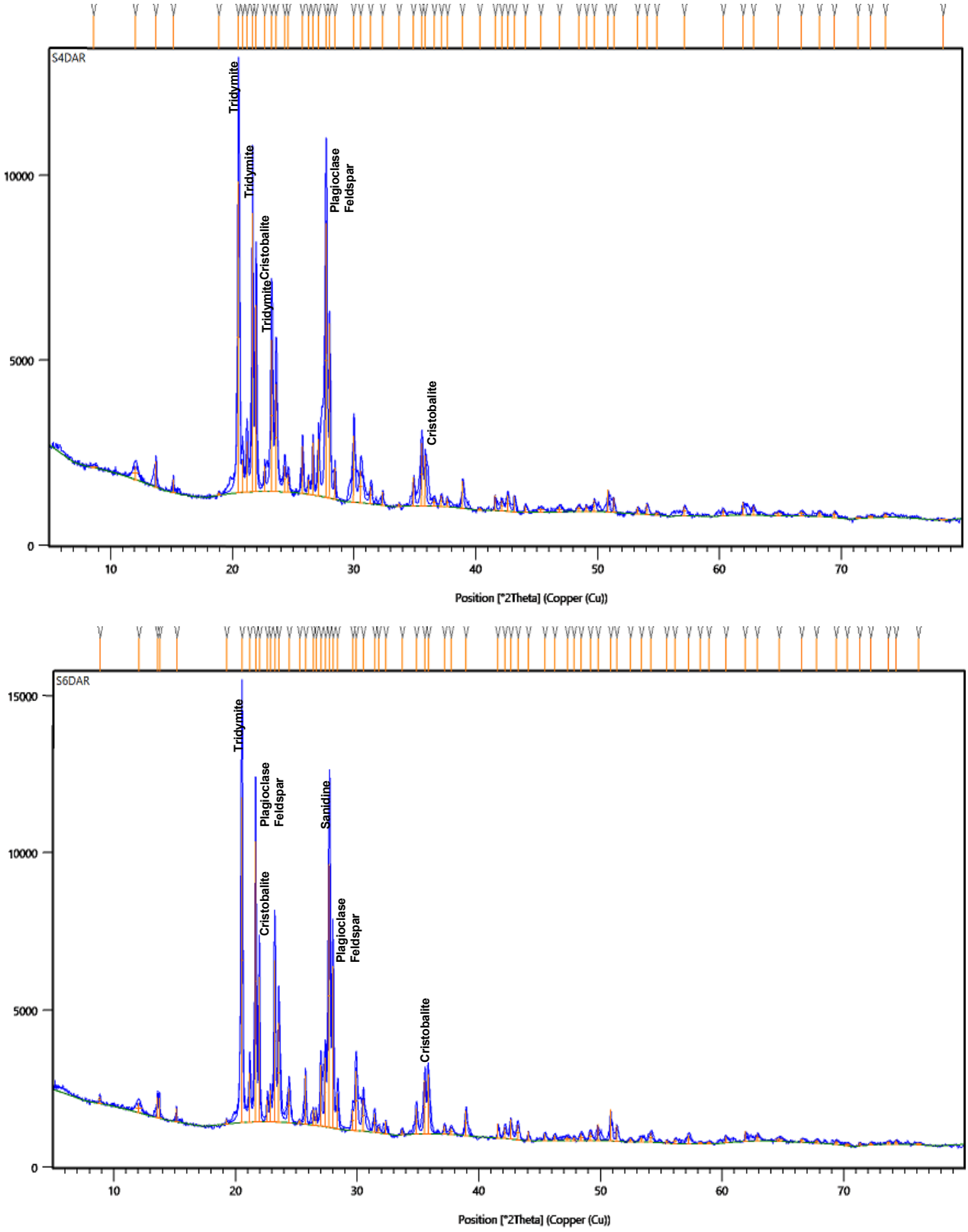

Figure 5.23: Diffraction patterns showing the presence of quartz mineral variations, and plagioclase feldspars for the two samples that show mineral variation from the Greenpark rhyolites.

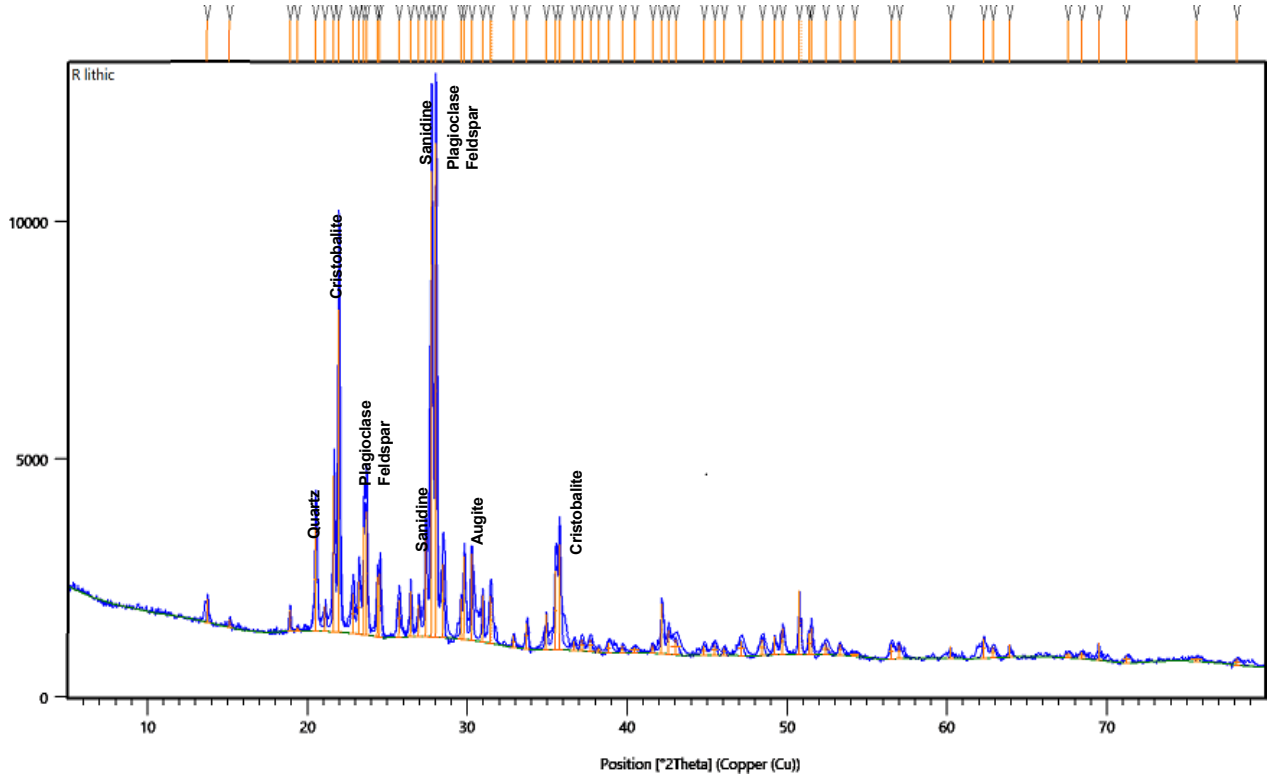

Figure 5.24: Diffraction patterns in sample R Lithic recorded by XRD analysis, showing a strong presence of plagioclase feldspars, augite, sanidine and quartz variations.

5.4 Scanning Electron Microscopy (SEM) results

SEM was used to finalise specific characteristics that were unable to be identified during previous steps. Five samples were analysed, using the polished thin sections and rough chips representing both the phenocrysts and groundmass.

5.4.1 Pukunui

Sample 1TB showed a thin band that made up a large amount of the field of view. Figure 5.25 and 5.26 (A - H) show alternating thin bands, and the composition and textural differences between the rough and smooth appearing areas. The smooth area was a quartz vein, with a consistent mineral composition throughout the entire area. The rougher textured area showed an interlocking texture comprised of K-feldspars.

The whole rock analysis showed a differing composition between the rough and smooth bands. The rough bands had smaller, interlocking textures and the smooth areas were larger, flat areas of quartz that interlock. This was seen in the thin section SEM analysis, comparing the rougher and smooth banded areas. Each crystal in the smooth band area appeared to exceed 10 μm in length, while the rough ones look to be on average around 5 – 6 μm (Figure 5.26G, H). The individual crystals within the rough area of the whole rock analysis had sharper, well-formed and blocky characteristics. The contact between the bands was transitional over 30 – 60 μm.

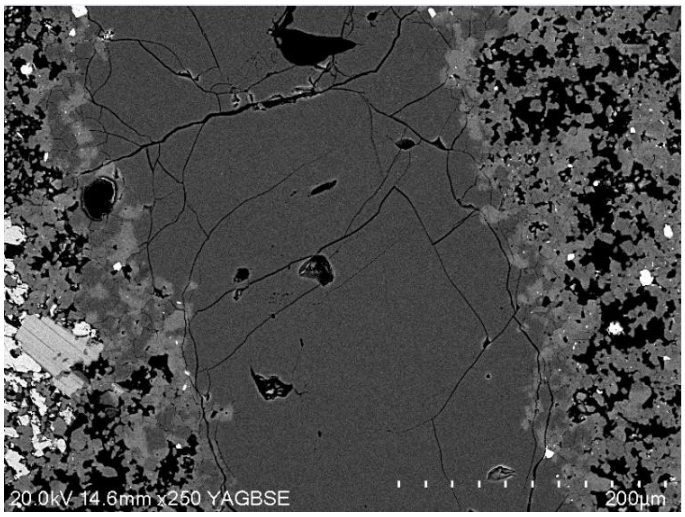

Figure 5.25: Scanning electron microscopy in BSE mode of the flow banded sections showing an area of ~ 400 μm with a different rough and smooth texture, representing flow banded rhyolite.

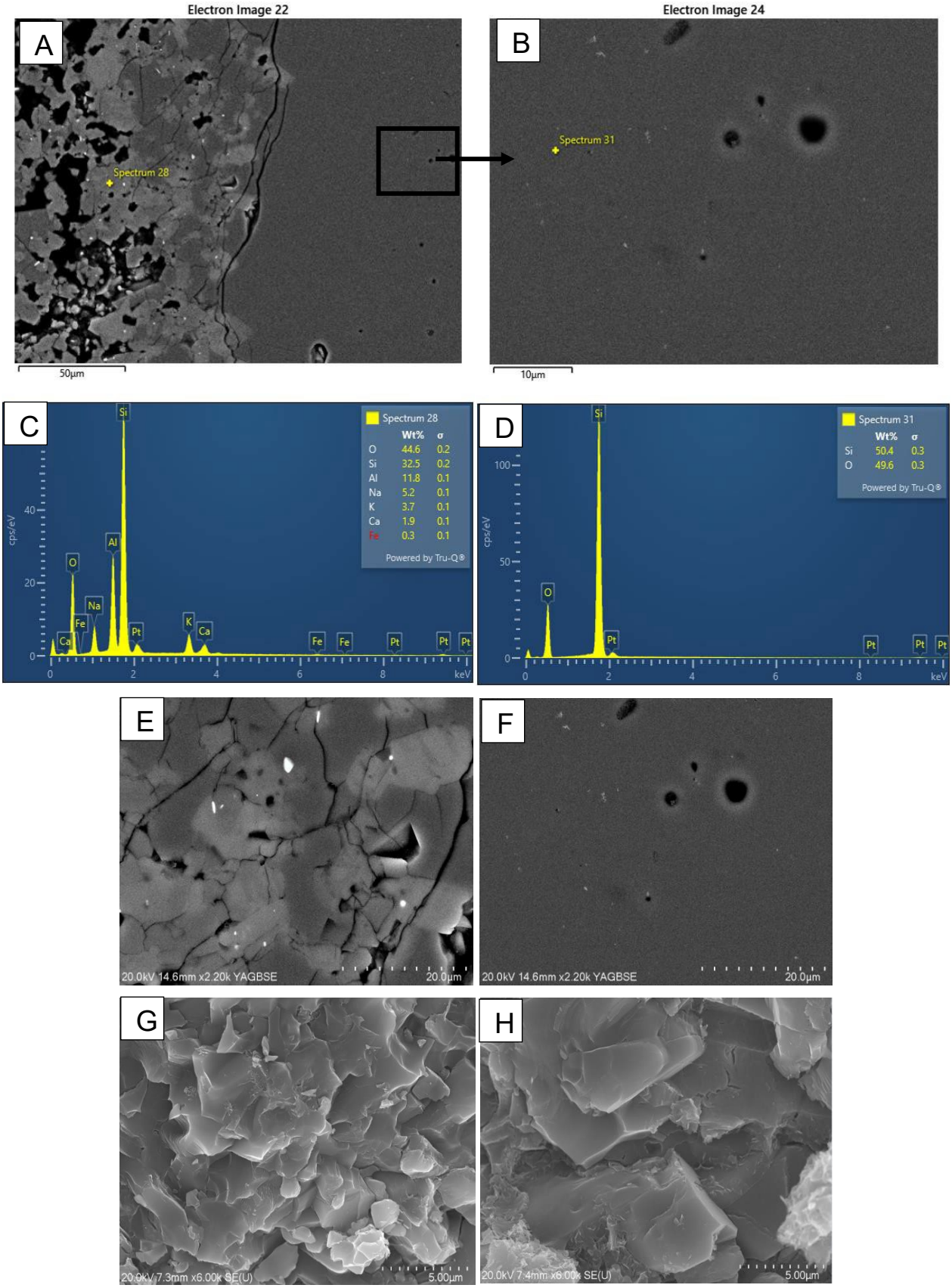

Figure 5.26: SEM images and EDS analysed the composition and the texture of the alternating thin banding in the Pukunui Rhyolite. (B, D, F, H) showing the textures and elemental composition of the smooth area of the flow banding. (A, C, E, G) shows the textures and elemental composition of the rough area of the flow banding. (G-H) images from whole chip pieces.

5.4.2 Maungatūtū/Mount Misery

Most of the rhyolite sample examined is devitrified glass, of alkali feldspar composition; a crystalline groundmass, showing poorly formed crystallites of sanidine that comprised a feathery-like habit. The groundmass had a microlitic texture, with needle like structures (feathery-like surface) visible in a semi radiating pattern. The elements that made up the needle-like structures within groundmass are K, Na, Si, O and Al, which confirmed them as K-feldspars (sanidine), which likely formed as a result of devitrification of the original glass groundmass. Whole rock pieces that were analysed confirmed the microlitic groundmass texture.

Figure 5.27 (A-D) shows a series of SEM images and corresponding EDS analysis for the groundmasses. The thin section groundmass showed a radiating pattern with light and dark areas, and the EDS confirms the alkali feldspar composition. The lighter area, shown in Figure 5.27B, had a mineral composition resembling sanidine, while the groundmass in its entirety appeared to be devitrified glass. Both samples that were run in the SEM confirmed the sanidine groundmass.

Many large (~400 μm) phenocrysts were found, including orthopyroxenes with highly altered areas in the centre of them, typically appearing large and euhedral, with zones of alteration or weathering. The minerals had elemental compositions consistent with orthopyroxene (high silica, iron, magnesium) which defined them as clinoferrosilite structures, as their elemental $FeSiO_2$ was above 50 %. Iron oxides were found scattered throughout sample TM. It featured a 100 μm euhedral phenocryst of iron titanium oxide (ilmenite).

One whole rock piece and a thin section were looked at, where images captured allowed for the comparison of the groundmass textures. As seen in Figure 5.27 (E, F) the groundmass in the thin section had a microlitic texture, with needle-like structures that appear in an almost radiating or circular pattern. The elemental composition of these lighter areas were high in K and Na, which defined them as sanidine. The whole rock pieces analysed from Maungatūtū/Mount Misery confirmed the microlitic textures.

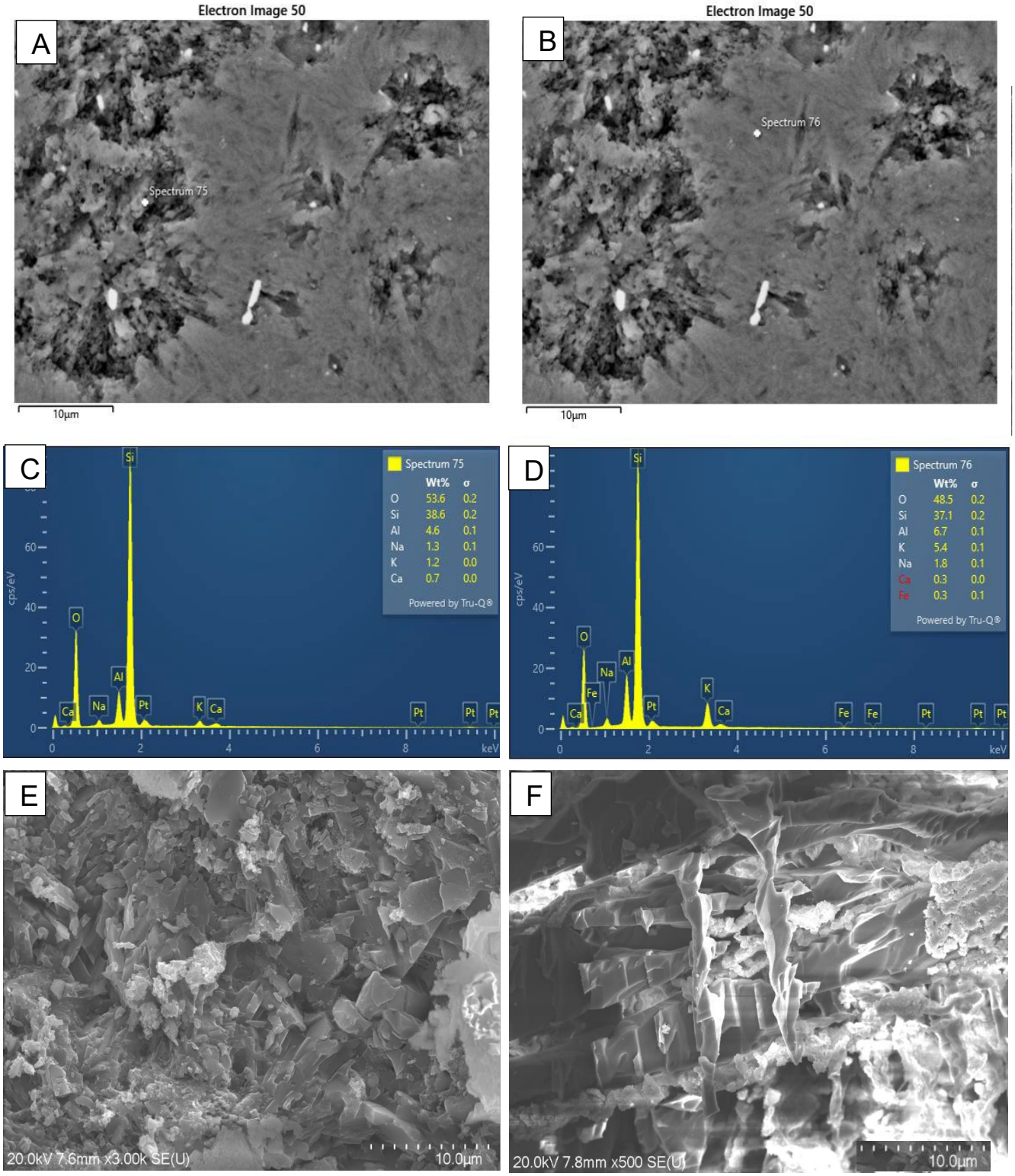

Figure 5.27: Groundmass textures of the Mount Misery lavas, (A,B) different EDS points marked to determine the mineralogical difference between the alternating light and dark colours, as well as the radial pattern of the crystalline groundmass. (C, D) corresponding EDS results. (E, F) whole rock chip images showing the needle like structures within the groundmass (K-feldspars).

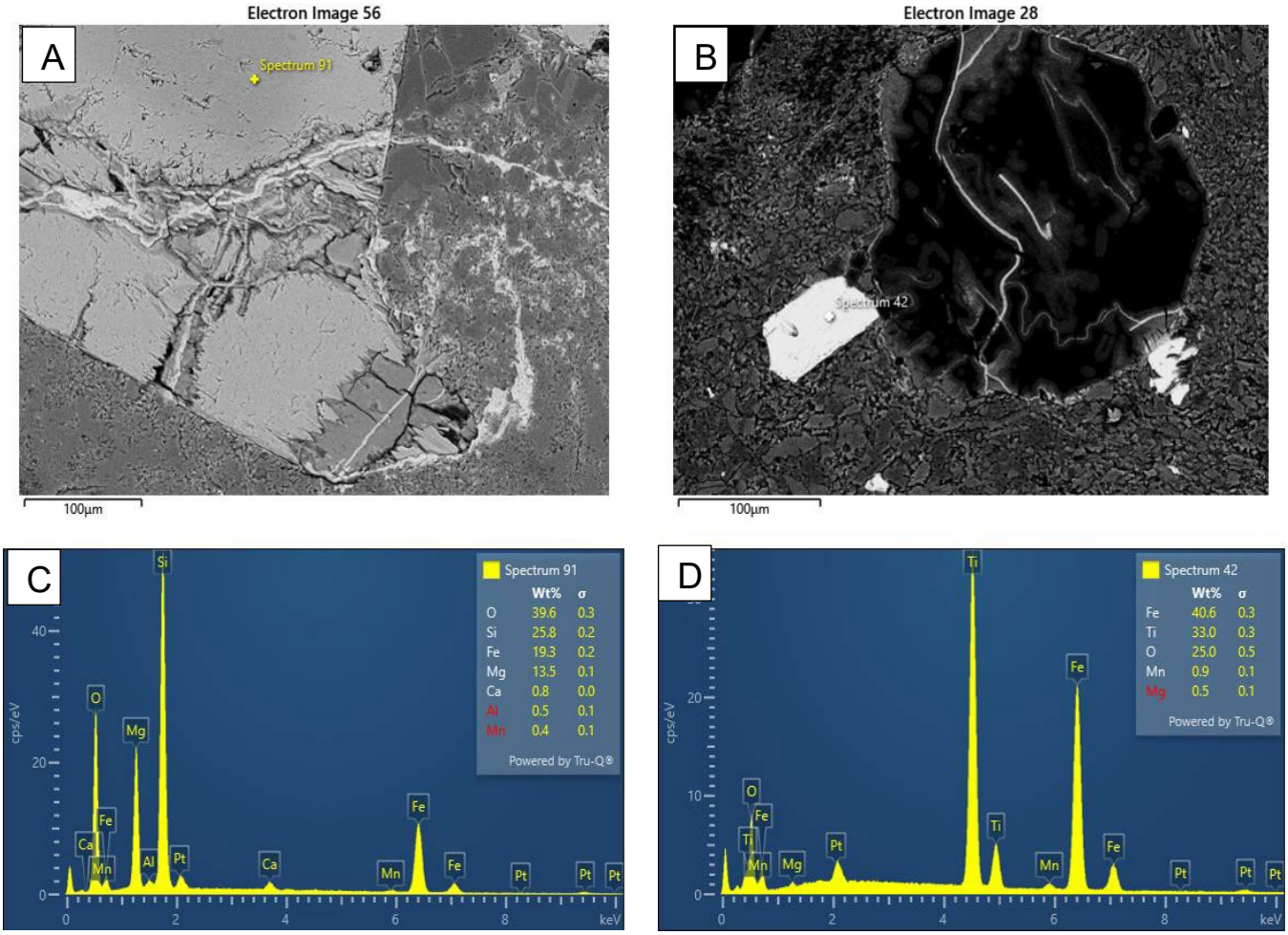

Figure 5.28: SEM images in BSE mode showing phenocrysts found in the Mount Misery lavas. (A) Pyroxene phenocryst, cut through the middle with a vein featuring alteration on the edges with a corresponding EDS graph (C). (B) Ilmenite phenocryst next to an empty phenocryst space, with a corresponding EDS graph (D).

5.4.3 Greenpark

Sub-circular inclusions were common groundmass features observed in thin section under the optical microscope, and so SEM was used to identify the composition within and outside of these features. Under the optical microscope, these circles appeared to be 130 μm and so in the SEM, this scale was used to identify these circular inclusions. Under SEM, the scale of this ranged from around 120 – 150 μm. They were found to be consistently round in shape, varying in the internal texture compared to the external texture. These sub-circular inclusions were not visible during whole rock analysis of sample S1.1. Few subcircular inclusions were joined (Figure 5.29).

Figure 5.30 (C, D) shows that there is a clear difference between the internal texture and external texture of the sub-circular inclusions. The first notable feature was the size of the minerals that were present. The shading and compactness also shows the difference between the internal and external textures. In Figure 5.30 (D) showing the internal structure, the minerals were visibly larger, lighter grey in shade and much more compact than (C), which showed small minerals in both light and darker colours. The average size of a mineral in Figure 5.30D was 8.0 μm, compared to Figure 5.30C which showed a 2.0 μm average. The internal texture, analysed through SEM-EDS had a K-feldspar composition of the larger minerals, as the main elements were oxygen, silica, aluminium and potassium (sanidine). Looking at a whole circle, there was a clear outline in both microscope modes as shown in Figure 5.30 (A, B).

Minor minerals found within the sample were apatite (Figure 5.31) which was found in a plagioclase phenocryst (Figure 5.31A, C) in one sample, and again in another, on the cusp of an altered plagioclase (Figure 5.31B, D). Pyroxene phenocrysts were also found at ≥ 500 μm, characterised by a holey appearance and subhedral shapes.

The groundmass was composed of sanidine. Similar to the Maungatūtū/Mount Misery rhyolites, the glass has an interlocking texture of more elongated minerals but they do not appear radial (Figure 5.32A, B). The groundmass has interchanging dark and light grey areas, on average 20 μm long, but thin and needle like. Sanidine was measured on the EDS as the lighter grey area of the groundmass. Veining was a common feature in both Greenpark samples and appeared to be within the groundmass.

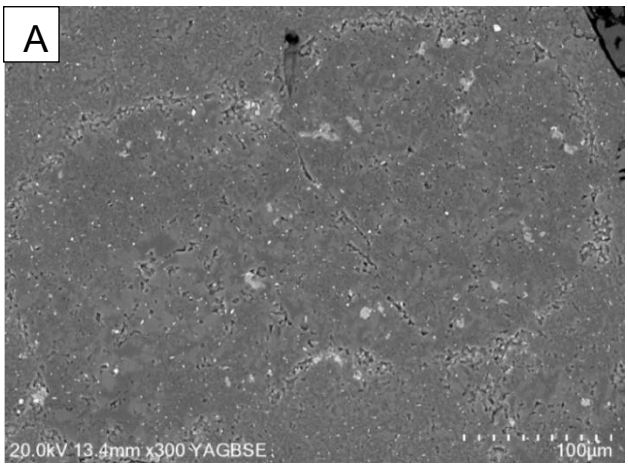

Figure 5.29: SEM image in BSE mode showing two conjoining sub-circular shapes.

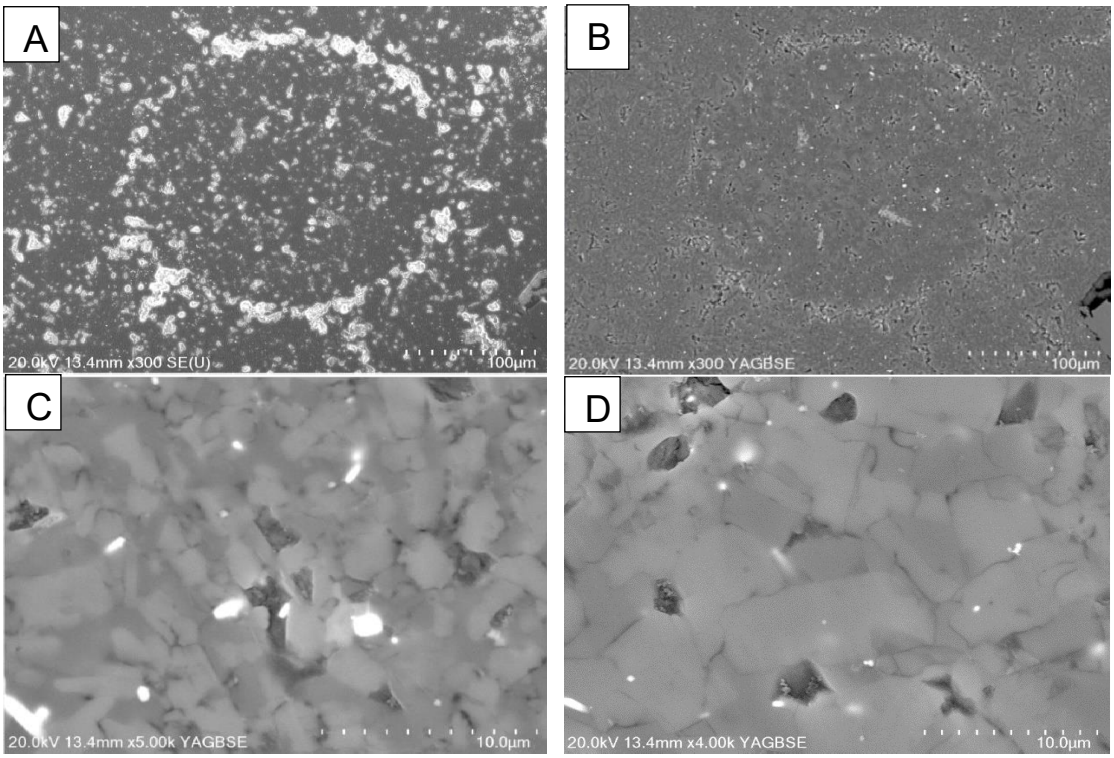

Figure 5.30: SEM images of sub-circular shapes. (A) SE image of a joined sub-circular inclusions, (B) BSE image of the same sub-circular inclusions. (C) zoomed in BSE mode of the outside of a sub-circular, and (D) zoomed in image of the inside of the sub-circular shape.

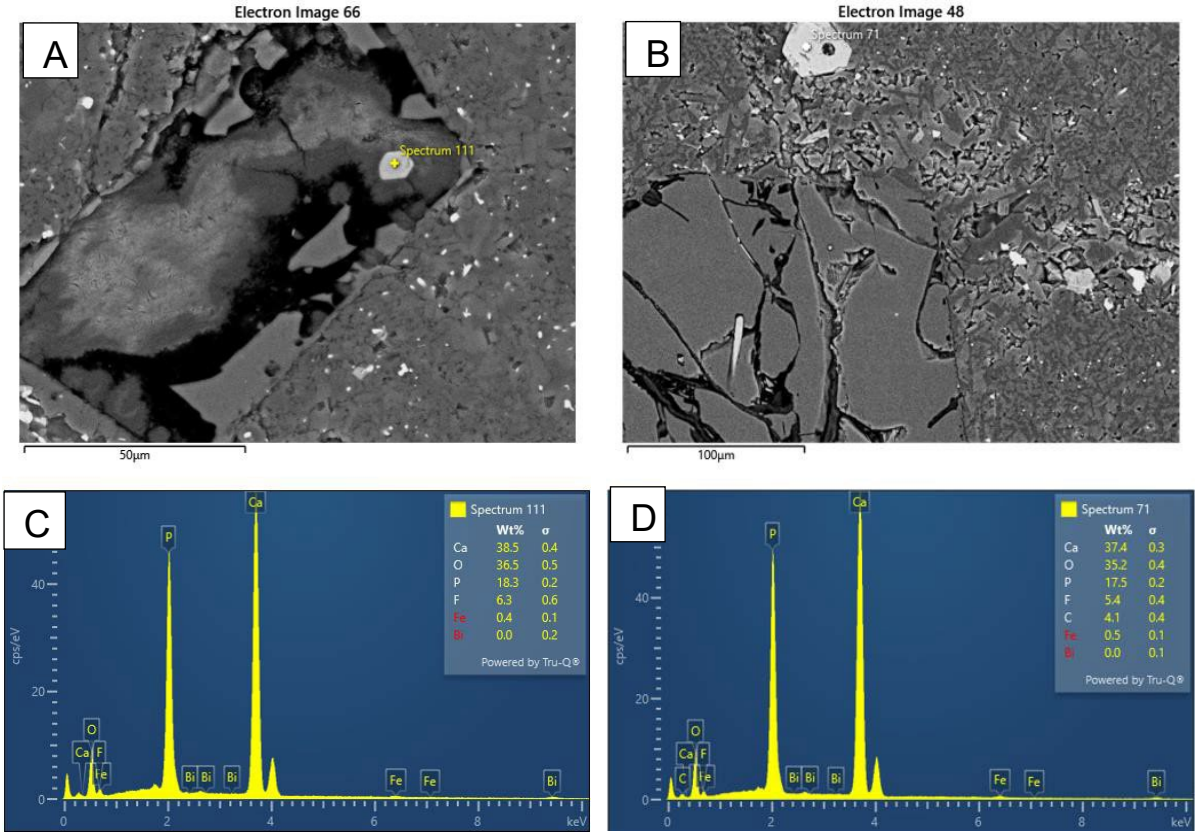

Figure 5.31: SEM imaging of apatite phenocrysts found in the Greenpark rhyolites, use BSE mode and EDS graph analysis. (A) A highly altered, plucked phenocryst with apatite, (C) the corresponding EDS analysis. (B) Apatite on the edge of another altered mineral, with (D) as the corresponding EDS analysis.

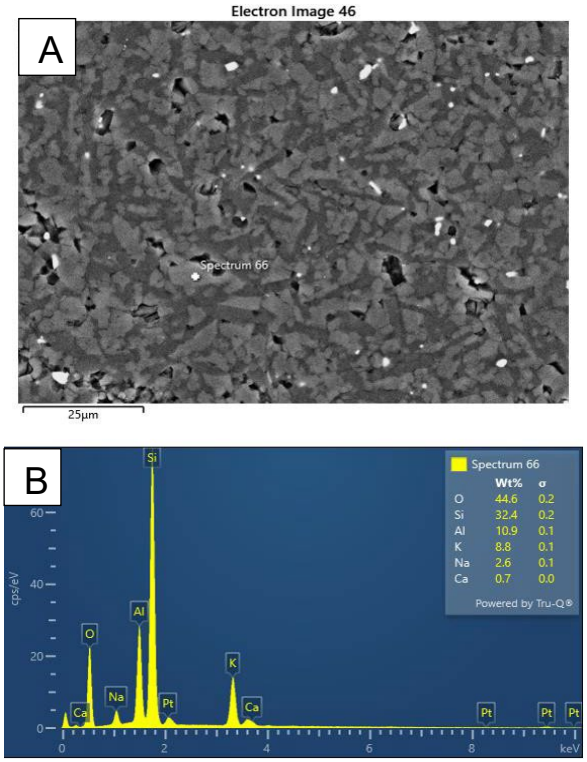

Figure 5.32: SEM imaging of groundmass textures from the Greenpark rhyolites. (A) interlocking elongated sanidine that is shown in (B) as K-feldspars.

Chapter Six

Geochemistry

6.1 Introduction

This chapter describes the geochemical characteristics of whole rock samples, including major and trace elemental compositions of 13 lava samples from the Pukunui, Maungatūtū/Mount Misery and Greenpark domes, and six from the Otawera ignimbrite pumices. Older data of glass from Otawera ignimbrites sourced from M. Prentice was also included here as an indicator for the Otawera pumice samples. The Otawera pumice has been comparatively analysed to try and correlate the Pukunui dome data with the ignimbrite data. The raw results for the geochemical analysis are supplied in Appendix B.

6.2 X-ray fluorescence spectroscopy (XRF) results

X-ray fluorescence spectrometry (XRF) was run to define the thin section and XRD results by testing the major, trace and rare earth element geochemistry. The whole rock samples used for geochemical analyses were normalised to 100 % and volatile free for major elements. A series of Harker plots were created, as well as a total alkali versus silica (TAS) plot.

Loss of ignition (LOI) data represented the change of weight in a whole rock sample after it has been heated, which removes the volatile content of the rock. Fresh rock samples would be expected to have an LOI of <2.5 %, and higher values (around 2.5 – 5+ %) are associated with the alteration of feldspars, which have been consistent with previous observations. Approximately half of the measured LOIs exceeded 2.5 %, which would be expected when looking at the samples that already display alteration and weathering. These values were still displayed to give a greater analysis of each of the three field locations.

Major elements analysed were Si, Al, Ti, Fe, Mn, Mg, Ca, Na, K, and P. Trace elements analysed were Sc, V, Cr, Co, Ni, Cu, Zn, Ga, As, Rb, Sr, Y, Zr, Nb, Mo, Sn, Sb, Cs, Ba, La, Ce, Nd, Tl, Pb, Th and U. The data obtained from XRF analysis was used in the TAS diagram, and many of the major and trace elements were used in the composition of the Harker plots.

6.2.1 Rock classification

The Mount Misery series has been classified as rhyolites by using a total alkali versus silica (TAS) diagram, shown in figure 6.1. The samples are all rhyolitic, with the Maungatūtū/Mount Misery samples showing on the diagram as borderline rhyolite-dacite. The separation between rock compositions was determined by Le Maitre et al. (2002) where rock types are split as follows: basalts contain 45-52 wt. % SiO_2; basaltic andesite, 52-57 wt. % SiO_2; andesite, 57-63 wt. % SiO_2 and dacite, 63-77 wt. % SiO_2.

The TAS diagram showed a relationship between the Mount Misery group lavas, and the Otawera glass and pumices. Samples on the boundary of rhyolite-dacite tended to have higher LOI values. The Maungatūtū/Mount Misery dome (green) and one point from Greenpark (yellow) show a rhyolite-dacite

composition, which was likely due to the high amount of weathering that occurred at this site. The data points followed a moderately positive linear trend, where Pukunui rhyolite shows a close relationship with the Otawera data.

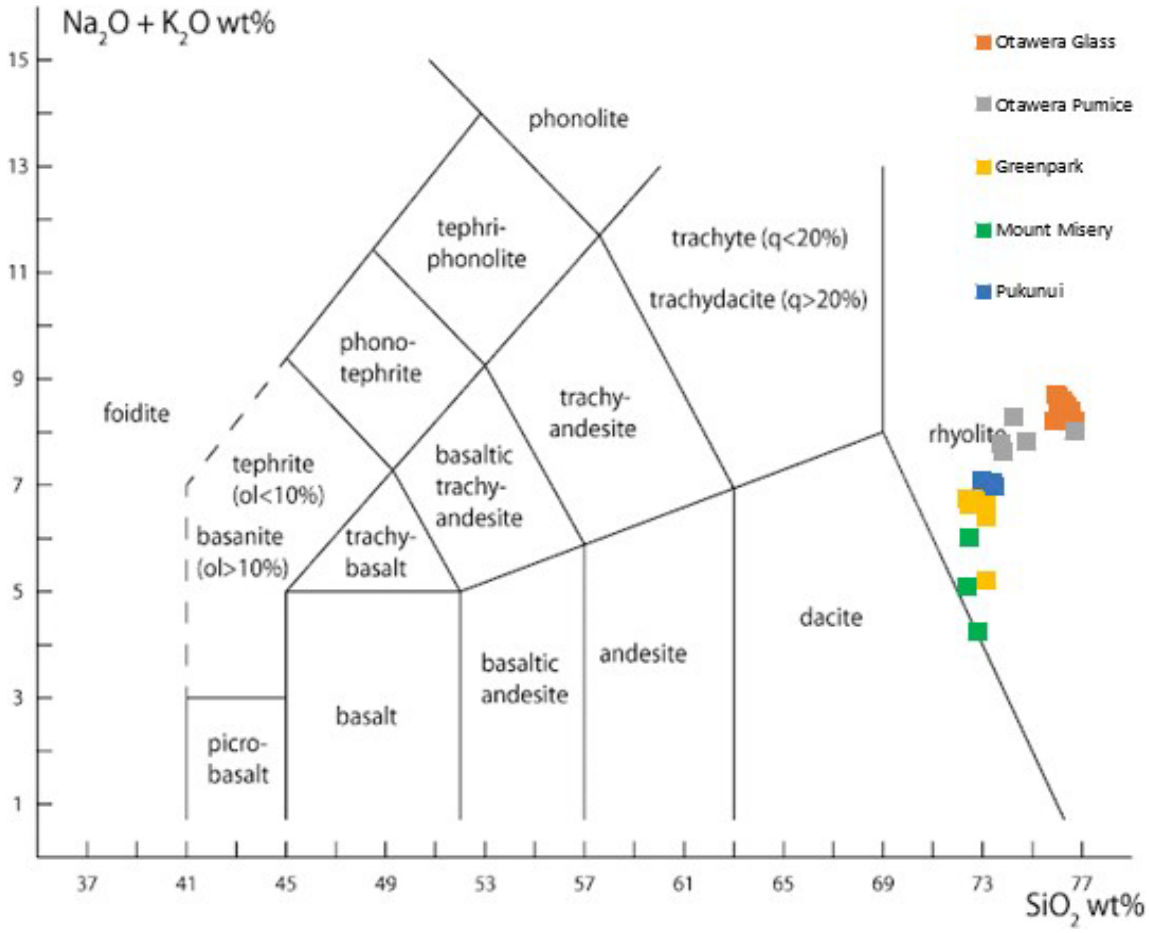

Figure 6.1: Chemical classification of volcanic rocks using total alkalis versus silica (TAS) diagram, from Le Maitre et al. 2002.

6.3 Major element geochemistry

The major element compositions are shown in Figure 6.2, with Harker variations diagrams for SiO_2 against Al_2O_3, TiO_2, Fe_2O_3, Na_2O, CaO, and MgO, where Fe is expressed as Fe_2O_3. Major element composition shown in Harker plots demonstrates the relationships between whole rock major elements against silica. This was done for both the Otawera glass and pumice, and the Mount Misery group lavas.

6.3.1 Mount Misery Lavas

Measured SiO_2 abundances range from 72.11 to 73.29 wt. % (normalised to 100% volatile free). As the SiO_2 content increases, there was a progressive increase for Na_2O and CaO, while there was a decrease shown for Al_2O_3, TiO_2 and Fe_2O_3. The trends shown are moderate in strength and appeared reasonably

well defined for Al_2O_3, TiO_2, Na_2O, and Fe_2O_3. The Maungatūtū/Mount Misery lava commonly had values slightly differing from Pukunui and Greenpark, likely due to weathering. The Maungatūtū/Mount Misery dome shows higher concentrations of Al_2O_3, and lower amounts of Na_2O, relative to the other two lavas.

With respect to each major element, the abundance of Fe_2O_3 ranges from 2.49 – 3.43 wt. %. TiO_2 ranges from 0.35 – 0.41 wt. %, and Al_2O_3 from 14.79 – 18.58 wt. %. CaO from 0.51 – 1.94 wt. %, and MgO ranges between 0.09 – 0.30 wt. %. Na_2O had abundances between 1.37 – 3.82 wt. %.

CaO and MgO show no recognisable trends, with significant spread in both Harker variation diagrams. The MgO range was very low, with a maximum value of 0.30 wt. %, however MgO is not an expected major element in rhyolites. The CaO graph has three outliers, which are the weathered samples with a higher LOI value, however the other data points are strongly grouped together, showing a genetic relationship. The TiO_2 graph shows another strong genetic relationship between the three lavas, where the numbers have a small range of 0.06 wt. %, which are low values.

6.3.2 Otawera ignimbrites, glass and pumice

The Otawera glass and pumice data showed strong correlations across all major Harker variation plots. The Pukunui lava data and the Otawera pumice samples tended to share similar values across the major element geochemistry, and where they didn't overlap they tended to fit along a moderately positive trendline. The pumice data had more variation, although less data points than the glass. Pumice had lower silica than the glass but higher amounts of Al_2O_3, TiO_2, Fe_2O_3, CaO, and lower Na_2O.

The SiO_2 values for the pumice data ranges from 73.47 – 74.50 wt. %, and for the glass data was 75.62 – 76.47 wt. %. With respect to the other major elements range, Fe_2O_3 ranges from 2.06 - 2.30 wt. % for pumice, 1.30 – 1.70 wt. % for glass; TiO_2 from 0.16 – 0.21 wt. % for pumice, and 0.08 – 0.14 wt. % for glass. CaO from 1.46 – 1.80 wt. % for pumice and 0.79 – 1.14 wt. % for glass; and MgO ranges between 0.18 – 0.38 wt. % for pumice and 0.02 – 0.10 wt. % for glass. Na_2O had abundances between 3.89 – 4.28 wt. % for pumice, and 4.33 – 4.90 wt. % for glass. The pumice and glass values did not overlap but were close together.

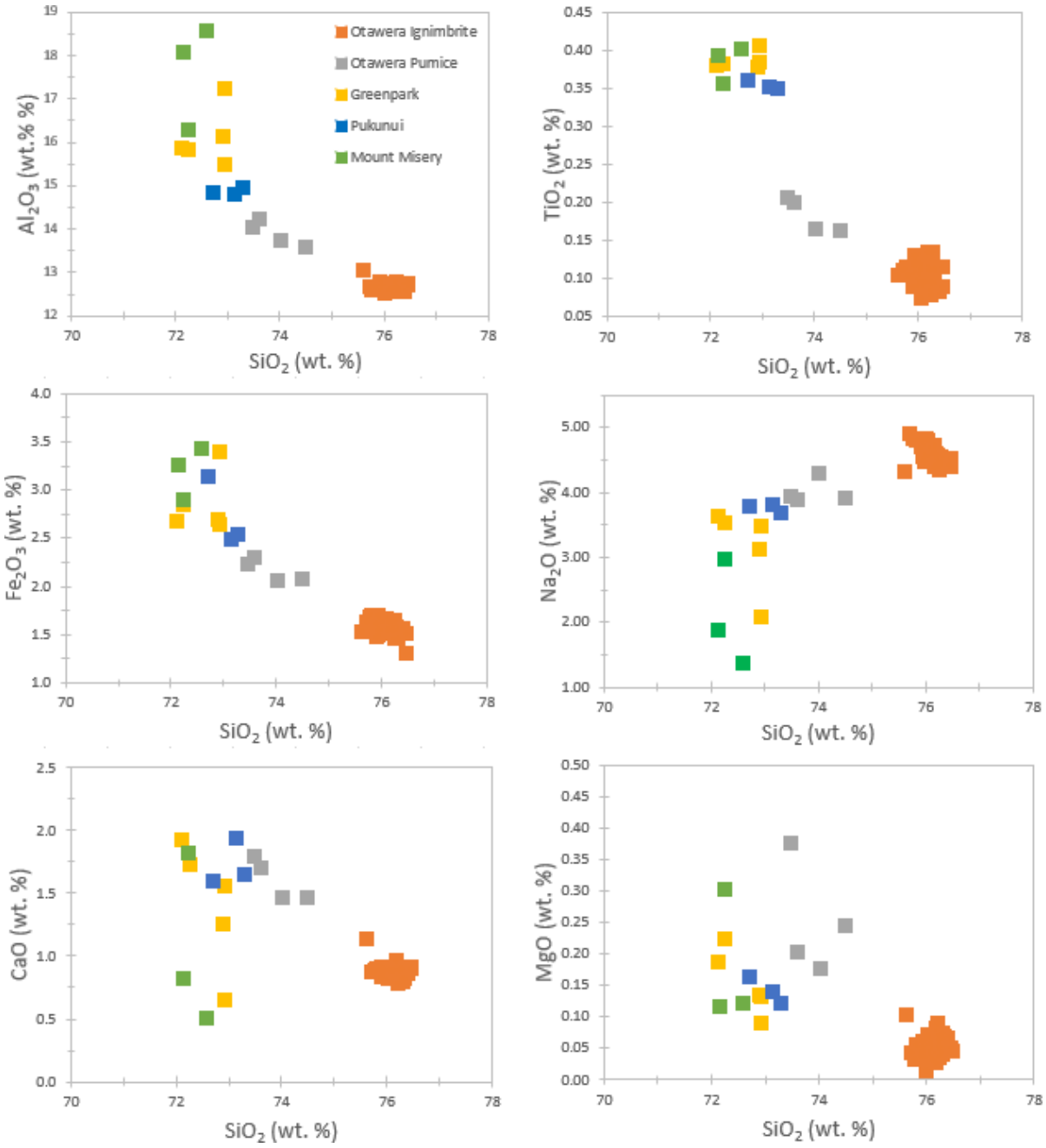

Figure 6.2: Harker plots for the SiO2 versus Al2O3, TiO2, Fe2O3, Na2O, CaO, MgO major elements, measured in wt. % with a legend shown in the top left graph.

6.4 Trace element geochemistry

Harker variation plots were made for five trace elements, niobium (Nb), zirconium (Zr), rubidium (Rb), strontium (Sr), and barium (Ba), which are shown in Figure 6.3. The trace elements selected had relatively high concentrations and were commonly used trace elements in other studies.

6.4.1 Mount Misery lavas

The Rb values showed flat profiles with an indiscernible trend. The zirconium and strontium plots, when only considering the lava data points, show a positive linear relationship. Maungatūtū/Mount Misery often sat on the lower end of the ranges for each plot excluding rubidium, showing the data points as slightly different from the other two domes.

The relationships shown in the Harker plots are linear, with weak to moderate trend-lines. The trace element data for Nb had an abundance ranging from 5 – 8 ppm, Zr from 174 – 252 ppm. Rb from 110 – 124 ppm. Sr ranges from 46 – 134 ppm, while Ba had abundances between 646 – 934 ppm.

High zirconium is a characteristic used in previous studies to separate the Minden rhyolites, with the Mount Misery series expected to range between 207 – 285 ppm (Briggs et al. 2005). The data from the 13 samples analysed gives a current zirconium range slightly lower than this, from 174 – 252 ppm. Maungatūtū/Mount Misery is shown on the Harker variation plot as having the lowest zirconium content. The zirconium content for all three domes appears to be high enough to continue to classify the Mount Misery group as high zirconium.

6.4.2 Otawera ignimbrite, pumice and glass

The glass and pumice data (Figure 6.3) show moderate to strong linear trends. The glass data for zirconium shows a large range, greater than both the pumice and lava data. Niobium shows a strong positive relationship, while strontium is showing a moderate negative relationship between pumice and glass, which are the trends that are the most easily identifiable. Most appeared as flat profiles from pumice to glass, especially rubidium and barium, because of the range of each element from the glass data and the small sample size of pumice.

In these rock concentrations, the abundance for Rb was 112 – 121 ppm for pumice, and 126.65 – 199.32 ppm for glass. The concentrations of Sr were 143 - 117 ppm for pumice and 36.46 – 92.23 ppm for glass. Zr abundance values were 199 – 228 ppm for pumice and 110.88 – 292.32 ppm for glass. The pumice data for Ba showed a smaller range than the lavas at 736 – 785 ppm, and the glass data had a Ba abundance from 436.45 – 983.60 ppm, much larger than both the lavas and pumice. Nb ranges from 5 – 6 ppm for the pumice data, and 7.33 – 10.14 ppm for glass. The trace element data from the Otawera glass and pumice are very similar to the Mount Misery series lavas, where only the SiO_2 content separates them.

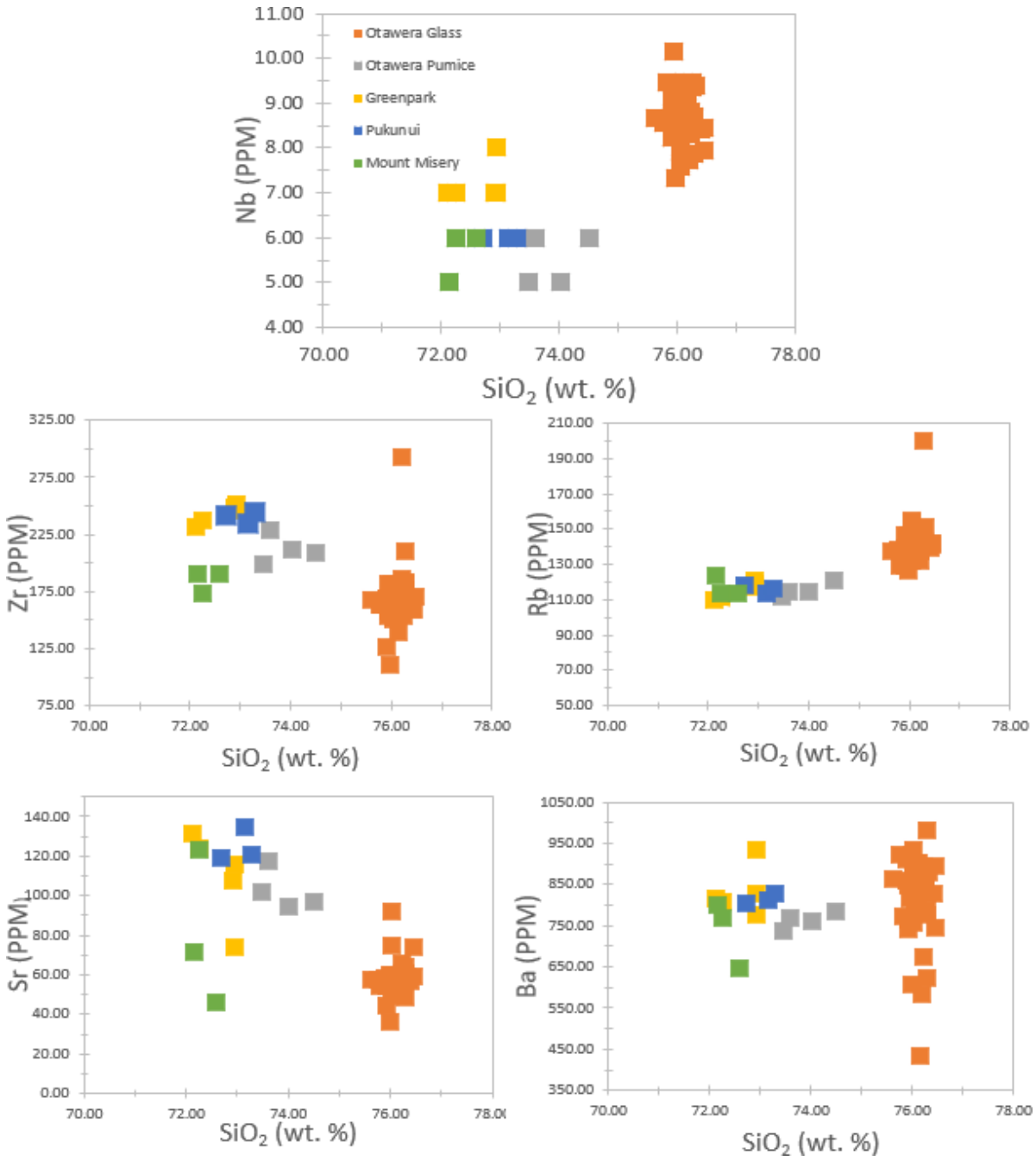

Figure 6.3: Harker variation diagrams for trace elements niobium (Nb), zirconium (Zr), rubidium (Rb), strontium (Sr), and barium (Ba) versus SiO_2 for glass, pumice and lava samples from the Mount Misery group and Otawera ignimbrite pumice and glass.

Chapter Seven

Discussion and Conclusions

7.1 Introduction

This chapter discusses the devitrification and alteration processes occurring within the Mount Misery rhyolites, the link between the Otawera ignimbrite and Pukunui rhyolite and emplacement mechanisms. Secondary and weathering alteration will be addressed. The interpretation is then followed by a discussion regarding like origins and influences of the Mount Misery series dome growth, and the conclusions.

7.2 Pukunui

The current peak of the Pukunui Dome is at 364 m above sea level while the base is 90 m above sea level, meaning the dome height is 274 m; with a width of ~ 1230 m. As this is a quarry, the original peak would have been higher as there is a pā site present, that would have been part of the peak, which has remained untouched at the top of the quarry (Figure 7.1). The key feature of the Pukunui rhyolite was quartz veining, outlined in the petrology chapter, present in both optical microscopy and SEM-EDS. The veins appeared in the rock samples as flow bands. There were no whole quartz phenocrysts present in the bands, implying that they are present as a feature of secondary alteration.

Figure 7.1: Peak of the Pukunui dome, showing the pā site at the top, with flow folding visible above the car.

There was a sub-vertical altered zone at the south side of the quarry face (Figure 4.3A), likely to be a zone of shearing that had undergone alteration through weathering fluids. In the field, this had a clay texture and appeared to be friable. This appears to be an area of massive rhyolite that has undergone secondary alteration or weathering to clay. Adjacent to the altered zone, there was an area with large-scale flow folding present (Figure 7.1). The strain rate of lava deformation commonly decreases downslope, as the lava loses heat through cooling as it moves away from the source (Smith, 2002). This implies that the area shown with large flow folds must have been close to the vent source. As Pukunui is situated atop the Otawa andesite, the morphology of the original Otawa area is likely to have influenced the morphology of the dome. The vent may have been positioned in a scar in the Otawa andesite, so the Pukunui dome infilled it. As the lava filled the scar and moved over ridges of the Otawa andesite, the lava folded internally to produce the flow folds seen today.

7.3 Maungatūtū/Mount Misery

The Maungatūtū/Mount Misery dome is presently 478 m a.s.l, > 130 m high above its base, and ~ 4877 m wide, covering a far greater width than the other two domes. The phenocrysts found in all Maungatūtū/Mount Misery samples were larger than at the other two domes, with a greater abundance of quartz, as well as pyroxenes. The abundance of large pyroxene phenocrysts and quartz may be indicative of a crystal rich magma, which means the Maungatūtū/Mount Misery dome differs from Pukunui and Greenpark in this regard.

An autobrecciated outcrop was found at stop three, identified by a breadcrust texture. Autobrecciation is when the surface of a lava cools and hardens, while the internal lava flow consistently breaks up the cooled crust and carries blocks of the solidified rock further forward (Kilburn, 2004). There needs to be large enough strain conditions imposed by the new lava, causing failure within the solid rock and transforming the lava from continuous to fragmented. The limiting conditions created by an autobreccia mean that for a lava to flow, complete autobrecciation must occur for the front to continue (Kilburn, 2004).

7.4 Greenpark

The Greenpark dome is ~379 m a.s.l, presently ~ 115 m high above its base, and ~ 902 m wide, which is the smallest width of the three domes. The quarry was visibly split into an area of lighter on the east and darker rhyolite on the west. The quarry owners have referred to the darker rhyolite as andesite and the lighter as rhyolite, however after petrographic and geochemical analysis of each type, they have both been classified as rhyolite. The lighter rhyolite had higher levels of devitrification, and had a more crystalline groundmass than the darker side. The darker rhyolite has a glassier composition, giving it a darker appearance. The

upper west side of the quarry was not as weathered as the lower east half. Common devitrification products are quartz, sanidine and tridymite (Rowe et al. 2012), which were typical minerals found in the lighter half of Greenpark [section 5.3.3] but not in the darker half.

The sub-circular crystalline inclusions identified in five of the twelve samples were an intriguing find. They were found in samples from all areas of the quarry, not limited to the 'light' and 'dark' sides. They appear similar to radiating spherulites, but smaller and with different internal textures. They are an alteration feature within a groundmass, also composed of K-feldspars. The internal crystals forming these sub-circular inclusions are not needle like, as seen in spherulites, but are blockier. This may imply that the internal part of an original spherulite may have been recrystallised into a compact, intergranular quartz-feldspar aggregate through alteration, forming these inclusions (McPhie et al. 1993).

7.5 Comparisons

The groundmasses of each dome vary; however, they have similar elemental compositions at various stages of secondary alteration. Flow bands were present in Pukunui and Greenpark, while Maungatūtū/Mount Misery had more spherulitic textures and a devitrified groundmass. They were all fine-grained, almost cryptocrystalline, with euhedral laths of feldspar. Each dome included sanidine in the groundmass, at different stages of alteration.

Phenocryst growth shown [sections 5.2.1 – 5.2.4] varies between domes. Maungatūtū/Mount Misery had much larger phenocrysts, and a greater abundance of quartz than the other two domes. As well as this, radiating spherulites were a common feature. The crystal abundance of the Maungatūtū/Mount Misery lavas implies that the magma drew up a crystal rich part of the chamber. Pyroxenes were found in both Maungatūtū/Mount Misery and Greenpark, however in Maungatūtū/Mount Misery they were much larger, with resorption features such as embayments present.

Flow banding was found at Pukunui and Greenpark, while Maungatūtū/Mount Misery appeared massive. The geomorphological differences between Pukunui, Greenpark and Maungatūtū/Mount Misery may be because the first two have been quarried, showing more of the inner dome features, and Maungatūtū/Mount Misery has not. The flow banding was quartz and feldspar dominated, showing a crystal alignment along linear planes. Often, the banding was thin (<1 cm) but was found at both domes to be thicker (> 3 cm) with an increase in elevation. The Pukunui thin bands were analysed under SEM-EDS and determined to be pure quartz. Folds and flows are typical of silicic lavas, and are found laterally at Pukunui

and Greenpark. Flow bands may be primary; directly related to the lava flow, or secondary; occurring during synemplacement deformation of the lava (Cioni and Funedda, 2005). Flow banding is a characteristic of flow related deformation, and occurs commonly in lower units depending on strain and the progressive deformation of the lower lava flows (Cioni and Funedda, 2005). This was an obvious feature at the Greenpark dome, where only the bottom layers (stops 1-3) showed thin flow banding. The Pukunui dome flow bands are likely enhanced by secondary alteration due to quartz dominant composition.

In chapter six, the Mount Misery series geochemical compositions for the three individual domes show a relationship. This implies that these lavas are related, sharing the same magma source but erupting from three different vents. Figures 6.2 and 6.3 show some differences between the domes, such as CaO and MgO for major elements, and Sr for trace elements. However, with other elements the trends in each dome are comparable.

7.6 Pukunui pyroclastic succession

Chapter five analysed the thin sections of the Pukunui pyroclastic succession, Otawera ignimbrite pumice and the Pukunui lavas. All three showed similar mineral compositions, with dominant plagioclase phenocrysts as well as hornblende and opaques being common in both ignimbrites and lava. Otawera pumice clasts were taken from M. Prentice from a separate ignimbrite unit, as the pumice clasts found at Pukunui were too small to be sampled for geochemistry, and also weathered. The andesite lithic analysed matches the Otawa andesite, which underlies the Pukunui dome. Characteristically, Otawa andesite is hornblende and pyroxene rich, comparable to the crystal rich andesite found in the Pukunui pyroclastic succession.

Results show that there is a strong correlation between the Pukunui lava and the Pukunui pyroclastic succession. The data presented in chapters five and six give provide petrographic and field evidence to support that the Pukunui pyroclastic deposit correlates to the Otawera ignimbrite, which was probably emplaced as a result of a collapse at the Pukunui rhyolite dome. After establishing that the Pukunui pyroclastic succession correlates to the Otawera ignimbrite, the relationship between the Otawera ignimbrite and the three domes of the Mount Misery series was assessed. To achieve this geochemical pumice and glass analysis from samples of the Otawera glass and pumice were compared to geochemical analysis of the domes.

The Otawera pumice and glass had a similar elemental composition to the lava, consistent with a correlation. In the major element geochemistry data, Pukunui and the Otawera glass

data showed relationships in the plots for CaO, Na_2O, Fe_2O_3 and Al_2O_3 (Figure 6.2). In these Harker plots, they had either a close data set or showed an obvious trendline. In Figure 6.3, every minor element Harker plot showed a relationship between Pukunui and Otawera data.

Prentice et al. (2022) identified the Otawera ignimbrite as a new ignimbrite unit that was non-welded and composed of multiple sub-units. Typically, it is fine-grained, with lithic (dominantly andesite) concentration zones in its basal layers, and phenocrysts of plagioclase, orthopyroxene and hornblende set in a crystal-rich vitroclastic matrix. This description compares with findings in chapters four and five, where the outcrop was described in the field area and through the stratigraphic log. Primary phenocrysts found in the Pukunui pyroclastic succession were pyroxene, plagioclase and hornblende, matching the Otawera ignimbrite description, with the same crystal-rich matrix, matching the Otawera ignimbrite with the Pukunui dome petrographically.

Units A-F identified at Pukunui have been characterised as one eruption event, and match the characteristics described above of the Otawera ignimbrite. The stratigraphic log (Figure 4.5) visualises the units found. Unit A is an ignimbrite with an andesite rich basal layer, representing the initial pyroclastic flow of the eruption. Unit B was an ash layer, possibly caused by air-fall, or settling of the ash cloud above the unit A ignimbrite. Unit C was a thin ignimbrite unit with the same fine-grained texture, crystal and pumice rich characteristics. Unit D was a thin ignimbrite layer featuring an upper accretionary lapilli zone. Units E-F were massive ignimbrites, with unit F featuring a layer of ash at the top of the pyroclastic succession. These changes in units from ignimbrites to ash fall may imply changes in eruption intensity, with the ignimbrites representing pulses and flows in the eruption, or partial collapse of the dome. Mild lava dome eruptions, linked to collapsing plumes may commonly result in thin pyroclastic deposits dominated by fine ash, which is what is seen in the field at Pukunui (Calder et al. 2015). The two separate units appear to both be the Otawera ignimbrite based on the petrographic analysis, with an ash flow in between units representing a change in eruption style.

The accretionary lapilli found in unit D are tightly bound, spherical particles which are common in phreatomagmatic eruptions, appearing at Pukunui as a nucleus surrounded by fine ash. Being found in a pyroclastic flow is rare, and not all require water condensation for formation (Gilbert and Lane, 1994). Aggregates tend to grow within plumes through contact with other particles, followed by binding of solid and liquid phases. Breaking up of aggregates is common in violent eruptions and tend to not lead to accretionary lapilli formation (Gilbert and Lane, 1994), so this implies the eruption occurring at Pukunui may have been steadier to avoid this happening at the time of eruption.

7.7 Devitrification of the Mount Misery Rhyolites

Glass alteration is common in older rocks, as glass tends to be thermodynamically unstable and devitrifies over long periods of time (G. Lofgren, 1971). Spherulites are an identifiable feature of high temperature devitrification within natural glass, and the morphology of spherulites depends on their temperature at formation (McPhie et al. 1993). The length of the individual crystals comprising the spherulite increases with the temperature of formation, and the internal fibre of the crystal can be recrystallised to a quartz-feldspar aggregate in later alteration stages; but typically, they are formed from alkali feldspars or quartz (McPhie et al. 1993).

Spherulites, radiating and non-radiating tended to be found in brown groundmass areas. The brown groundmass areas, especially in the Maungatūtū/Mount Misery samples are composed of sanidine. The groundmass of the Maungatūtū/Mount Misery rhyolite comprises microlitic glass, with microlites appearing in a non to partially radiating pattern, which through SEM-EDS analysis identifies these microlites as K-feldspars (sanidine), which is consistent with McPhie et al. (1993). Fan shaped and irregular fibrous arrays are observed as a result of overgrowth, meaning not all sanidine crystals appear as perfectly radiating. Sanidine also comprised the sub-circular crystalline inclusions found at Greenpark, with the possibility that they are a form of spherulite as they have similar circular shapes.

Sanidine was a commonly detected mineral in every XRD sample that was analysed. This was an unexpected result as sanidine does not normally occur in the Tauranga Volcanic Centre as a phenocryst, except in the Bowentown dome (Cook, 2016; Namaliu, 2021; Prentice et al. 2022). There were no whole phenocrysts of sanidine found. Hence, sanidine was only identified as a part of the groundmass in SEM-EDS.

Quartz flow banding features may be indicative of shear strain deformation within the rhyolites (White et al. 1982), occurring at lower temperatures (above ground) that favour the dislocation creep of minerals within the rhyolite that were present at the time of eruption. Slow strain rates can cause deformation by dislocation processes within the rock, with re-crystallisation acting as a key part of the process. There is a continuous reduction of the recrystallised grains, and deformation creates a homogenous, ultra-fine-grained texture within the quartz veins (White et al. 1982). The flow banding present in sample 1TB was shown under the SEM to have alternating ‘smooth’ and ‘rough’ textures. The mineralogical

compositions were determined by running EDS analysis, which showed the rougher looking areas as plagioclase feldspar-rich and the smooth areas as pure quartz. The implication of quartz occurring in the form of alternating bands is that SiO_2 was segregated after emplacement. There are no large quartz phenocrysts present in the quartz banding, which would imply that they had developed during cooling and so therefore needed to occur as a groundmass crystallisation or devitrification (dislocation creep) process. The transition contact within the veins may imply fluidal mixing along the boundary.

7.8 Dome emplacement

The Otawa andesite is the oldest in this field area at 2.95 to 2.54 Ma, with Maungatūtū/Mount Misery being dated close in age at 2.69 Ma (Briggs et al. 2005), meaning these two volcanic areas would have been active at the same time. The Otawera ignimbrite is likely the youngest in the area, at 2.21 ± 0.13 Ma. Pukunui and Greenpark have not been dated individually, but Pukunui must be younger than the Otawa andesite yet older than Otawera due to the law of superposition.

Lava dome growth can be endogenous or exogenous, and this emplacement style can be determined by specific rock characteristics. Shearing commonly changes the physical property of the lava, indicating the kinetics involved in the eruption process, as shearing is usually related to exogenous growth (Hale and Wadge 2008). Shear bands are normally formed on the junction of the conduit and base of the dome where pressure is the greatest, and so would be an identifiable feature if present because they would form early on in an eruption and move down the dome as growth continues. Endogenous dome growth tends to expand laterally, followed by vertically, and vertical growth tends to reduce the flow laterally at the base of the dome. In endogenous domes, crystal formation within the magma is greater because there is more time for crystal growth, and a fluidal lava is more likely due to ongoing higher temperatures (Hale et al. 2008). Shearing was not seen as a primary feature at Pukunui, Maungatūtū/Mount Misery or Greenpark, however secondary shear strain deformation was noted, while features such as large crystals and flow banding were common. These factors therefore imply that the Mount Misery series are the result of endogenous lava dome growth. There may have been a transition between endogenous and exogenous dome growth at points, but in the field areas there was no solid evidence to prove this.

Pukunui and Greenpark are localised domes covering a small spatial area, making it likely that they are a singular, individual dome from source, with potentially each from a fissure sourced from the main vent. Pukunui and Greenpark are both heavily quarried areas and would have previously extended over larger areas. Maungatūtū/Mount Misery covers a larger

spatial area, appearing to extend through Rowe Road based on comparative petrographic analysis of samples from both locations. Maungatūtū/Mount Misery is also likely sourced from a single, crystal rich magma. Although it covers a large spatial area, there is only one notable peak, which may imply a greater volume of magma erupted that was able to flow over a larger area, while Pukunui and Greenpark may have had lower volumes. The autobrecciation of the Maungatūtū/Mount Misery lava may imply the lava flow moved with force downslope, which would support the idea that it covers a larger spatial area.

7.9 Conclusions

The overall conclusions of this study are outlined below:

- The Mount Misery series are a group of rhyolite domes in the Bay of Plenty, north-east of Tauranga. The Pukunui dome overlies the Otawa andesite, and has an ignimbrite succession attached to its flank, which was correlated to the Otawera ignimbrite of the Papamoa Formation.

- Maungatūtū/Mount Misery was identified as the largest rhyolite dome of the three, which also had the largest phenocrysts. Autobrecciation was a characteristic at the Maungatūtū/Mount Misery dome, and so the lava flow here would have experienced cooling and the rebreaking of a crust of the lava, creating a forced flow directed by large volumes of magma moving downslope.

- Greenpark was previously segregated by its ‘light’ rhyolite and ‘dark’ andesite areas of the Oropi quarry. Petrographic and geochemical analysis has proven these areas of the quarry to both be rhyolitic in composition, with no andesite present. The difference in colour is a result of devitrification.

- The Pukunui pyroclastic succession includes proximal ignimbrites and intercalated fall deposits on the flank of the Pukunui dome, and was correlated to the Otawera ignimbrite. The pyroclastic succession was two massive ignimbrites separated by pyroclastic fall, which highlighted a change in eruption style from flows to fall. Accretionary lapilli were found in unit D, are rare find in a pyroclastic flow. This discovery may imply the steady state required of the eruption plume for accretionary lapilli to form.

- The lava compositions of the Mount Misery series are similar, showing petrogenetically related magmas. Maungatūtū/Mount Misery had a more crystal rich magma than the other two domes. Common phenocrysts found at all three are plagioclase, quartz, and pyroxenes; at Maungatūtū/Mount Misery the phenocrysts were more abundant and were larger in size than Pukunui and Greenpark.

- Devitrification is a common process altering all domes. Sanidine is common in the groundmass as radiating spherulites or as a new find of sub-circular crystalline inclusions. Slow strain caused deformation as a secondary process, forming pure quartz veins found in Pukunui, which shows that there was alteration occurring after the deposition of the rock at lower temperatures.

- The dome emplacement processes that occurred involved endogenous growth of each dome, with the volume of magma erupting varying. Shearing was not seen as a primary feature at any of the domes, while flow banding and large crystal growth was noted, which classified the Mount Misery rhyolites as endogenous. It is likely that Pukunui, Maungatūtū/Mount Misery and Greenpark were sourced from a single, crystal rich magma and erupted from separate vents along a fissure.

7.10 Future work

Work that would benefit the Mount Misery rhyolite series and the general Tauranga area in the future would entail greater detail in mapping and aging of all units in the area. Limitations throughout this thesis have been the lack of current detail on the Mount Misery series. Dating done on both Pukunui and Greenpark as individual domes would contribute to the understanding of the eruptive history of the three domes, as this would give definitive timelines of oldest to youngest units in the area. Better spatial constraints of each dome would be beneficial for the land and quarry owners. In future, more detailed geochemistry of trace elements for a greater volume of samples could be used to find out the temperature the domes were during emplacement. Melt inclusions within phenocrysts were found in all three domes, could be geochemically analysed to understand the changes to the mineral assemblage.

References

Adams, C.J., Graham, I.J., Seward, D., Skinner, D.N.B., & Moore, P.R. (1994). Geochronological and geochemical evolution of late Cenozoic volcanism in the Coromandel Peninsula, New Zealand. *New Zealand Journal of Geology and Geophysics, 37* (3). 359-379.

Allen, S.R., & McPhie, J. (2003). Phenocryst fragments in rhyolitic lavas and lava domes. *Journal of Volcanology and Geothermal Research, 126* (3-4). 263-283.

Ashwell, P.A., Kennedy, B.M., Gravley, D.M., von Aulock, F.W., & Cole, J.W. (2013). Insights into caldera and regional structures and magma body distribution from lava domes at Rotorua Caldera, New Zealand. *Journal of Volcanology and Geothermal Research, 258*. 187-202.

Ashwell, P.A. (2014). Controls on rhyolite lava dome eruptions in the Taupo Volcanic Zone. *(PhD Thesis, University of Canterbury).*

Ball, J.L., Stauffer, P.H., Calder, E.S., & Valentine, G.A. (2015). The hydrothermal alteration of cooling lava domes. *Bulletin of Volcanology, 77* (102).

Barker, S.J., Wilson, C.J.N., Illsley-Kemp, F., Leonard, G.S., Mestel, E.R.H., Mauriohooho, K., & Charlier, B.L.A. (2020). Taupo: an overview of New Zealand's youngest supervolcano. *New Zealand Journal of Geology and Geophysics, 64* (2-3). 320-346.

Bebbington, M.S. (2020). Temporal-volume probabilistic hazard model for a supervolcano: Taupo, New Zealand. *Earth and Planetary Science Letters, 536*. 116-141.

Briggs, R.M., & Fulton, B.W.J. (1990). Volcanism, structure, and petrology of the Whiritoa-Whangamata coastal section, Coromandel Volcanic Zone, New Zealand: Facies model evidence for the Tunaiti caldera. *New Zealand Journal of Geology and Geophysics, 33* (4). 623-633.

Briggs, R.M., Hall, G.J., Harmsworth, G.R., & Hollis, A.G., Houghton, B.F., Hughes, G.R., Morgan, M.D., & Whitbread-Edwards, A.R. (1996). Geology of the Tauranga area: scale 1:50,000. *Waikato: Institute of Geological and Nuclear Sciences 1:50,000 map.* 5 p.

Briggs, R.M., Houghton, B.F., McWilliams, M., & Wilson, C.J.N. (2005). $^{40}Ar/^{39}Ar$ ages of silicic volcanic rocks in the Tauranga-Kaimai area, New Zealand: Dating the transition between volcanism in the Coromandel Arc and the Taupo Volcanic Zone. *New Zealand Journal of Geology and Geophysics, 48* (3). 459-469.

Brothers, R.N. (1984). Subduction regression and oceanward migration of volcanism, North Island, New Zealand. *Letters to Nature, 39*. 698-700.

Calder, E.S., Lavallee, Y., Kendrick, J.E., & Bernstein, M. (2015). Lava Dome Eruptions. In Sigurdsson, H., Houghton, B., McNutt, S., Rymer, H., & Stix, J (Eds.), *The Encyclopedia of Volcanoes* (pp. 343-363).

Cerling, T.E., Brown, F.H., & Bowman, J.R. (1985). Low-temperature alteration of volcanic glass: Hydration, Na, K, ^{18}O and Ar mobility. *Chemical Geology: Isotope Geoscience section, 52* (3-4). 281-293.

Chambefort, I., Lewis, B., Wilson, C.J.N., Rae, A.J., Coutts, C., Bignall, G., & Ireland, T.R. (2014). Stratigraphy and structure of the Ngatamariki geothermal system from new zircon U-Pb

geochronology: Implications for Taupo Volcanic Zone evolution. *Journal of Volcanology and Geothermal Research, 274*. 51-70.

Cioni, R., & Funedda, A. (2005). *Structural geology of crystal-rich, silicic lava flows: A case study from San Pietro island (Sardinia, Italy).* Kinematics and Dynamics of Lava Flows, Geological Society of America.

Cook, E.T. (2016). Felsic volcanism in the eastern Waihi area; process origins of the Corbett and Ratarua ignimbrites and the Hikurangi Rhyolite. *(MSc Thesis, University of Waikato).*

de Silva, S., & Lindsay, J.M. (2015). Primary Volcanic Landforms. In Sigurdsson, H., Houghton, B., McNutt, S., Rymer, H., & Stix, J (Eds.), *The Encyclopedia of Volcanoes* (pp. 273-299).

Downs, D.T., Rowland, J.V., Wilson, C.J.N., Rosenberg, M.D., Leonard, G.S., & Calvert, A.T. (2014). Evolution of the intra-arc Taupo-Reporoa Basin within the Taupo Volcanic Zone of New Zealand. *Geosphere*. 185-206.

Druitt, T.H., Young, S.R., Baptie, B., Bonadonna, C., Calder, E.S., Clarke, A.B., Cole, P.D., Harford, C.L., Herd, R.A., Luckett, R., Ryan, G., & Voight, B. (2002). The eruption of Soufriere Hills volcano, Montserrat, from 1995 to 1999. *Geological Society, London, Memoirs, 21*. 281-306.

Fink, J.H., & Griffiths, R.W. (1998). Morphology, eruption rates, and rheology of lava domes: Insights from laboratory models. *Journal of Geophysical Research: Solid Earth, 103* (B1). 527-545.

Fisher, R.V., & Schmincke, H.U. (1984). *Alteration of Volcanic Glass*. Pyroclastic Rocks. Springer, Berlin, Heidelberg. 312-345.

Gilbert, J.S., & Lane, S.J. (1994). The origin of accretionary lapilli. *Bulletin of Volcanology, 56*. 398-411.

Hale, A.J., & Wadge, G. (2008). The transition from endogenous to exogenous growth of lava domes with the development of shear bands. *Journal of Volcanology and Geothermal Research, 171 (3-4).* 237-257.

Hale, A.J., Calder, E.S., Loughlin, S.C., Wage, G., & Ryan, G.A. (2009). Modelling the lava dome extruded at Soufriere Hills volcano, Montserrat, August 2005-May 2006: Part II: Rockfall activity and talus deformation. *Journal of Volcanology and Geothermal Research, 187* (1-2). 69-84.

Harnett, C.E., & Heap, M.J. (2021). Mechanical and topographic factors influencing lava dome growth and collapse. *Journal of Volcanology and Geothermal Research, 420*.

Higgins, M.D. (1996). Magma dynamics beneath Kameni volcano, Thera, Greece, as revealed by crystal size and shape measurements. *Journal of Volcanology and Geothermal Research, 70* (1-2). 37-48.

Hollis, A.G. (1995). Volcanic geology of the central Tauranga basin, New Zealand. *(MSc Thesis, University of Waikato).*

Houghton, B.F., & Cuthbertson, A,S. (1989). *Sheet T14 BD, - Kaimai Geological map of New Zealand 1:50 000.* Wellington, New Zealand, Department of Scientific and Industrial Research.

Hughes, G.R. (1993). Volcanic geology of the eastern Tauranga basin and Papamoa range. *(MSc Thesis, University of Waikato).*

Huppert, H.E., Shepherd, J.B., Sigurdsson, H., & Sparks, R.S.J. (1982). On lava dome growth with application to the 1979 lava extrusion of the Soufriére of St. Vincent. *Journal of Volcanology and Geothermal Research, 14.* 199-222.

Jerram, D.A., Dobson, K.J., Morgan, D.J., & Pankhurst, M.J. (2018). *The Petrogenesis of Magmatic Systems: Using Igneous Textures to Understand Magmatic Processes.* Volcanic and Igneous Plumbing Systems. (192-224).

J Swap Contractors Ltd. (2022). *Tauranga Quarry.* Retrieved July 14th, 2022, from https://jswap.co.nz/location/tauranga-quarry/.

Julian, H.A. (2016). *Volcanology of the Owharoa and Waikino ignimbrites, Waihi, Coromandel Volcanic Zone*. (MSc Thesis, University of Waikato).

Kilburn, C.R.J. (2004). Fracturing as a quantitative indicator of lava flow dynamics. *Journal of Volcanology and Geothermal Research, 132 (2-3).* 209-224.

Kokelaar, B.P. (2002). Setting, chronology and consequences of the eruption of Soufriere Hills volcano, Montserrat (1995-1999). *Geological Society, London, Memoirs, 21*. 1-43.

Laird, M.G., & Bradshaw, J.D. (2003). The break-up of a long-term relationship: the Cretaceous separation of New Zealand from Gondwana. *Gondwana Research, 7* (1). 273-286.

Le Maitre, R. W., Streckeisen, A., Zanettin, B., Le Bas, M., Bonin, B., & Bateman, P. (2002). *Igneous rocks: a classification and glossary of terms: recommendations of the International Union of Geological Sciences Subcommission on the Systematics of Igneous Rocks.* Cambridge University Press.

Leonard, G. S. (2003). *The evolution of Maroa Volcanic Centre, Taupo Volcanic Zone, New Zealand*. (MSc Thesis, University of Canterbury).

Leonard, G.S., Begg, J.G., & Wilson, C.J.N. (2010). *Geology of the Rotorua area*. GNS Science, Lower Hutt, New Zealand.

Lofgren, G. (1971). Experimentally produced devitrification textures in natural rhyolitic glass. *GSA Bulletin, 82* (1). 111-124.

Malengreau, B., Skinner, D., Bromley, C., & Black, P. (2000). Geophysical characterisation of large silicic volcanic structures in the Coromandel Peninsula, New Zealand. *New Zealand Journal of Geology and Geophysics, 43* (2). 171-186.

Marshall, R.R. (1961). Devitrification of Natural Glass. *GSA Bulletin, 72*. 1493-1520.

McPhie, J., Doyle, M., & Allen, R. (1993). Volcanic textures: a guide to the interpretation of textures in volcanic rocks. *Centre for Ore Deposit and Exploration Studies, University of Tasmania, Hobart.*

Moore, P.R. (2011). Obsidian sources of the Coromandel Volcanic Zone, Northern New Zealand. *Journal of the Royal Society of New Zealand, 43* (1). 38-57.

Mortimer, N., Herzer, R.H., Gans, P.B., Laporte-Magoni, C., Calvert, A.T., & Bosch, D. (2007). Oligocene-Miocene tectonic evolution of the South Fiji Basin and Northland Plateau, SW Pacific Ocean: Evidence from petrology and dating of dredged rocks. *Marine Geology, 237* (1-2). 1-24.

Namaliu, M.D.M. (2021). Volcanic geology of the early Pleistocene ignimbrite succession in the western Papamoa Region, Bay of Plenty. *(MSc Thesis, University of Waikato).*

Pittari, A., Prentice, M.L., McLeod, O.E., Zadeh, E.Y., Kamp., P.J.J., Danisik, M., & Vincent, K.A. (2021). Inception of the modern North Island (New Zealand) volcanic settings: spatio-temporal patterns of volcanism between 3.0 and 0.9 Ma. *New Zealand Journal of Geology and Geophysics, 64* (2-3). 250-272.

Prentice, M., Pittari, A., Lowe, D.J., Kilgour, G., Kamp, P.J.J., & Namaliu, M. (2022). Linking proximal ignimbrites and coeval distal tephra deposits to establish a record of voluminous early quaternary (2.4-1.9 Ma) volcanism of the Tauranga Volcanic Centre, New Zealand. *Journal of Volcanology and Geothermal Research, in press*.

Rait, G., Chanier, F., & Waters, D.W. (1991). Landward-and seaward-directed thrusting accompanying the onset of subduction beneath New Zealand. *Geology, 19* (3). 230-233.

Rissmann, C., Nicol, A., Cole, J., Kennedy, B., Fairley, J., Christenson, B., Leybourne, M., Milicich, S., Ring, U., & Gravley, D. (2011). Fluid flow associated with silicic lava domes and faults, Ohaaki hydrothermal field, New Zealand. *Journal of Volcanology and Geothermal Research, 204* (1-4). 12-26.

Romano, C., Mungall, J.E., Sharp, T., & Dingwell, D.B. (1996). Tensile strengths of hydrous vesicular glasses: An experimental study. *American Mineralogist, 81*. 1148-1154.

Rowe, M.C., Ellis, B.S., & Lindeberg, A. (2012). Quantifying crystallisation and devitrification of rhyolites by means of X-ray diffraction and electron microprobe analysis. *American Mineralogist, 97* (10). 1685-1699.

RPL Services. (2022). *Metal aggregates to meet the demand of local businesses, Oropi Quarry*. Retrieved July 14th, 2022, from https://rplservices.co.nz/quarries

Rutherford, N.F. (1978). Fission-track age and trace element of geochemistry of some Minden Rhyolite obsidians. *New Zealand Journal of Geology and Geophysics, 21* (4). 443-448.

Scott, J.M. (2013). A review of the location and significance of the boundary between the Western Province and Eastern Province, New Zealand. *New Zealand Journal of Geology and Geophysics, 56* (4). 276-293.

Seebeck, H., Nicol, A., Stern, T.A., Bibby, H.M., & Stagpoole, V. (2010). Fault controls on the geometry and location of the Okataina Caldera, Taupo Volcanic Zone, New Zealand. *Journal of Volcanology and Geothermal Research, 190* (1-2). 136-151.

Shanks, W.C.P., Morgan, L., Balistrieri, L.S., & Alt, J.C. (2005). *Hydrothermal vent fluids, siliceous hydrothermal deposits, and hydrothermally altered sediments in Yellowstone Lake*. Montana State University.

Smith, J.V. (2002). Structural analysis of flow-related textures in lavas. *Earth-Science Reviews, 57 (3-4)*. 279-297.

Smith, N., Cassidy, J., Locke, C.A., Mauk, J.L., & Christie, A.B. (2006). The role of regional-scale faults in controlling a trapdoor caldera, Coromandel Peninsula, New Zealand. *Journal of Volcanology and Geothermal Research, 149* (3-4). 312-328.

Sparks, R.S.J. (1997). Causes and consequences of pressurisation in lava dome eruptions. *Earth and Planetary Science Letters, 150* (3-4). 177-189.

Swanson, S.E., Naney, M.T., Westrich, H.R., & Eichelberger, J.C. (1989). Crystallization history of Obsidian Dome, Inyo Domes, California. *Bulletin of Volcanology, 51*. 161-176.

Tauranga Historical Society. (1972). Journal of the Tauranga Historical Society (Inc.) *Publicity Printing Ltd., Tauranga,* (45). 8.

Vincent, K.A. (2012). *U-Pb dating of silicic volcanic rocks of the eastern Coromandel Peninsula*. (MSc Thesis, University of Waikato).

Voight, B. (2000). *Structural stability of andesite volcanoes and lava domes.* The Royal Society**.**

White, S.H., Evans, D.J., & Zhong, D.L. (1982). Fault rocks of the Moine Thrust Zone: Microstructures and Textures of Selected Mylonites. *Textures and Microstructures, 5.* 33-61.

Wilson, C.J.N., & Rowland, J.V. (2016). The volcanic, magmatic and tectonic setting of the Taupo Volcanic Zone, New Zealand, reviewed from a geothermal perspective. *Geothermics, 59B, 168-187.*

Appendices

Appendix A: Table of samples

Sample numbers:	W Number:	Location:	Easting (NZTM)	Northing (NZTM)	Elevation (m):	Analytical method applied on sample:	Sample type:
1CB, 1TB, 1CBA, 1WACB		Pukunui Quarry	1882219	5813947	365	TS *all* *1TB* – XRD, XRF, SEM	Rhyolite
2TB, 2CB		Pukunui Quarry	1882219	5813947	365	XRD, XRF, TS *all* *2CB* - SEM	Rhyolite
3TB, 3CB		Pukunui Quarry	1882219	5813947	365	TS *all* *3CB* – XRD, XRF	Rhyolite
S1		Mount Misery Farm	1880385	5810536	370	TS, XRD, XRF	Rhyolite
S2		Mount Misery Farm	1880442	5810658	370	TS, XRD, XRF	Rhyolite
S3, S3B		Mount Misery Farm	1880660	5810745	360	TS *all* *S3* - XRD, XRF	Rhyolite
TM		Mount Misery Farm	1880729	5810863	470	TS, XRD, XRF	Rhyolite
S7		Mount Misery Farm	1880829	5810822	440	TS	Rhyolite
S1, S1.1		Greenpark Quarry	1881720	5808987	285	TS *all* *S1.1* - XRD, XRF, SEM	Rhyolite
S2TB, S2MB		Greenpark Quarry	1881717	5809017	300	TS *all* *S2MB* – XRD, XRF	Rhyolite
S3MB, S3MBA		Greenpark Quarry	1881691	5809033	300	TS	Rhyolite
S4 DAR		Greenpark Quarry	1881678	5809086	330	TS, XRD, XRF	Rhyolite
S5E/L, S5W/H		Greenpark Quarry	1881732	5809118	340	TS	Rhyolite
S6AR, S6DAR		Greenpark Quarry	1881914	5809014	370	TS – *all* *S6DAR* – SEM, XRD, XRF	Rhyolite
Outcrop		End of Rowe Road, Tauranga	1882495	5811518	270	TS	Rhyolite
R Lithic, A lithic		Pukunui Quarry	1882624	5814712	150	TS *all*	Lithics

						R lithic - XRD, XRF	
1/1		Pukunui Quarry	1882624	5814712	150	TS	Bulk Ignimbrite
B/ ash		Pukunui Quarry	1882603	5814721	143	TS	Ash fall
C/ ign		Pukunui Quarry	1882603	5814721	143	TS	Ignimbrite
D/ ign		Pukunui Quarry	1882603	5814721	143	TS	Ignimbrite
E/ ign		Pukunui Quarry	1882603	5814721	143	TS	Ignimbrite
F/ ash		Pukunui Quarry	1882428	5814682	185	TS	Ash fall
F/ bottom		Pukunui Quarry	1882428	5814682	180	TS	Ignimbrite
P1, P2, P3, P4, P5, P6		Farm on Reid Road, Tauranga	1888211	5819449	80	TS – *P1, P2* XRF - *all*	Otawera Pumice

Appendix B: Raw XRF geochemical data

Sample Name	S1	S2	TM	2TB	2CB	3CB	R lithic	S1.1	S2TB
Major elements (XRF, wt.%) *(Raw data: all Fe expressed as Fe_2O_3)*									
SiO_2	72.58	72.14	72.25	73.14	72.71	73.29	61.99	72.93	72.93
Al_2O_3	18.58	18.07	16.27	14.79	14.84	14.97	17.5	15.5	17.26
TiO_2	0.4	0.39	0.36	0.35	0.36	0.35	0.75	0.38	0.41
MnO	0.06	0.06	0.03	0.01	0.02	0.02	0.08	0.02	0.02
Fe_2O_3	3.43	3.26	2.91	2.49	3.15	2.54	4.35	2.65	3.4
Na_2O	1.37	1.87	2.96	3.82	3.78	3.69	3.02	3.48	2.08
MgO	0.12	0.12	0.3	0.14	0.16	0.12	3.23	0.13	0.09
K_2O	2.9	3.23	3.06	3.25	3.33	3.33	1.5	3.29	3.14
CaO	0.51	0.82	1.82	1.94	1.60	1.65	7.44	1.56	0.66
P_2O_5	0.05	0.04	0.04	0.06	0.05	0.04	0.13	0.07	0.03
LOI (%)	5.52	4.91	2.86	1.51	1.64	1.82	0.64	2.3	5.01
Sum (%)	100.79	100.75	100.88	100.92	101.09	100.7	100.77	100.62	100.61
Trace elements (XRF, ppm)									
Sc	10	10	10	12	12	11	25	11	14
V	33	33	33	17	18	18	168	18	17
Cr	7	5	16	0	0	1	76	1	0
Co	8	12	9	7	10	8	38	12	9
Ni	3	3	4	3	3	3	12	3	3
Cu	9	11	7	7	7	6	17	7	8
Zn	61	47	56	40	46	50	58	44	47
Ga	19	19	19	17	17	16	18	17	19
As	6	7	7	8	9	9	8	6	5
Rb	113	124	113	114	118	116	51	117	121
Sr	46	72	123	134	119	121	287	116	74

Y	44	29	14	27	21	21	23	24	23
Zr	191	191	174	234	242	244	139	245	252
Nb	6	5	6	6	6	6	4	7	8
Mo	4	4	4	5	5	5	4	5	5
Sn	4	3	4	2	4	3	2	3	3
Sb	1	2	2	2	1	1	1	1	1
Cs	3	4	1	3	3	4	4	2	1
Ba	646	800	770	813	805	827	432	827	778
La	56	30	10	18	9	15	5	14	12
Ce	50	48	36	38	40	43	34	40	26
Nd	47	26	17	24	21	23	16	26	22
Tl	1	1	1	1	1	1	0	1	1
Pb	18	12	12	12	14	13	5	13	12
Th	14	14	13	13	14	12	6	13	13
U	3	4	3	3	3	3	3	3	4

Appendix B: Raw XRF geochemical data

Sample Name	S2MB	S4DAR	S6DAR	1	2	3	4
Major elements (XRF, wt.%) *(Raw data: all Fe expressed as Fe_2O_3)*							
SiO_2	72.9	72.25	72.11	74.02	73.6	74.5	73.47
Al_2O_3	16.15	15.83	15.85	13.73	14.23	13.61	14.03
TiO_2	0.38	0.38	0.38	0.17	0.2	0.16	0.21
MnO	0.02	0.02	0.03	0.05	0.05	0.05	0.05
Fe_2O_3	2.69	2.85	2.68	2.06	2.3	2.08	2.23
Na_2O	3.11	3.52	3.63	4.28	3.89	3.91	3.94
MgO	0.13	0.22	0.19	0.18	0.2	0.24	0.38
K_2O	3.29	3.14	3.13	4.01	3.78	3.95	3.86
CaO	1.26	1.73	1.92	1.46	1.7	1.46	1.8
P_2O_5	0.08	0.06	0.09	0.05	0.04	0.04	0.04
LOI (%)	2.98	2.36	2.07	4.63	4.22	4.61	5.55
Sum (%)	100.4	100.64	100.63	100.64	100.61	100.57	100.85
Trace elements (XRF, ppm)							
Sc	12	12	12	11	11	11	12
V	19	19	23	3	5	4	7
Cr	15	3	0	2	2	3	0
Co	9	7	7	19	12	11	9
Ni	3	3	3	3	3	3	3
Cu	8	7	6	6	5	7	5
Zn	46	49	47	52	51	51	51
Ga	17	17	18	16	17	16	16
As	7	6	8	8	9	9	9
Rb	119	111	110	115	115	121	112

Sr	108	124	131	95	117	97	102
Y	74	26	42	26	27	29	27
Zr	249	238	232	211	228	209	199
Nb	7	7	7	5	6	6	5
Mo	5	5	5	4	5	4	4
Sn	5	4	2	3	2	4	1
Sb	1	1	1	0	0	1	0
Cs	1	1	2	5	6	6	5
Ba	934	807	816	760	770	785	736
La	144	20	28	18	17	17	18
Ce	55	47	48	57	54	54	57
Nd	130	26	38	27	25	28	28
Tl	1	1	1	1	1	1	1
Pb	20	12	14	14	13	17	14
Th	13	13	12	11	11	13	11
U	4	3	3	4	3	4	3

Appendix C: XRD analysis and results

XRD ANALYSIS LIST

RHYOLITE	SAMPLE TYPE	SAMPLE NUMBER
PUKUNUI	**Bulk**	**2CB**
PUKUNUI	**Bulk**	**2TB**
PUKUNUI	**Bulk**	**3CB**
MT MISERY	**Bulk**	**TM**
MT MISERY	**Bulk**	**S1**
MT MISERY	**Bulk**	**S2**
MT MISERY	**Bulk**	**S3**
GREENPARK	**Bulk**	**S1.1**
GREENPARK	**Bulk**	**S2TB**
GREENPARK	**Bulk**	**S2MB**
GREENPARK	**Bulk**	**S4DAR**
GREENPARK	**Bulk**	**S6DAR**
PUKUNUI	**Bulk**	**R Lithic**

PUKUNUI RHYOLITES – 2CB

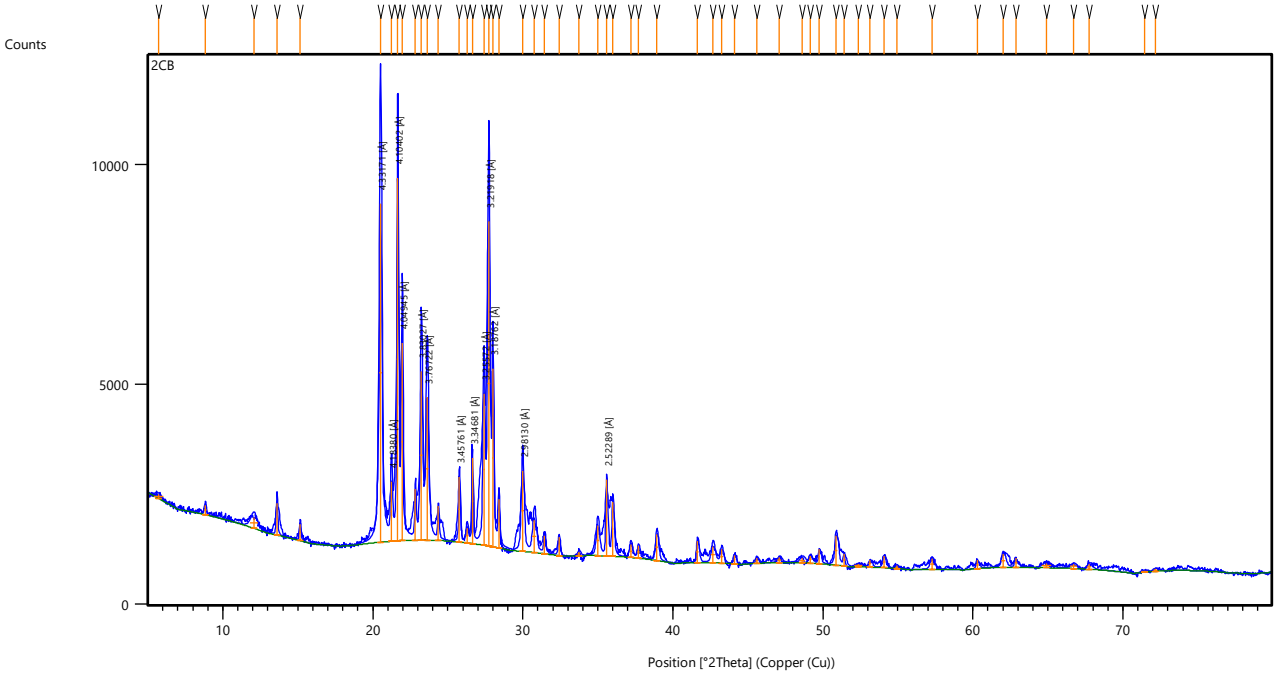

PUKUNUI RHYOLITES – 2TB

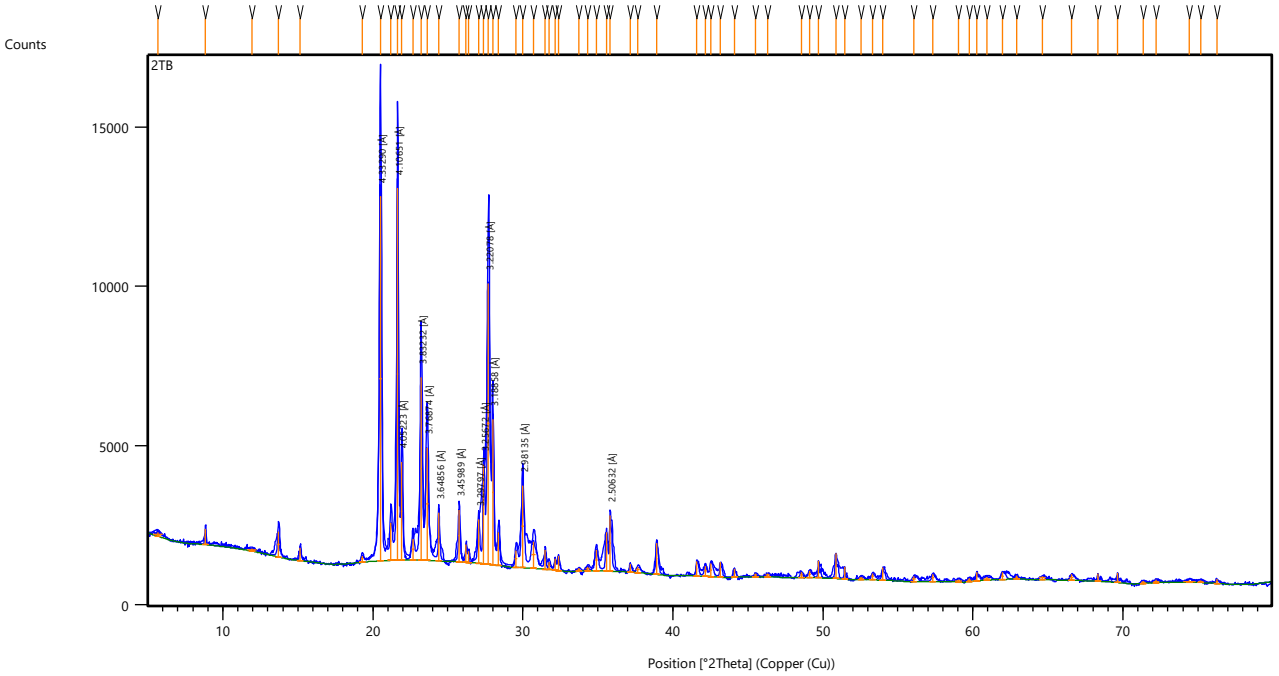

PUKUNUI RHYOLITES – 3CB

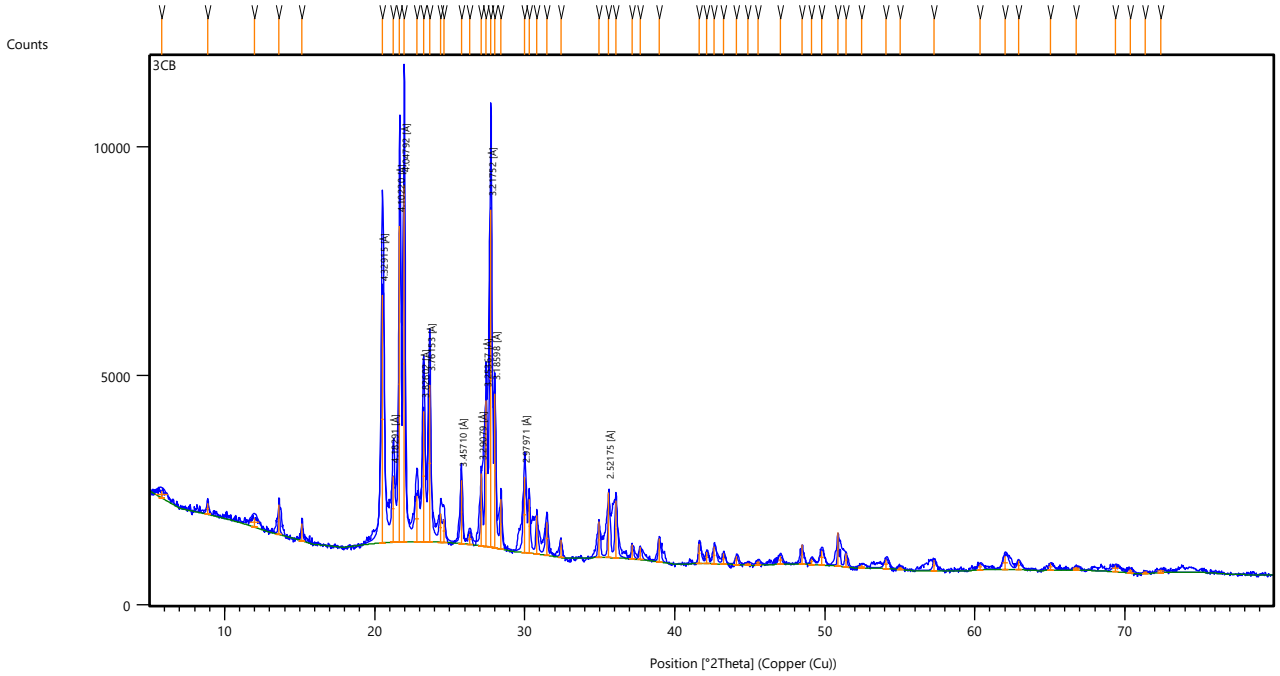

MAUNGATŪTŪ/MOUNT MISERY RHYOLITES – TM

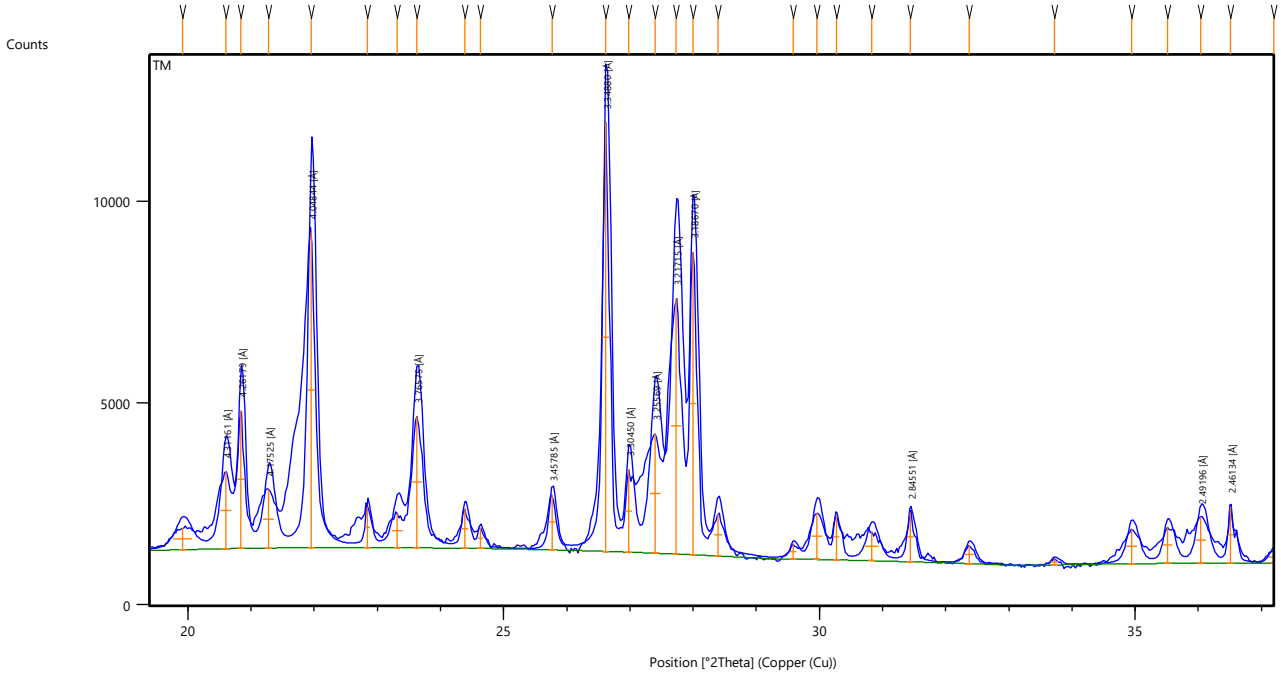

MAUNGATŪTŪ/MOUNT MISERY RHYOLITES – S1

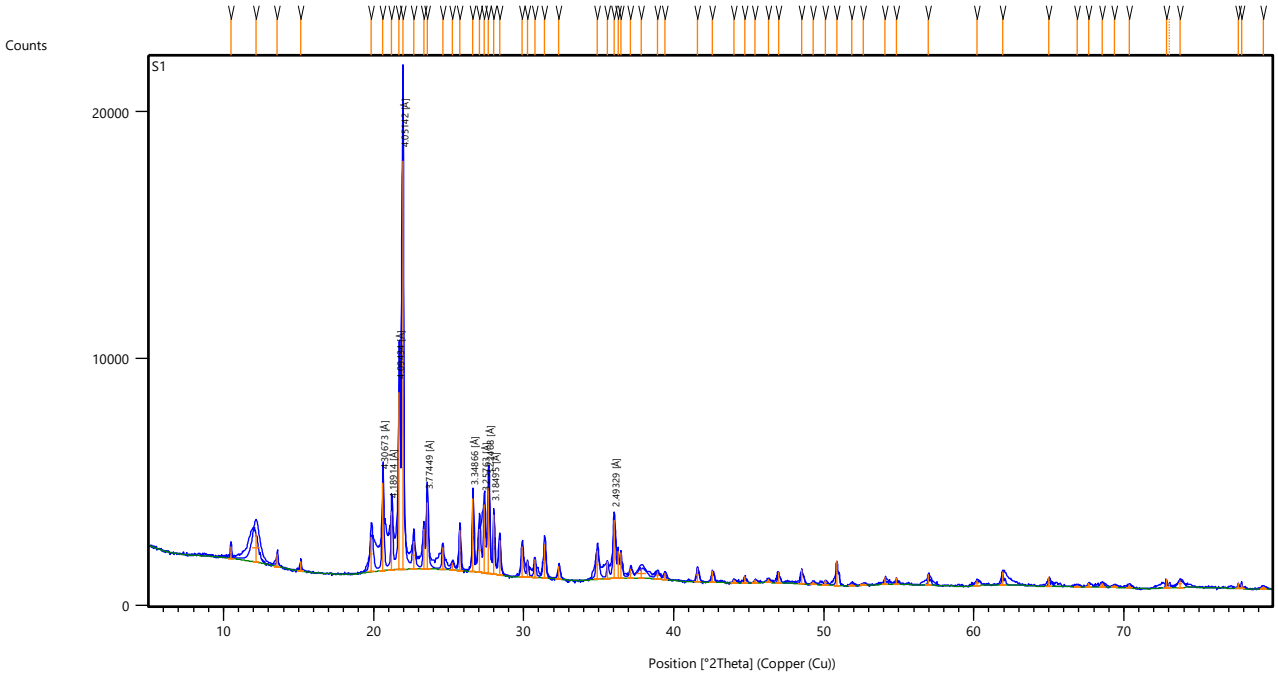

MAUNGATŪTŪ/MOUNT MISERY RHYOLITES – S2

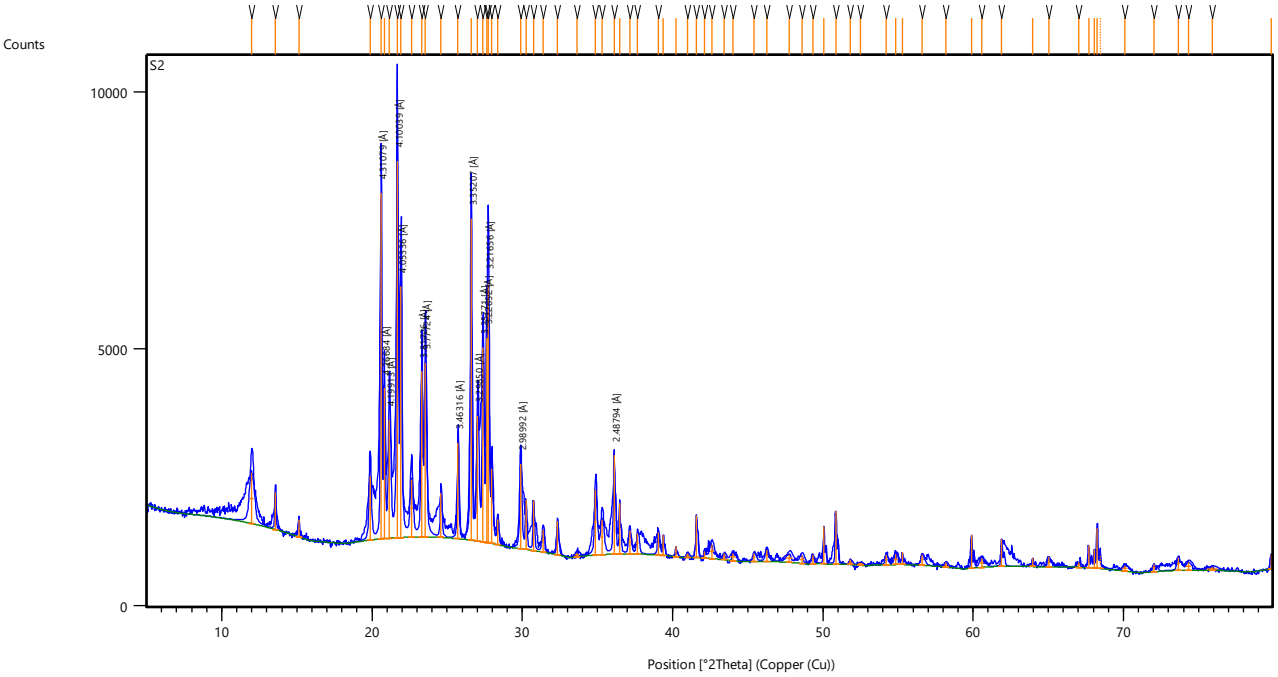

MAUNGATŪTŪ/MOUNT MISERY RHYOLITES – S3

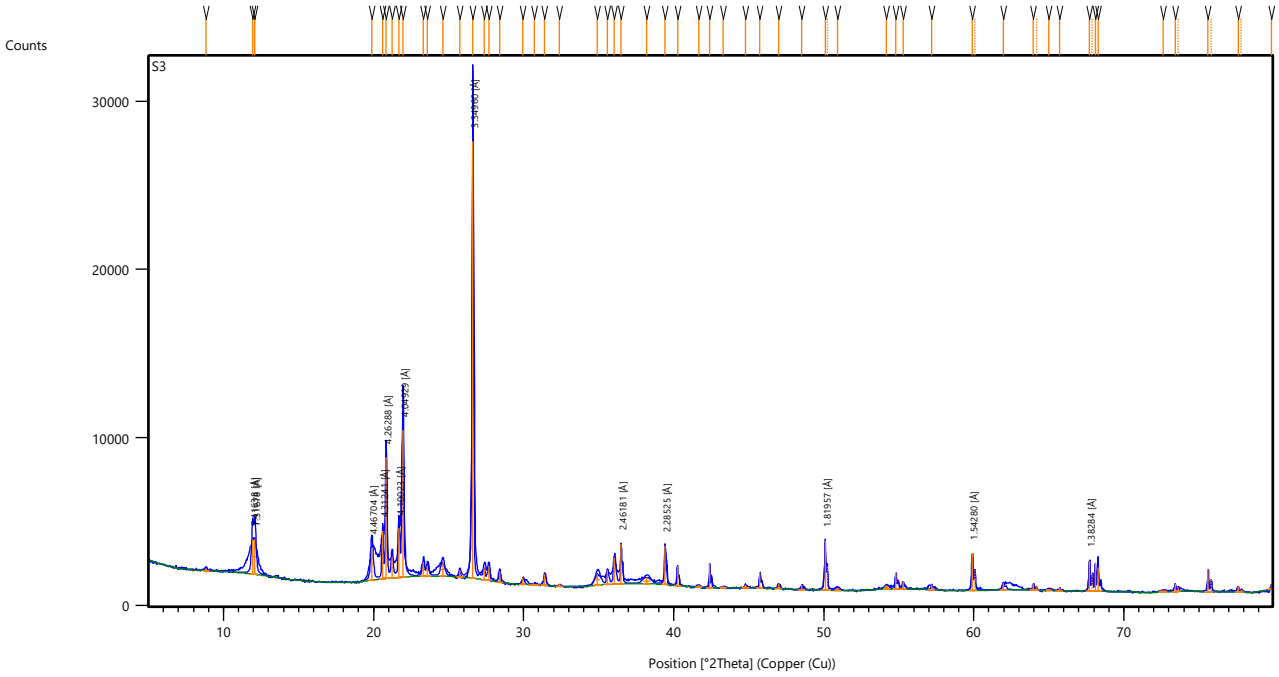

GREENPARK RHYOLITES – S1.1

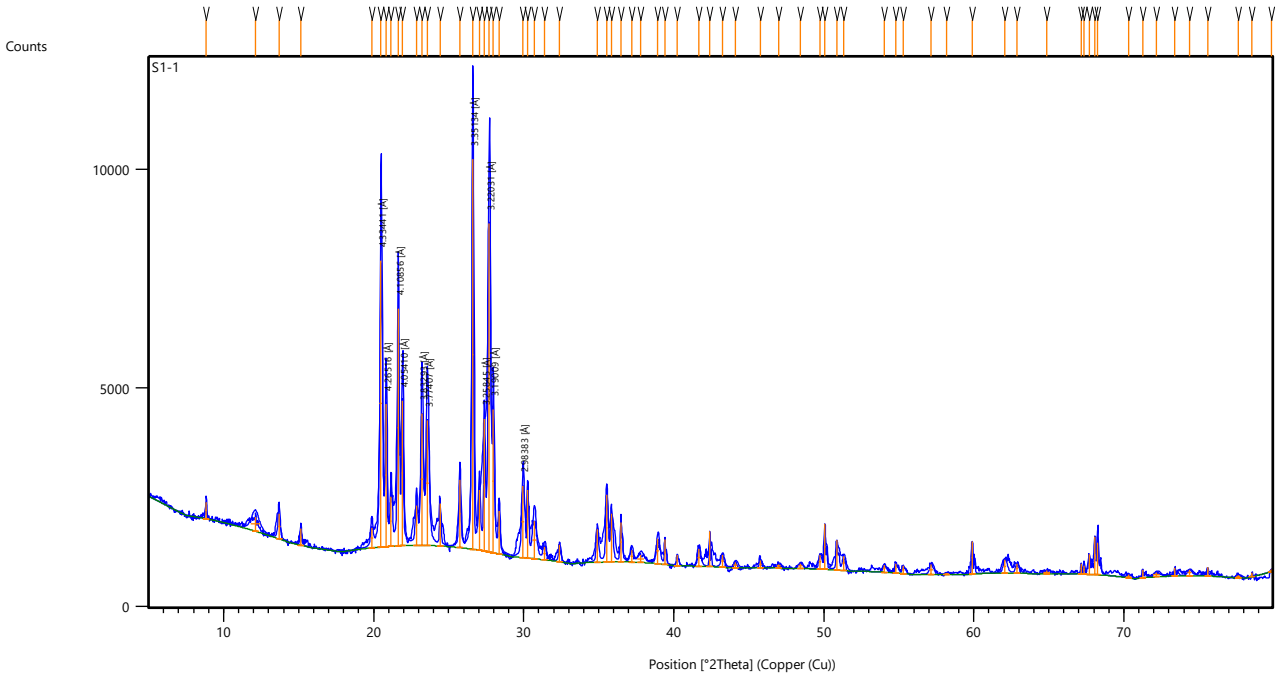

GREENPARK RHYOLITES – S2TB

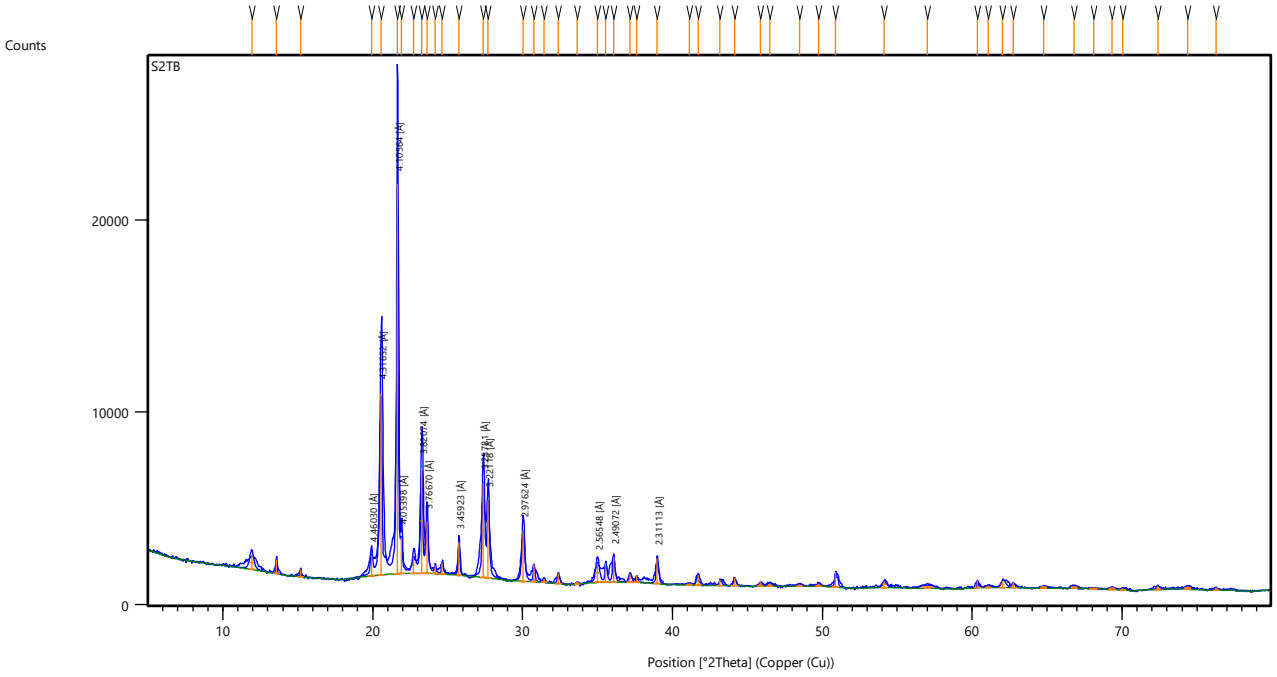

GREENPARK RHYOLITES – S2MB

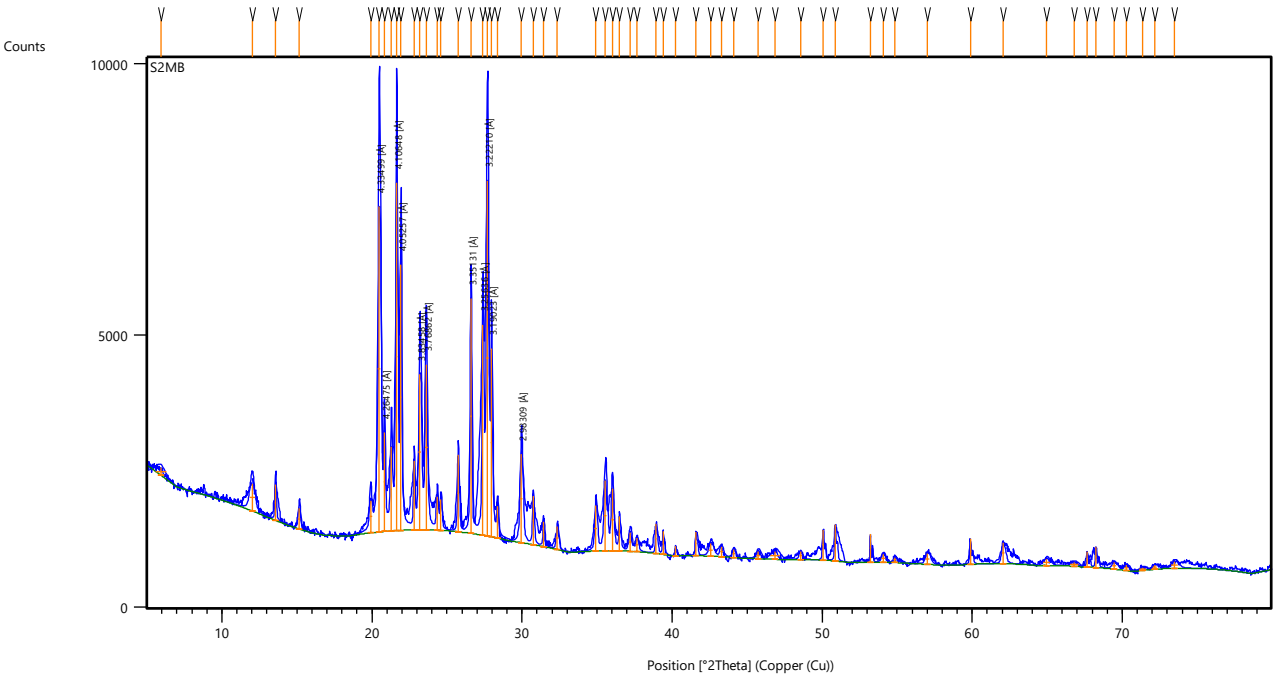

GREENPARK RHYOLITES – S4DAR

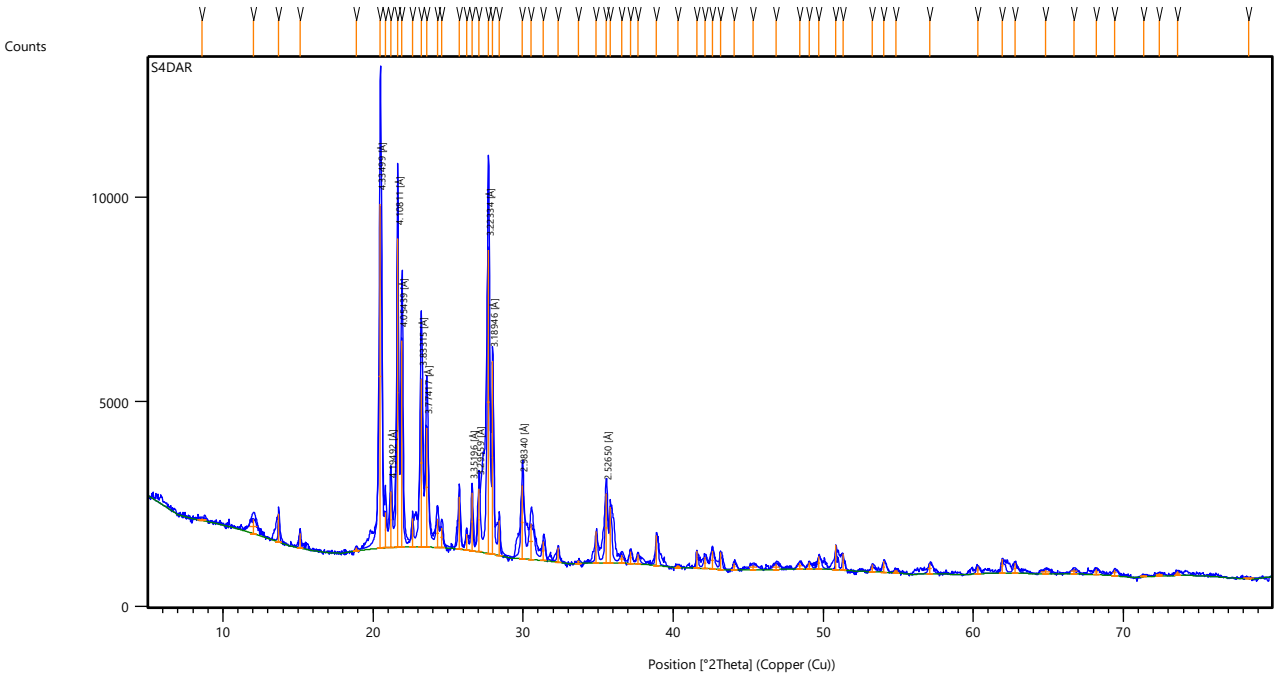

GREENPARK RHYOLITES – S6DAR

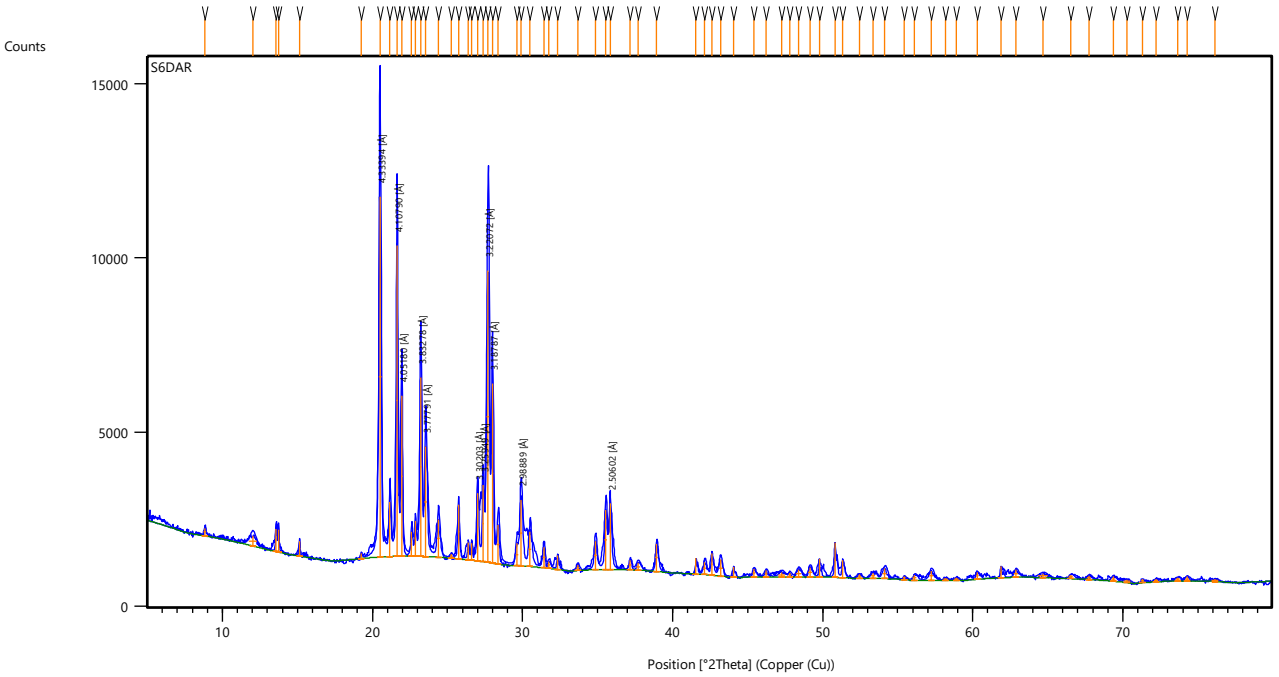

PUKUNUI RHYOLITES – R Lithic

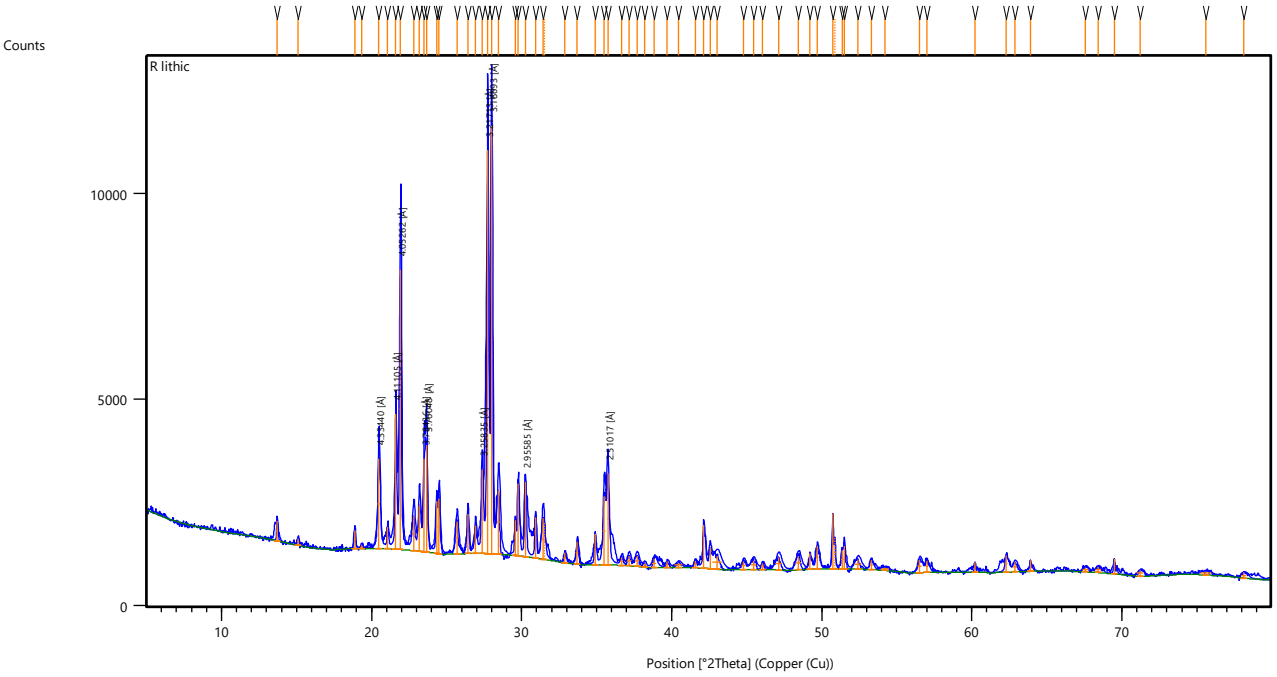

APPENDIX D: XRF analysis

XRF ANALYSIS LIST –

RHYOLITE/IGNIMBRITE	SAMPLE TYPE	SAMPLE ID
MT MISERY	**Bulk**	**S1**
MT MISERY	**Bulk**	**S2**
MT MISERY	**Bulk**	**S3**
MT MISERY	**Bulk**	**TM**
PUKUNUI	**Bulk**	**2TB**
PUKUNUI	**Bulk**	**2CB**
PUKUNUI	**Bulk**	**3CB**
GREENPARK	**Bulk**	**S1.1**
GREENPARK	**Bulk**	**S2TB**
GREENPARK	**Bulk**	**S2MB**
GREENPARK	**Bulk**	**S4DAR**
GREENPARK	**Bulk**	**S6DAR**
PUKUNUI	**Matrix**	**R Lithic**
OTAWERA	**Pumice**	**1**
OTAWERA	**Pumice**	**2**
OTAWERA	**Pumice**	**3**
OTAWERA	**Pumice**	**4**
OTAWERA	**Pumice**	**5**
OTAWERA	**Pumice**	**6**